



**The Abdus Salam
International Centre for Theoretical Physics**



2223-24

Winter College on Optics in Imaging Science

31 January - 11 February, 2011

Super Resolved Photonic Sensing

Z. Zalevsky
*Bar Ilan University
Israel*

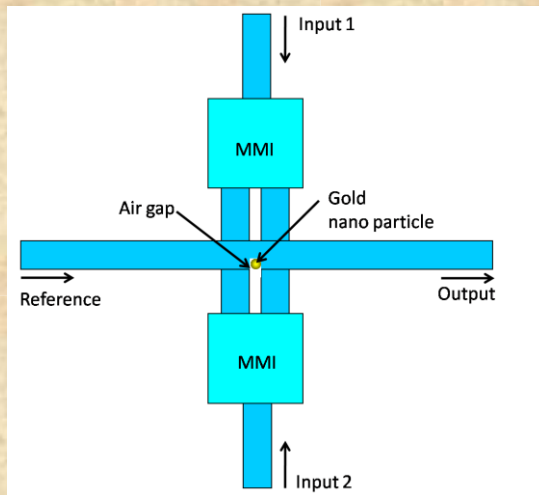


Super Resolved Photonic Sensing

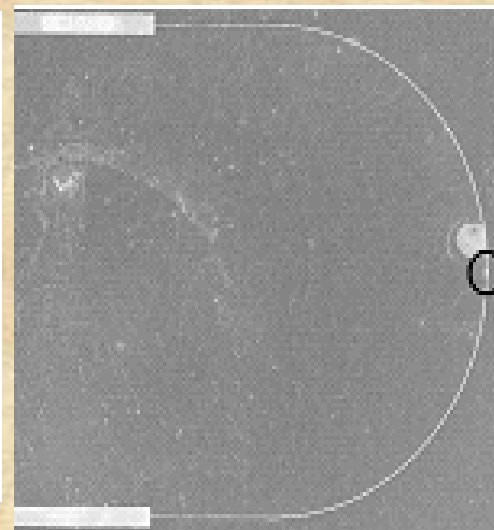
Zeev Zalevsky

**School of Engineering,
Bar-Ilan University, 52900 Ramat-Gan, Israel**

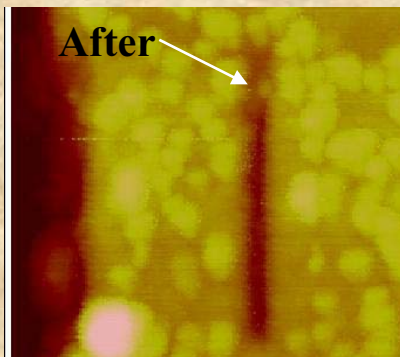
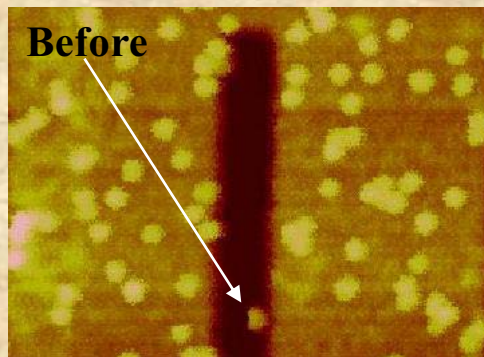
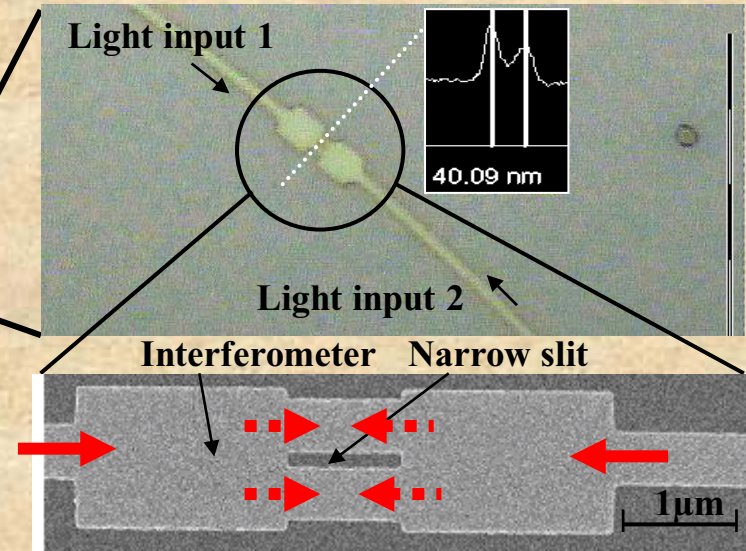
Trapped nano particle: all-optical modulator, sensor, wavelength converter, logic gate and flip flop



Operation Principle



Fabricated Prototype



Shifting particle along the slit with only 100nW! (coupled power)

Particle based electro-optical modulator

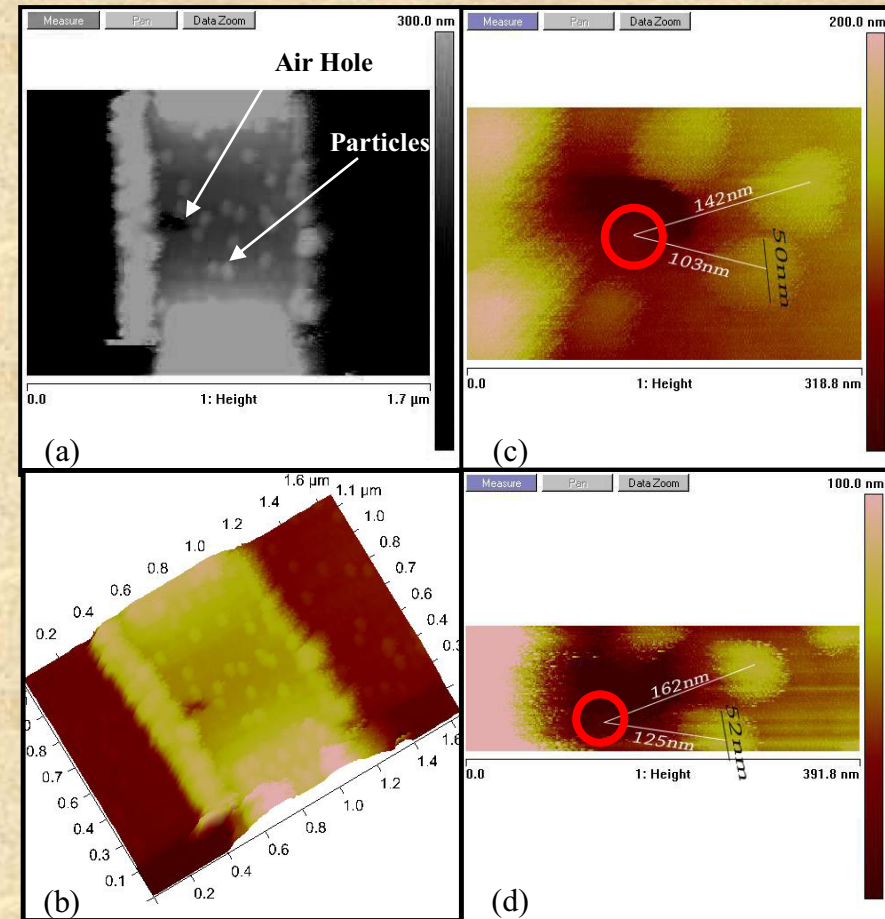
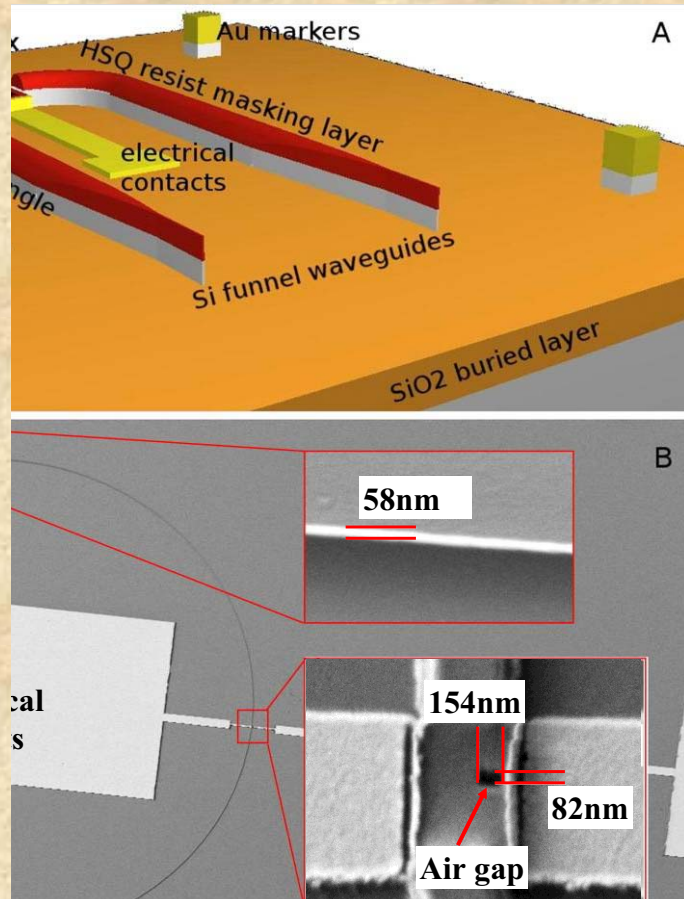
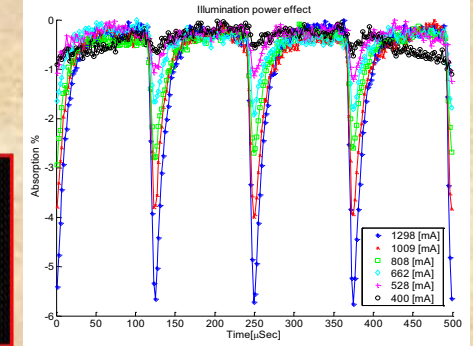
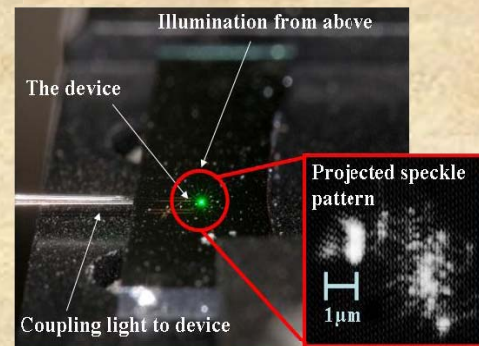
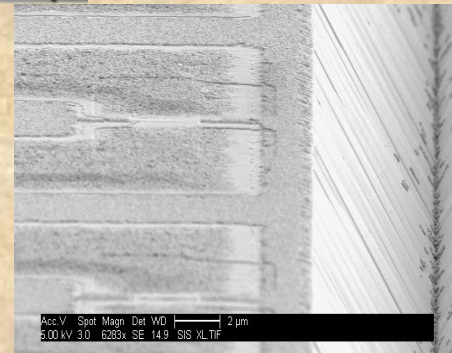
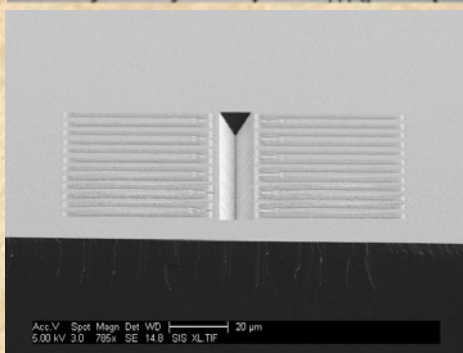
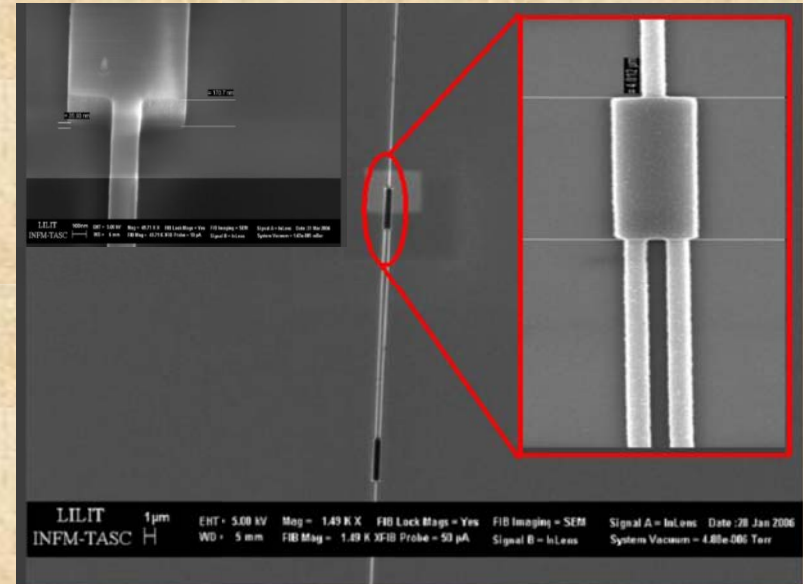
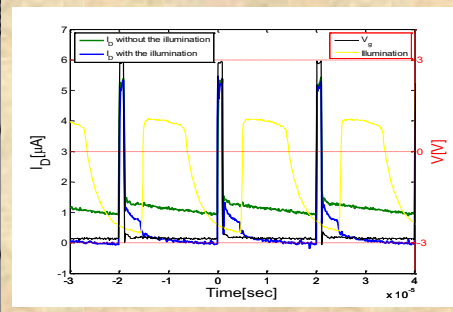
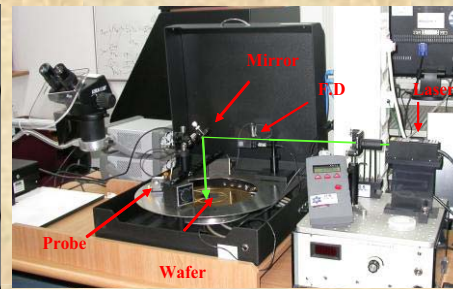
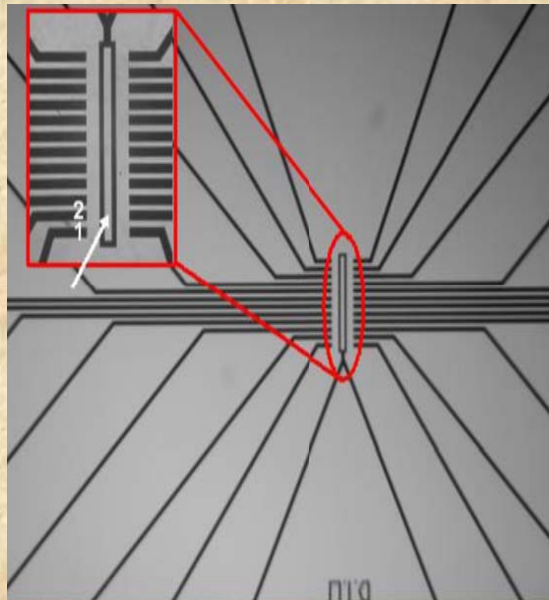
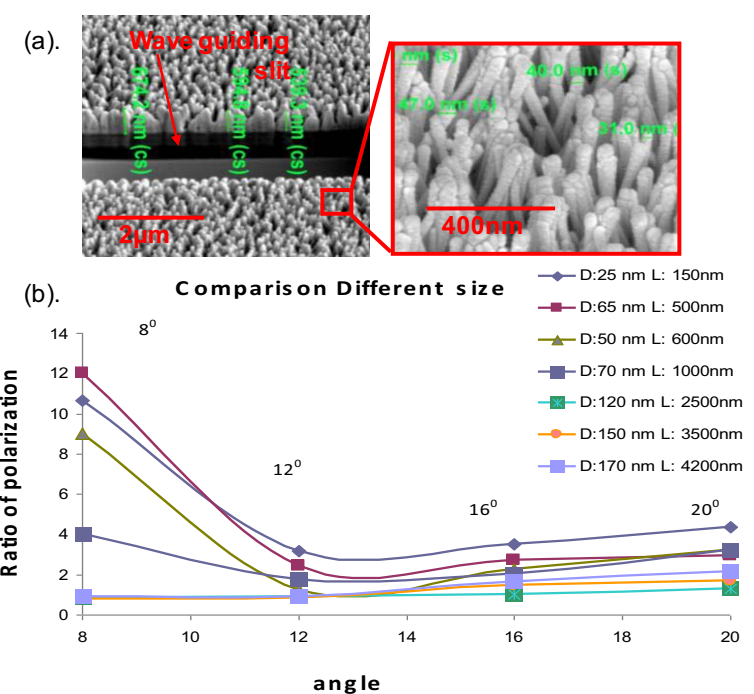
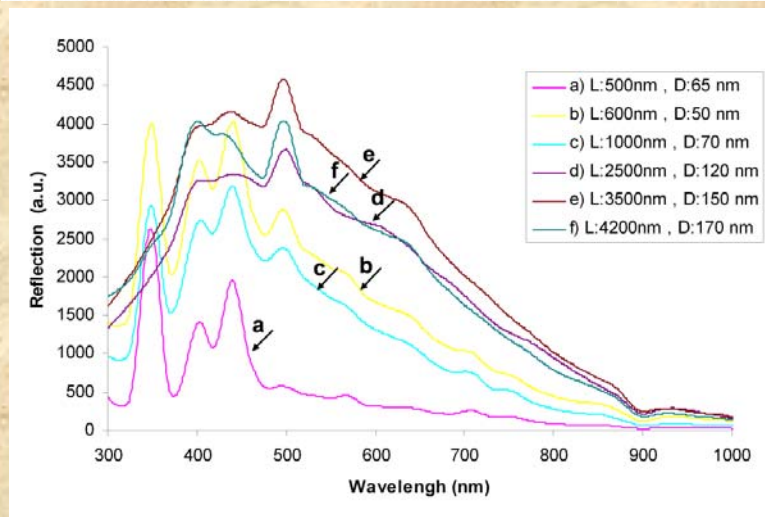
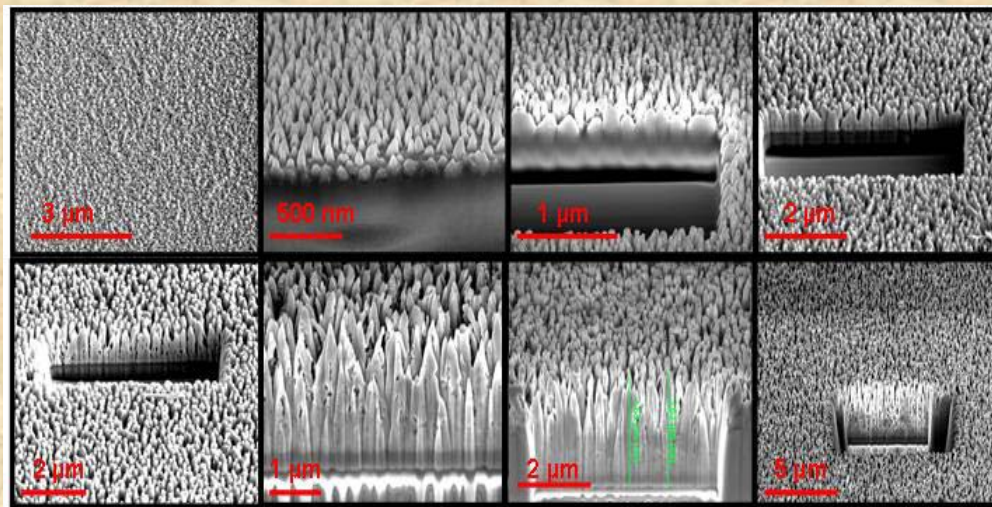


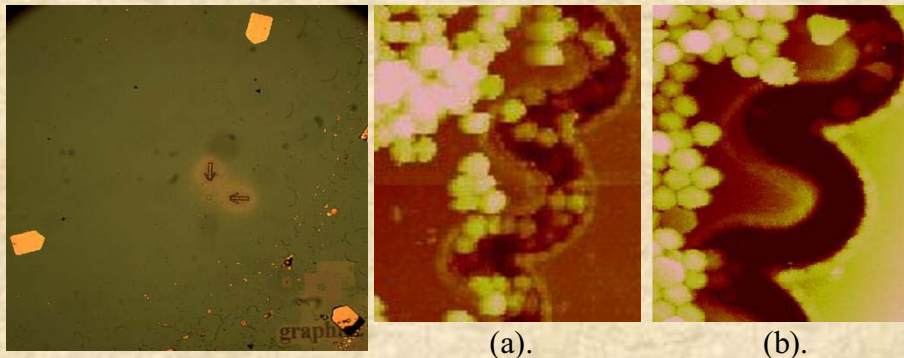
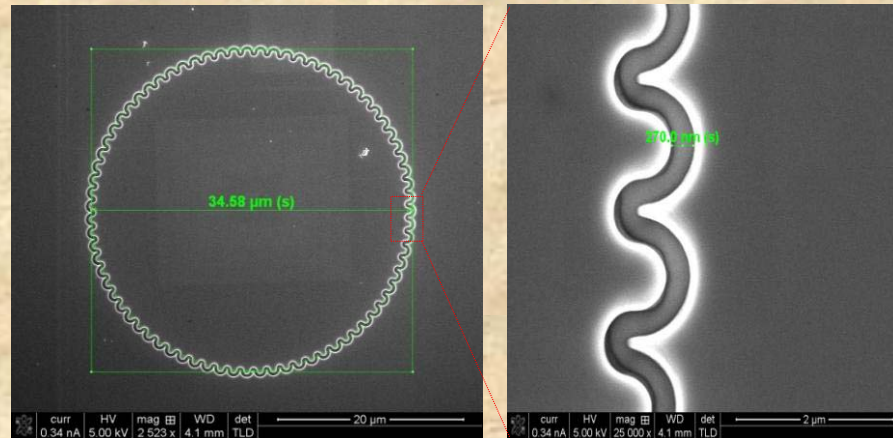
Photo-initiated and all-optical modulators



Nano rods based passive devices



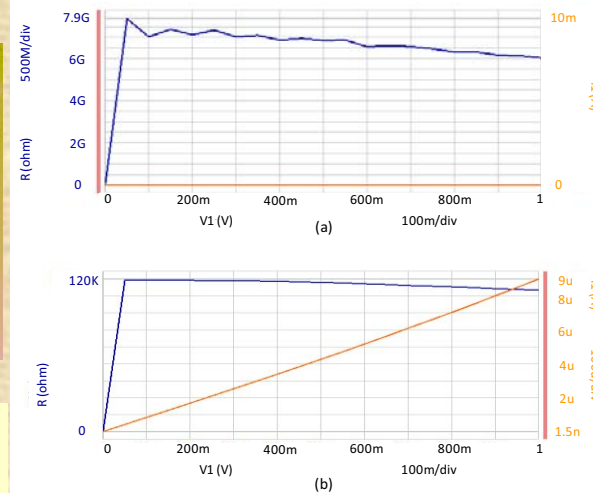
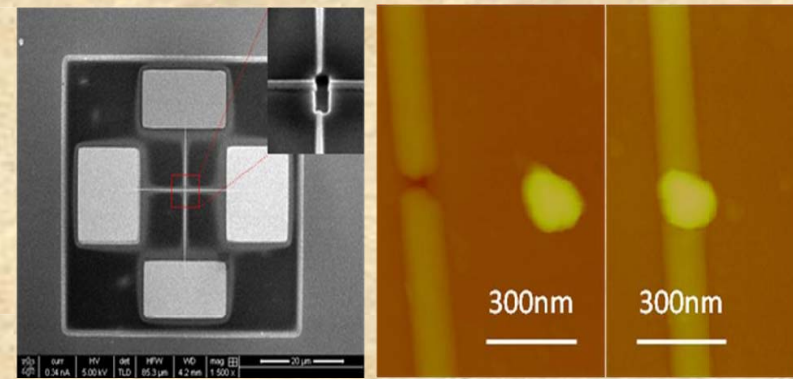
Tunable nano source



Preliminary experimental result for controlling the location of nano particles by applying voltage of a few volts across the tunnel. (a) Shows the deposition of the nano particles near the tunnel before applying external AC voltage. (b) Shows how we trapped the particles into the tunnel after applying a sine wave voltage with 1v peak-peak and at frequency of 10 KHz.

Other devices

Electronic nano transistor



R-V curve of the nano metric device, where the gold nanoparticle is being placed outside (a). and inside (b). the air gap, respectively (blue lines; left Y- axis). The orange curve presents the I-V (current-voltage) plot (right Y- axis). The horizontal X- axis is the same for both plots.



Collaborators

- **D. Mendlovic, *Israel***
- **E. Marom, *Israel***
- **A. Shemer, *Israel***
- **E. Sabo, *Israel***
- **D. Sylman, *Israel***
- **D. Fixler, *Israel***
- **A. Zlotnik, *Israel***
- **S. Ben-Yaish, *Israel***
- **O. Yehezkel, *Israel***
- **K. Lahav, *Israel***
- **M. Belkin, *Israel***
- **Y. Beiderman, *Israel***
- **A. Schwartz, *Israel***
- **A. Gur, *Israel***
- **E. Gur, *Israel***
- **Y. Garini, *Israel***
- **Y. Zdaka, *Israel***
- **A. Amsel, *Israel***
- **M. Meller, *Israel***
- **S. Rozentel, *Israel***
- **A. Lohmann, *Germany***
- **J. Garcia, *Spain***
- **C. Ferreira, *Spain***
- **V. Mico, *Spain***
- **P. Garcia, *Spain***
- **D. Cojoc, *Italy***



Outline

- **Introduction**
- **The “SW Adaptation” Process**
- **Diffraction type Super Resolution**
- **Geometrical type Super Resolution**
- **Hearing with light**
- **Conclusions**



Outline

- **Introduction**
- **The “SW Adaptation” Process**
- **Diffraction type Super Resolution**
- **Geometrical type Super Resolution**
- **Hearing with light**
- **Conclusions**

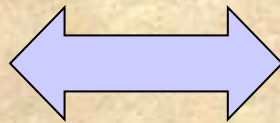
What is Resolution?



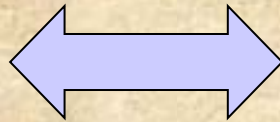
- **Resolution is finest spatial feature that an imaging system can resolve.**
- **Resolution of optical systems is restricted by diffraction (Lord Rayleigh, Abbe), by the geometry of the detector and by the noise equivalence of its pixels.**

Diffraction limitation of resolution is proportional to the F number of the imaging optics.

$$\delta x_{RES} = MIN \{ \Delta X \} = 1.22 \lambda f_{\#} = 1.22 \frac{\lambda f}{B}$$

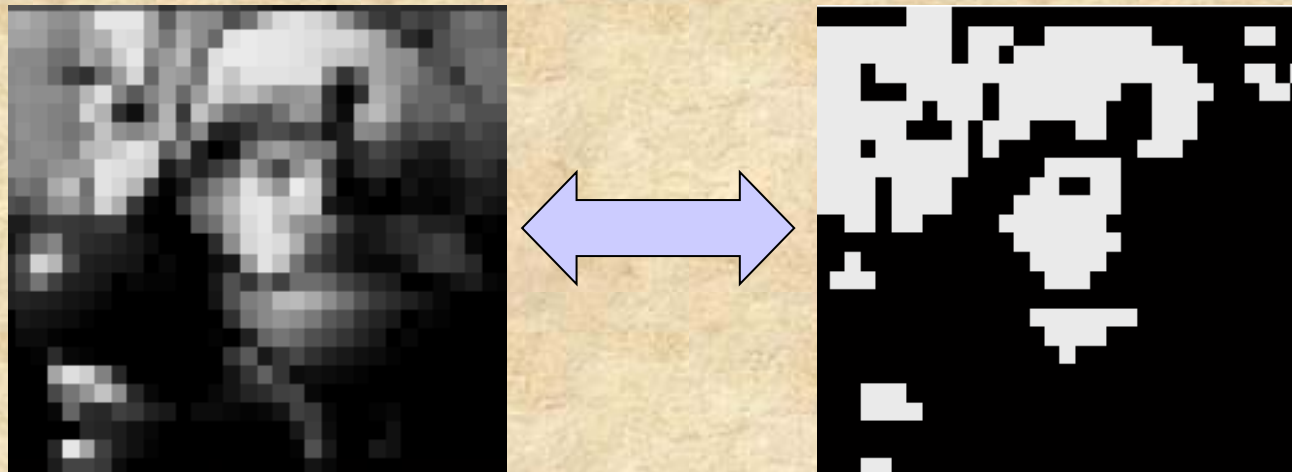


Geometrical resolution is limited by the number of detector's pixels and their size.



Introduction- Noise Equivalent Resolution

Noise equivalent resolution is originated by the internal noises existing within each pixel of the detector (electronic noises, shot noises etc).





Outline

- Introduction
- The “SW Adaptation” Process
- Diffractive type Super Resolution
- Geometrical type Super Resolution
- Hearing with light
- Conclusions

If not resolved, is it hopeless?

**No, if A Priori information
on the object is available!!!**

Types of a priori information:

- **A single dimensional object**
- **Polarization restricted information**
- **Temporally restricted signal**
- **Wavelength restricted signal**
- **Object shape**

The Suggested Solution:

Having a priori knowledge of the signal may lead to super resolution using an SW (space-bandwidth) adaptation process:

Adapt the SW of the signal to the acceptance SW of the system

$$SW(x, \nu) = \begin{cases} 1 & \text{for all } \langle W(x, \nu) \rangle > W_{\text{tresh}} \\ 0 & \text{otherwise} \end{cases}$$

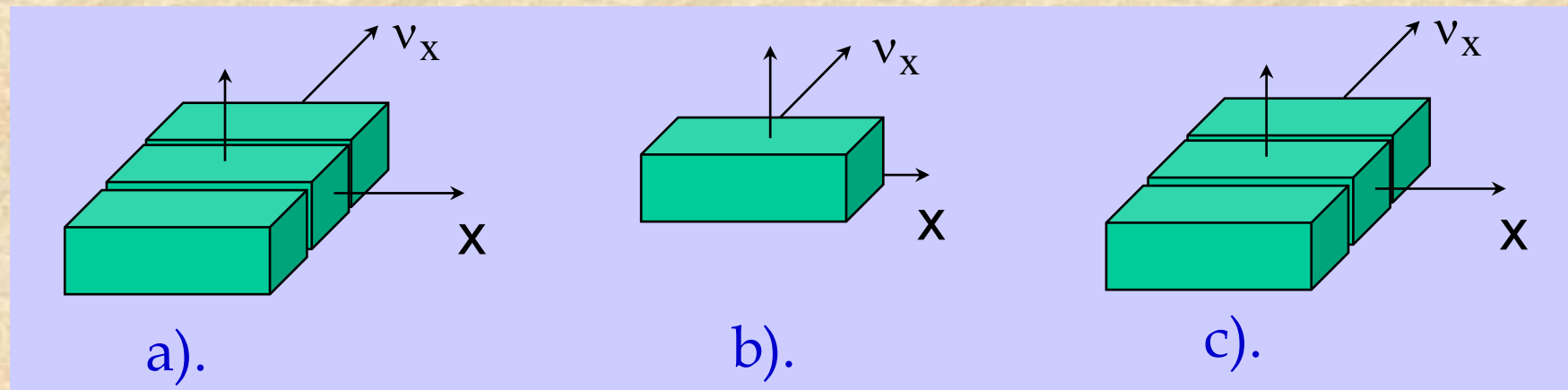
$$\iint SW(x, \nu) dx d\nu = N$$

Adaptation of Geometrical SR:

a). SWI

b). SWY

c). SWY after dividing each pixel to 3 regions



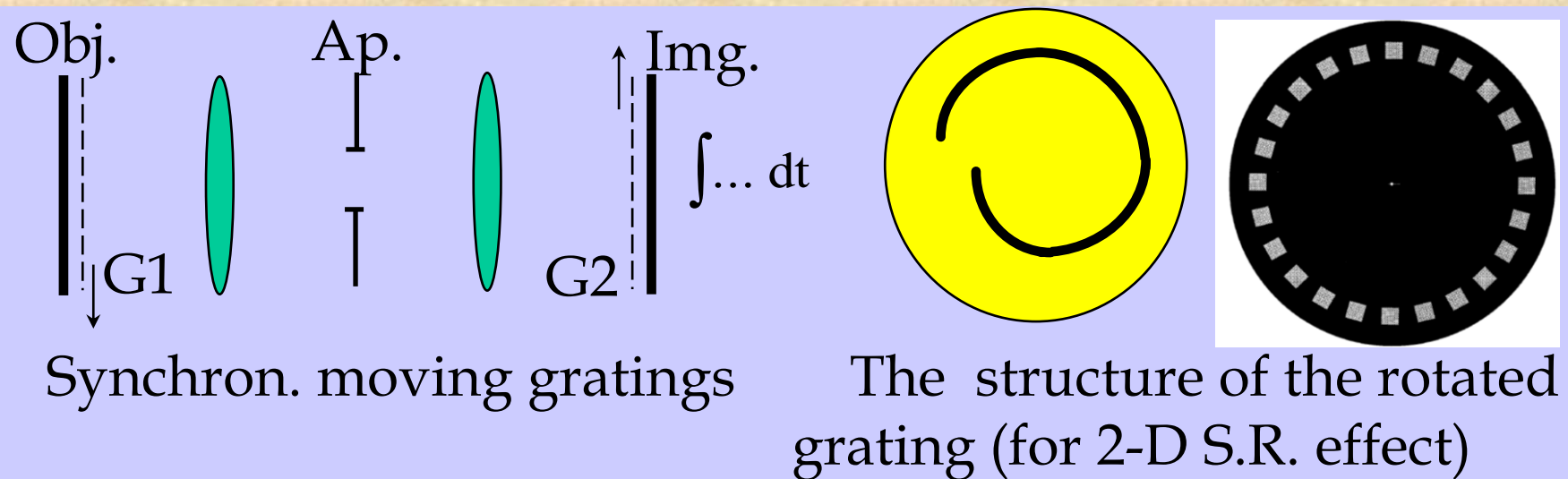


Outline

- Introduction
- The “SW Adaptation” Process
- **Diffractive type Super Resolution**
- Geometrical type Super Resolution
- Hearing with light
- Conclusions

Time Multiplexing:

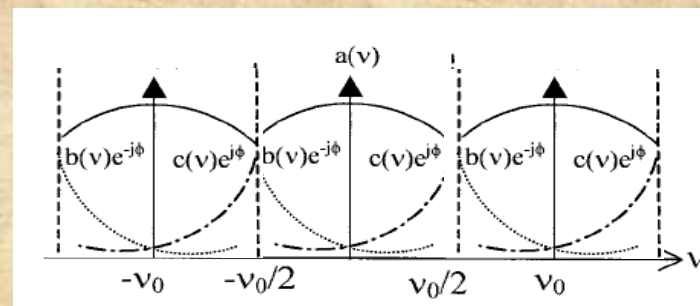
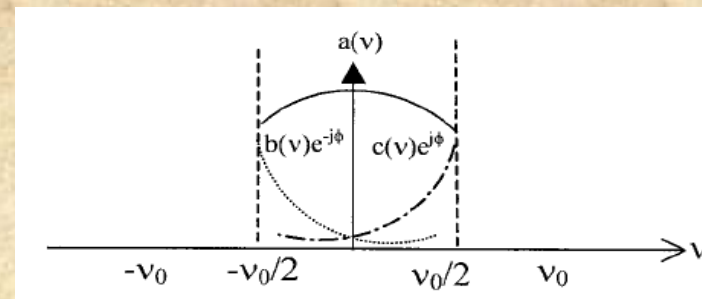
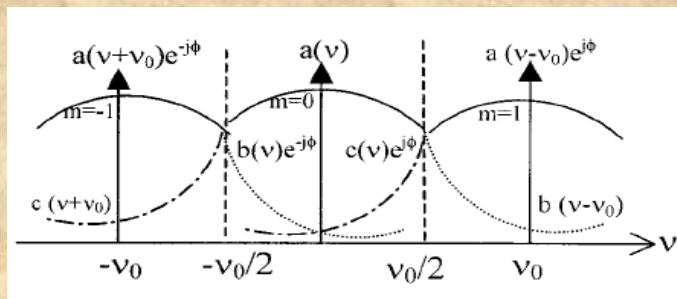
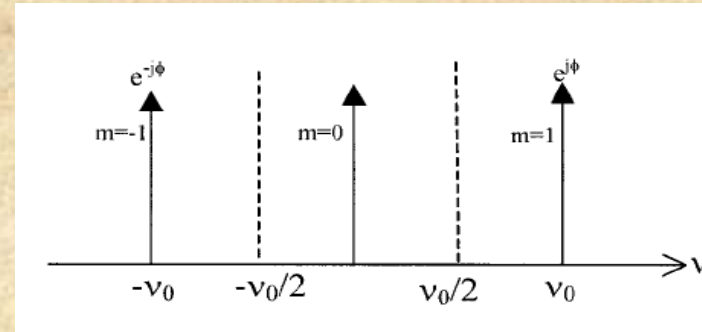
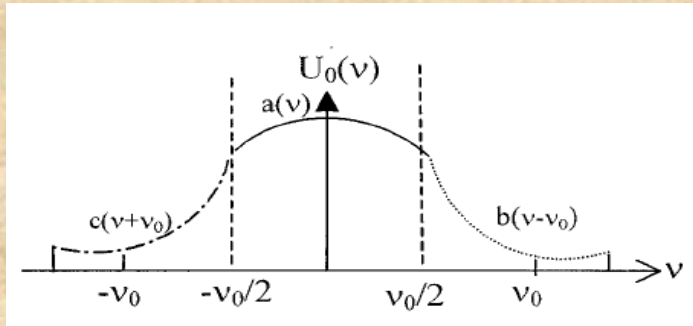
Conversion of temporal degrees of freedom to spatial domain (diffraction)



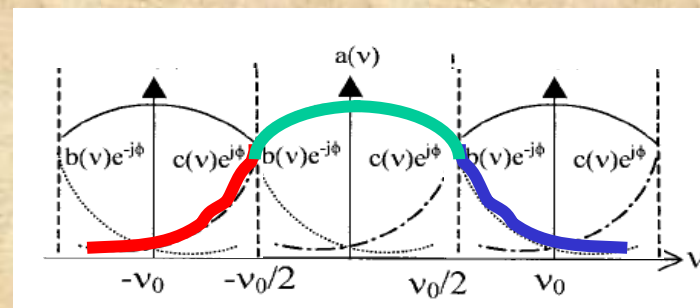
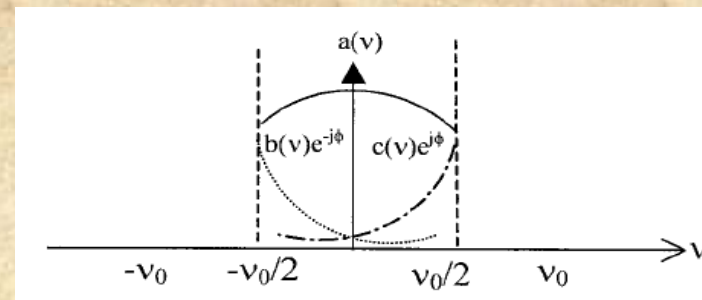
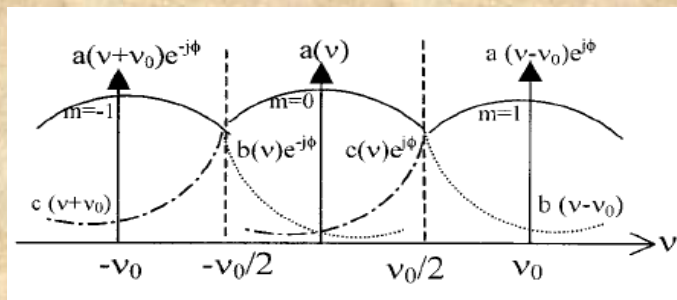
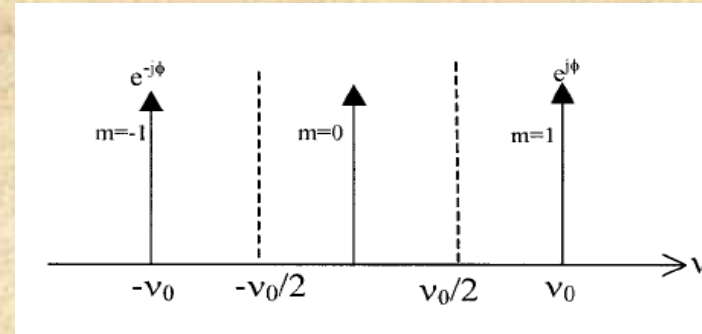
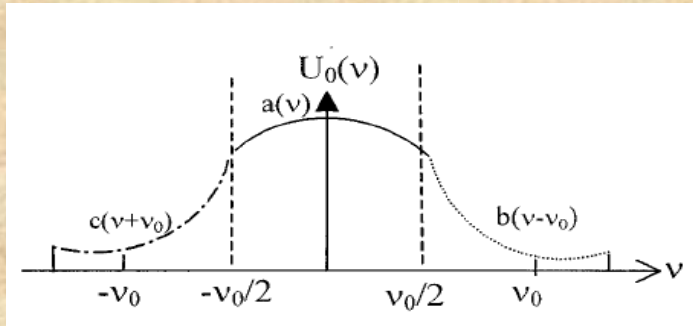
Recent improvements:

- Automatic synchronization (one grating, transmitted twice)
- 2-D objects, 2-D gratings
- Dammann gratings

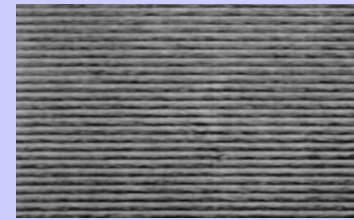
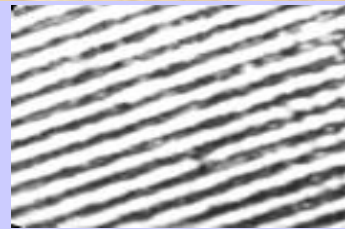
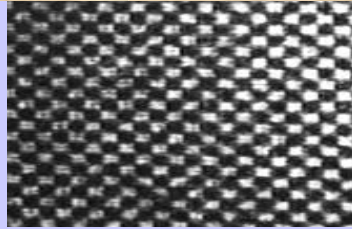
Diff. SR- Time Multiplexing



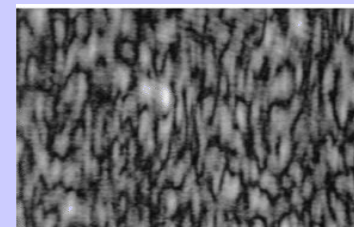
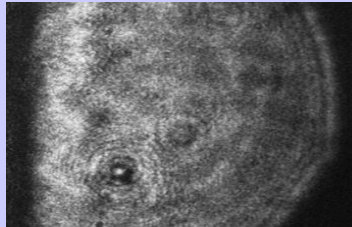
Diff. SR- Time Multiplexing



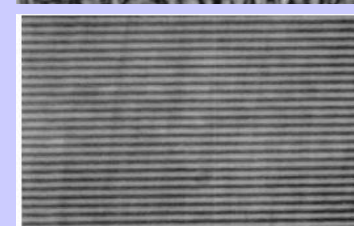
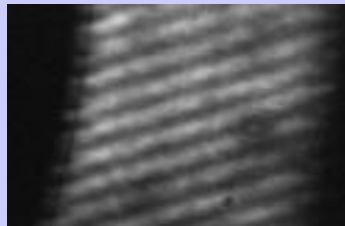
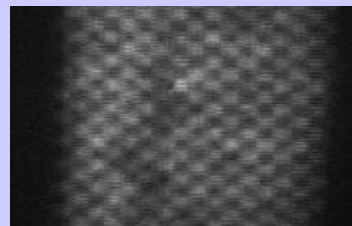
**With clear
aperture**



**Without time
multiplexing**

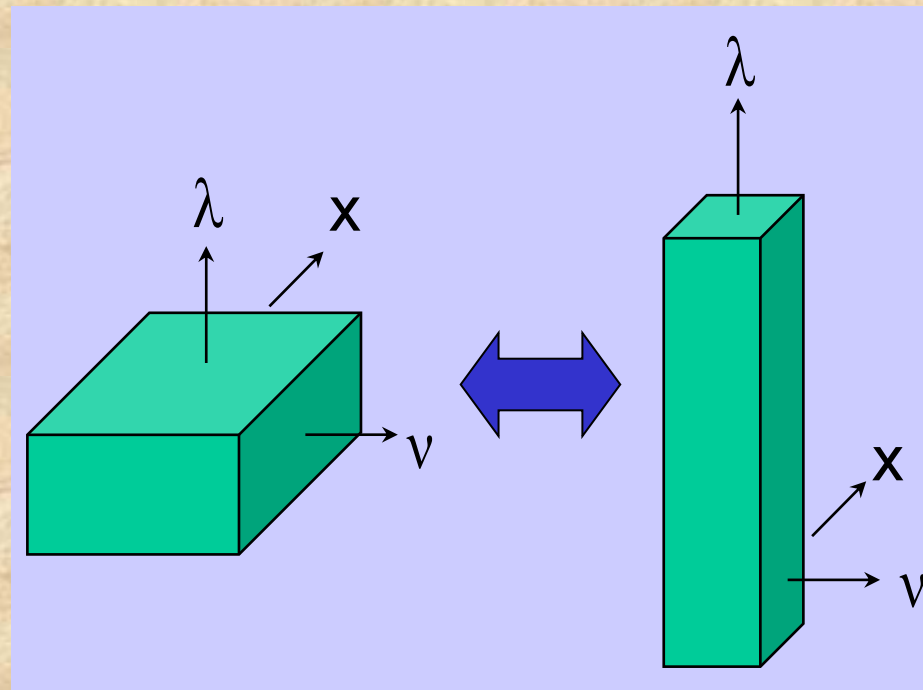


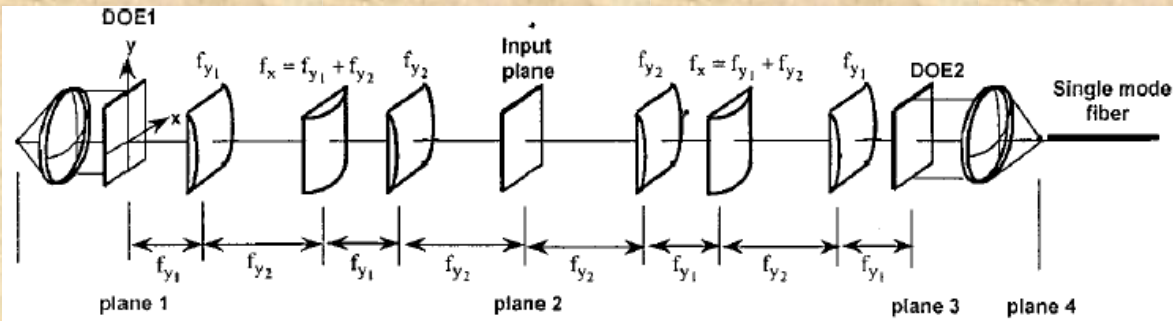
**With time
multiplexing**



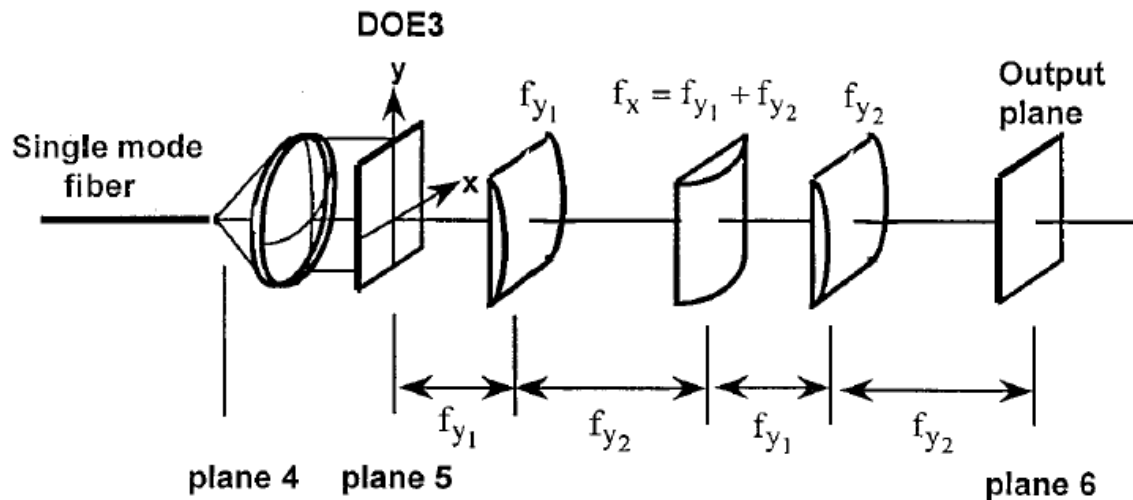
Wavelength Multiplexing:

The spatial coordinates of the input pattern are encoded by different wavelengths.

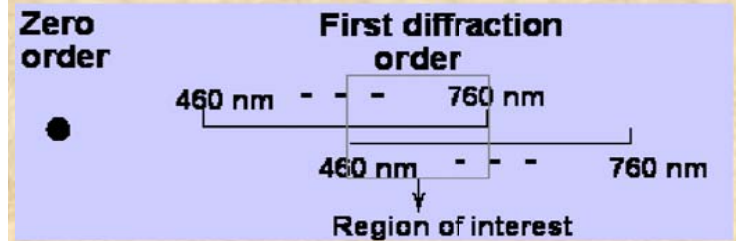
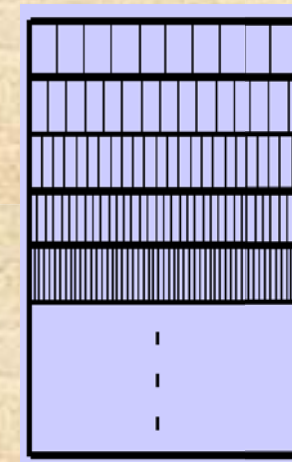




(a)

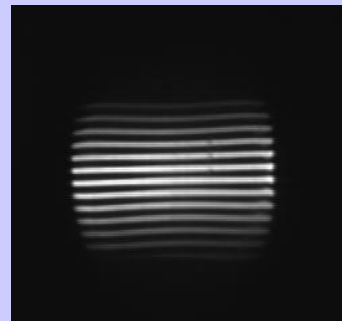
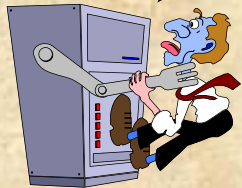


(b)

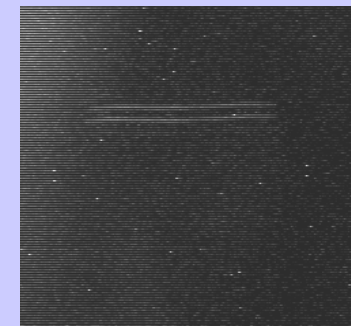


- a). Full spectrum
- b). Green
- c). Yellow
- d). Orange
- e). Red

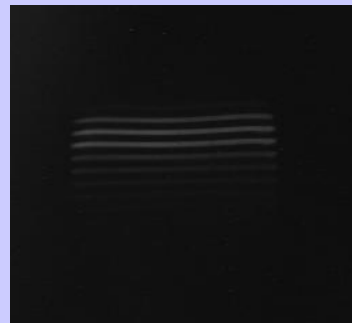
Filter's period=10 μ m
Input period= 1mm



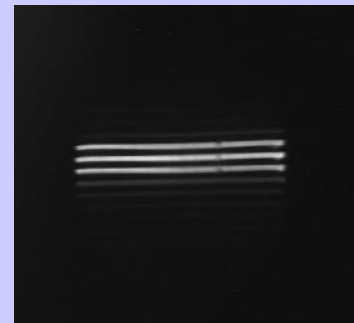
a).



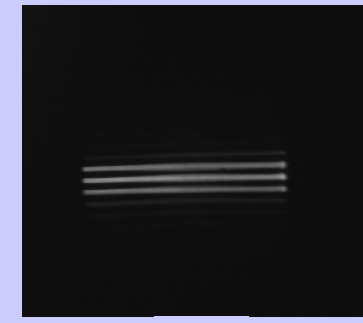
b).



c).

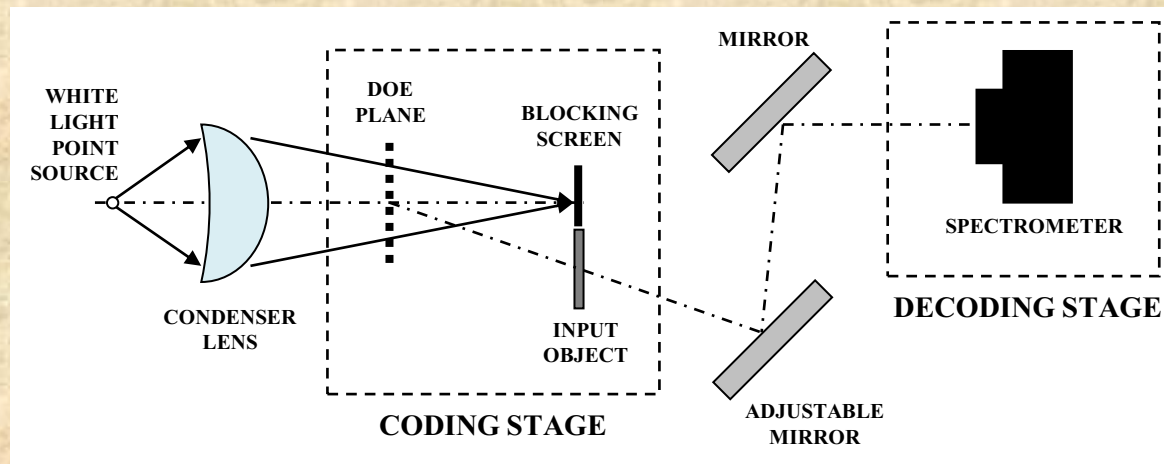
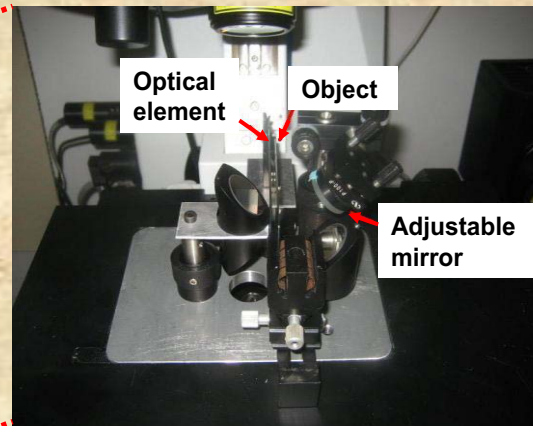
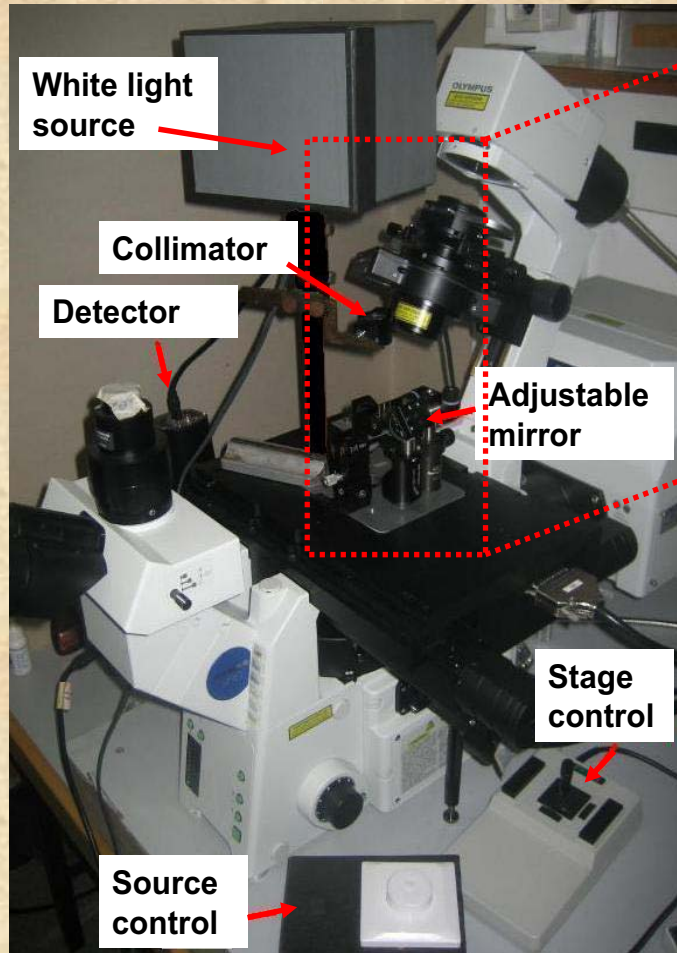


d).

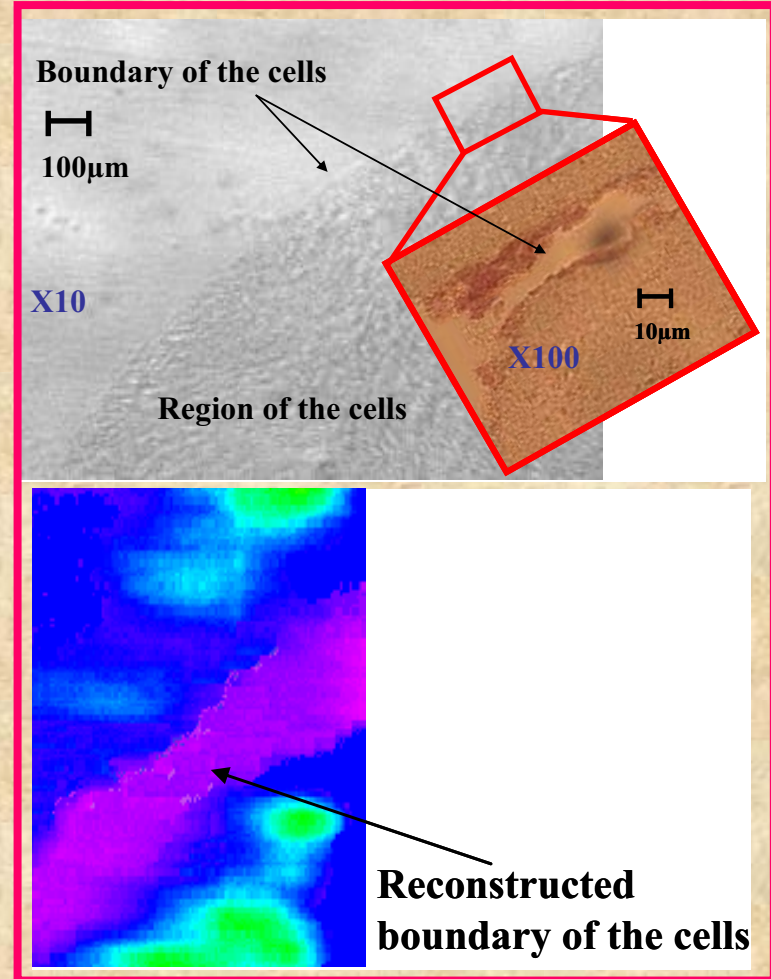
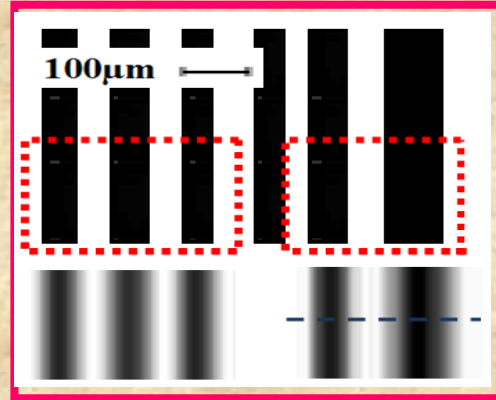
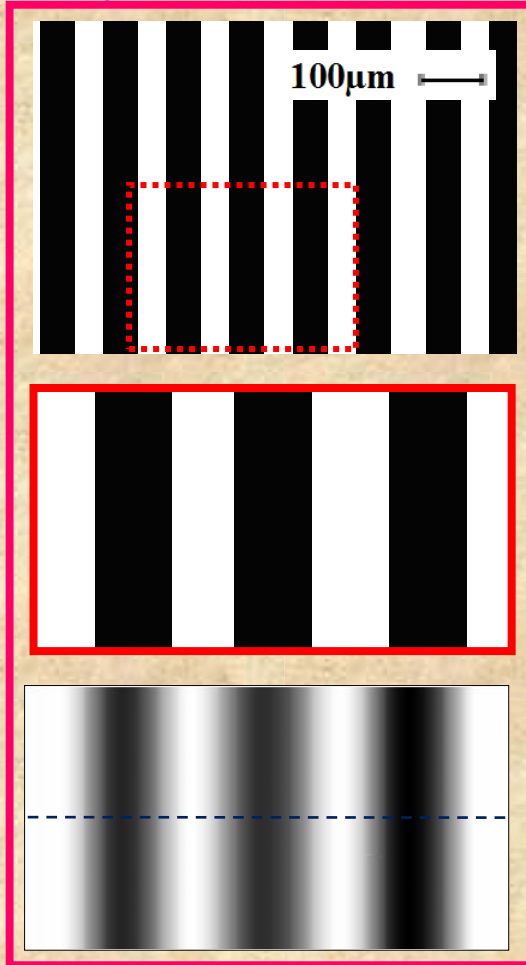


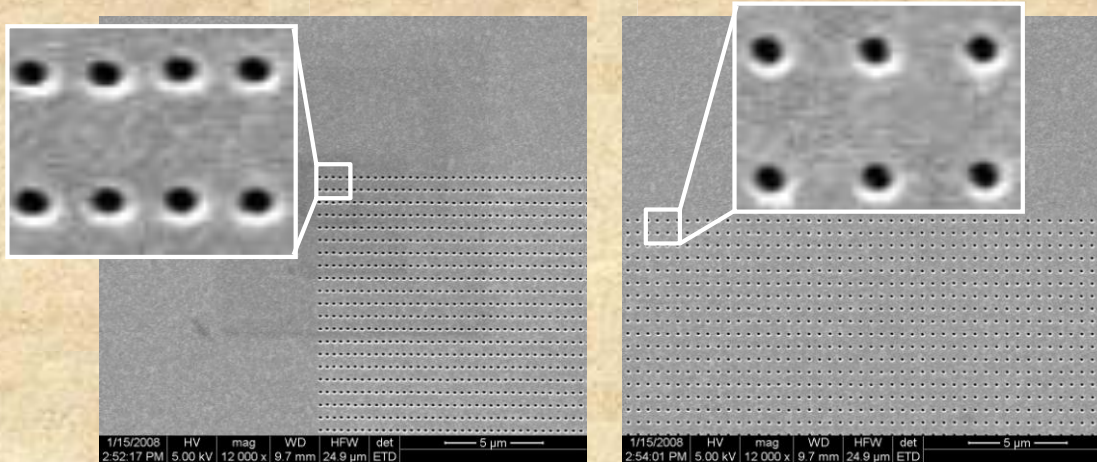
e).

Diff. SR- Wavelength Multiplexing2



Diff. SR- Wavelength Multiplexing2

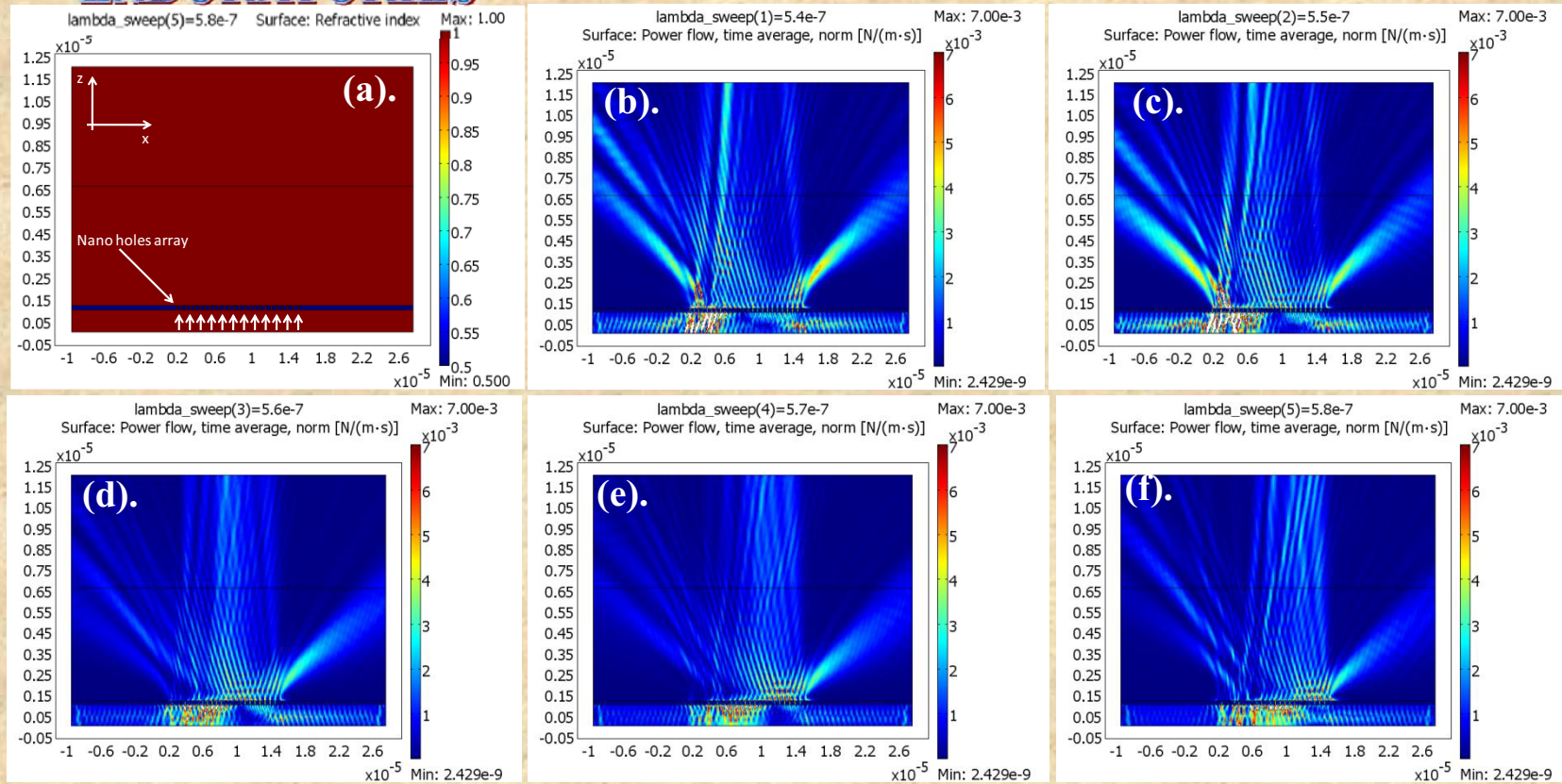




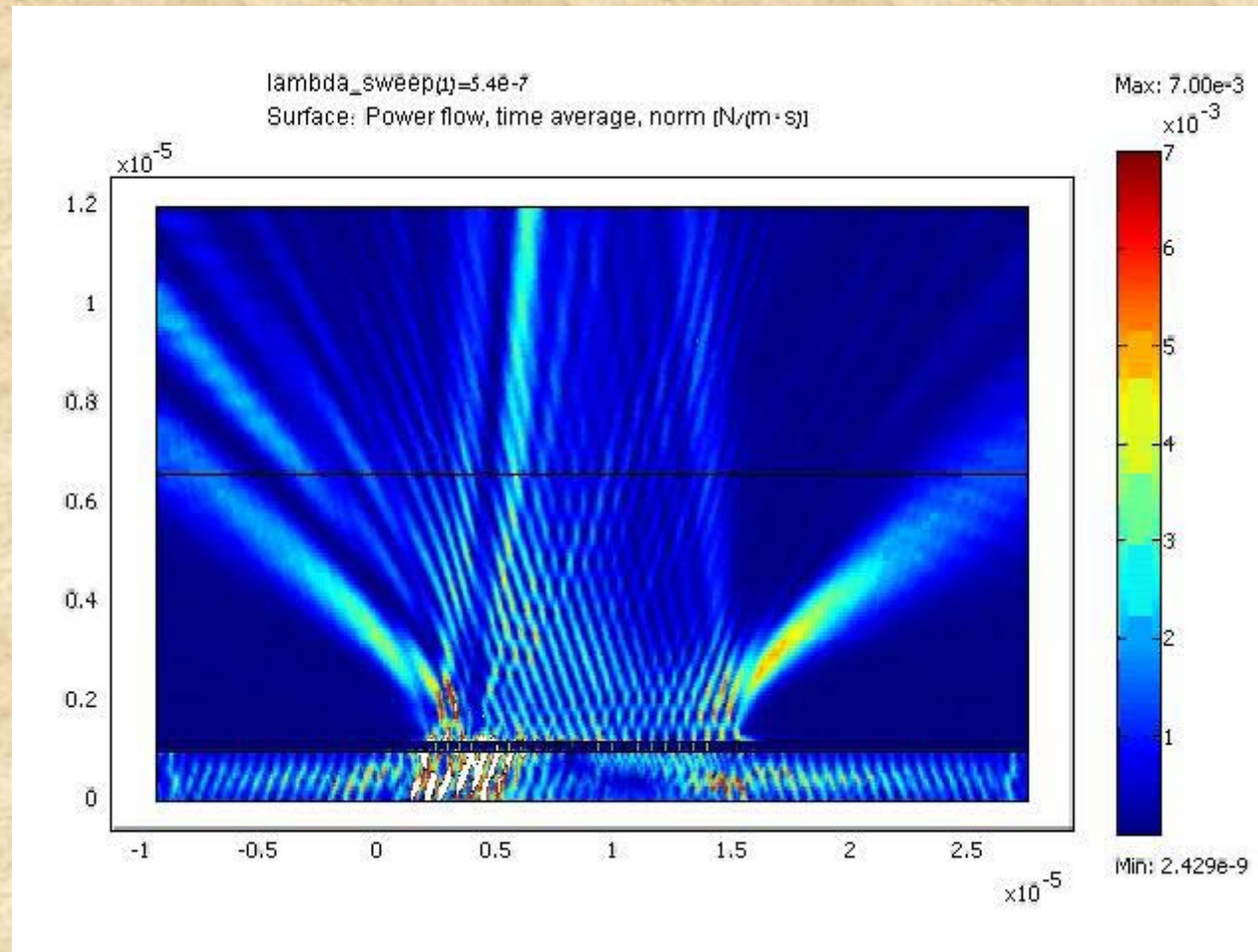
SEM image of the fabricated non periodic array of holes.

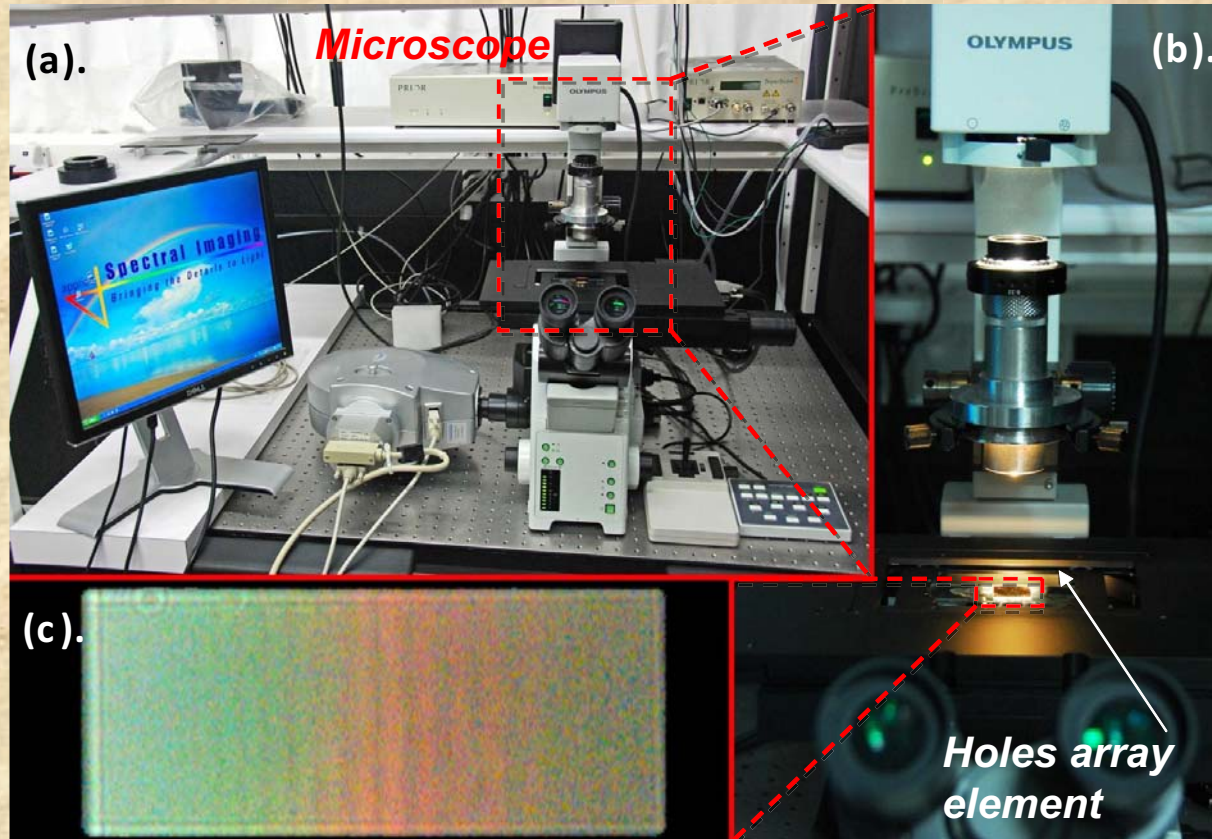
- No objective and no condenser
- 100% efficiency of transmission through the holes (plasmonic resonance).

Diff. SR- Wavelength Multiplexing³



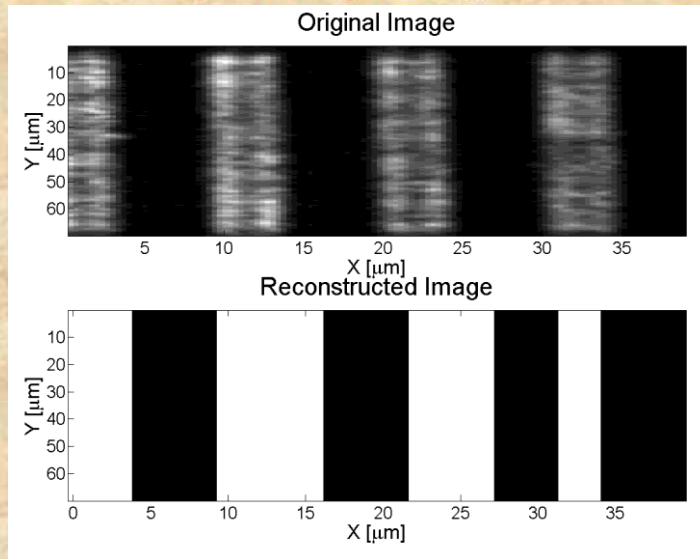
Numerical simulations of non periodic and wavelength sensitive sub wavelength holes array. (a) The nano holes array where the period of the holes was monotonically varied from 500nm up to 600nm in steps of 20nm. (b)-(f) The field pattern when illuminating the structure with different wavelength (540nm - 580nm in steps of 10nm).



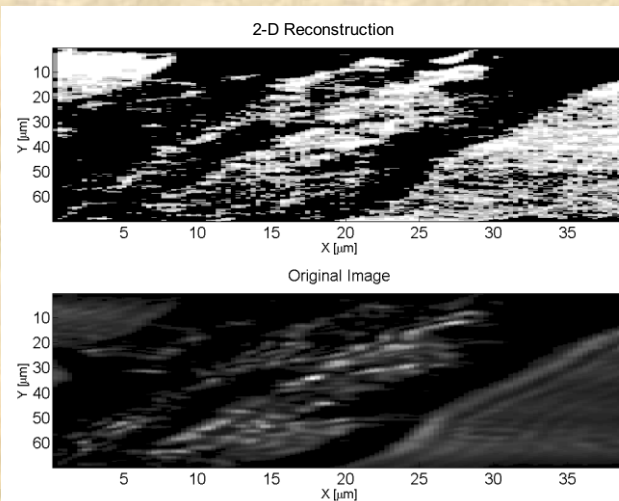
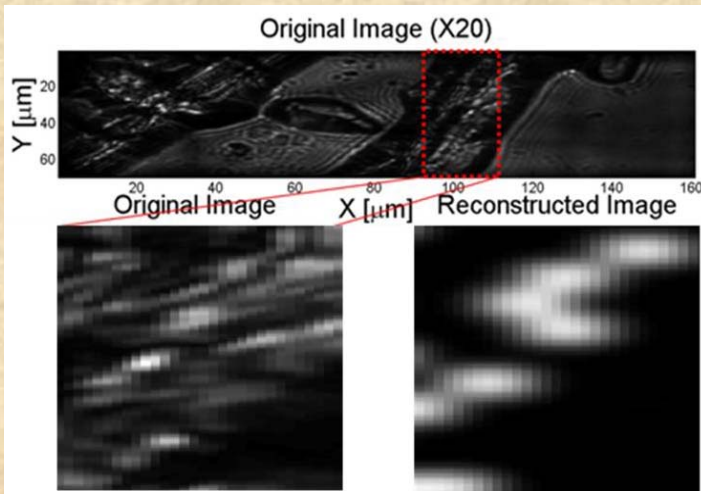


Preliminary experimental demonstration. (a). Microscope station in which we positioned the fabricated non periodic hole array (b). Collimated and polarized white light halogen lamp upon the fabricated element (c). The image seen in the microscope after illuminating the element with white light halogen lamp.

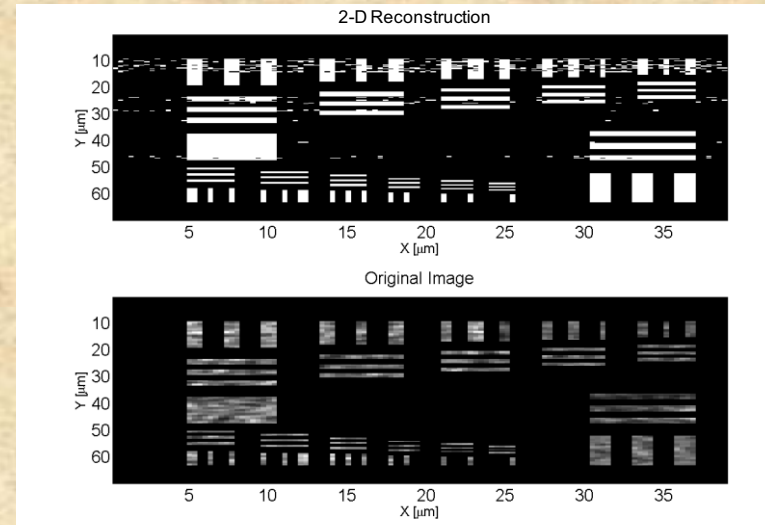
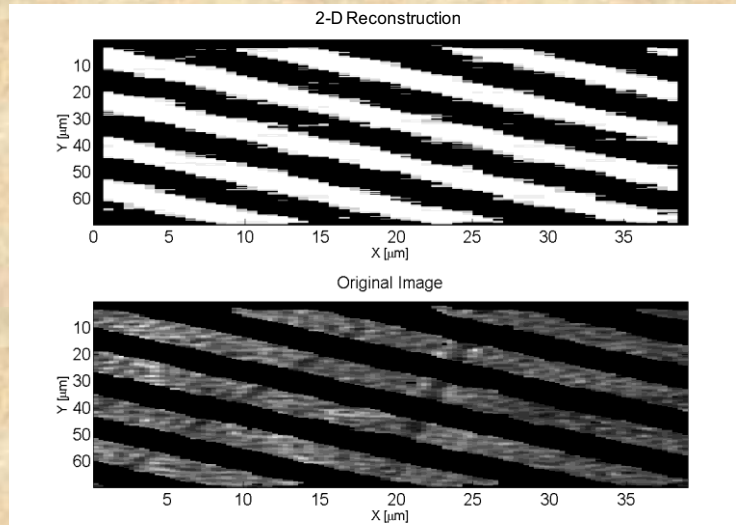
Diff. SR- Wavelength Multiplexing³



Experimental results including mapping of grating of 100 lp/mm



Experimental results including 2D mapping of 6 μ m polystyrene beads

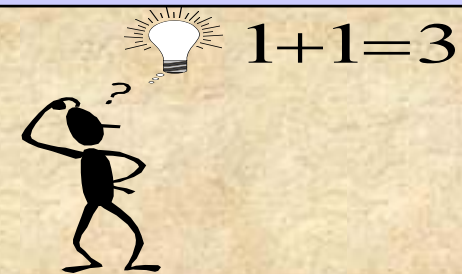
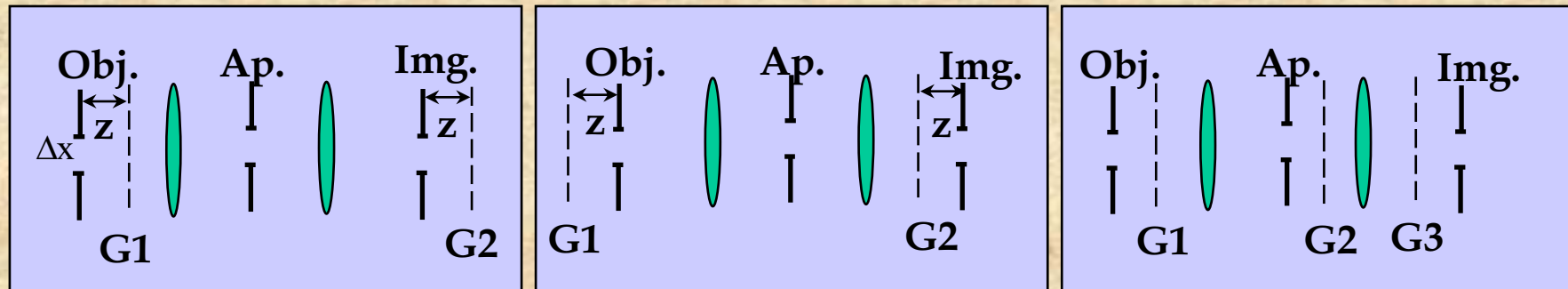


Physical numerical simulations for 2D tilted grating and a resolution target.

Direction Multiplexing:

The size ΔX of object (field of view) is restricted.

Three possible setups:



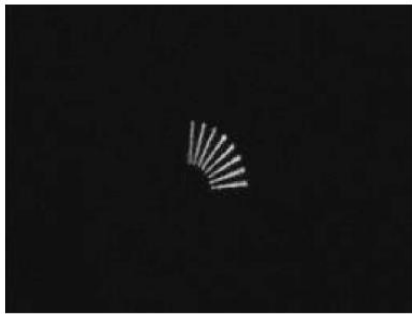
Direction Multiplexing:

$$mv_0 + nv_1 + lv_2 = 0$$

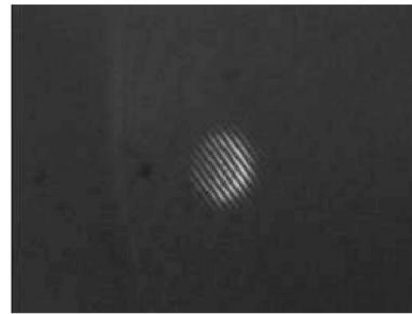
$$z_0mv_0 - z_1nv_1 - z_2lv_2 = 0$$

$$\frac{z_0\lambda}{2}m^2v_0^2 - z_1\lambda mnv_0v_1 - \frac{z_1\lambda}{2}n^2v_1^2 - z_2\lambda mlv_0v_2 - \frac{z_2\lambda}{2}l^2v_2^2 - z_2\lambda nlv_1v_2 = N$$

- **Adding all the spectral slots with the same linear phase.**
- **Obtaining all the spectral slots in the same location of the output plane.**
- **Adding all the spectral slots with the same constant phase factor (Talbot effect).**

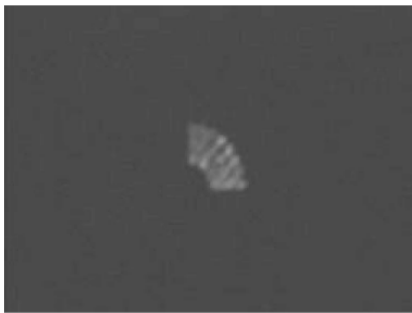


(a)



(b)

Open aperture

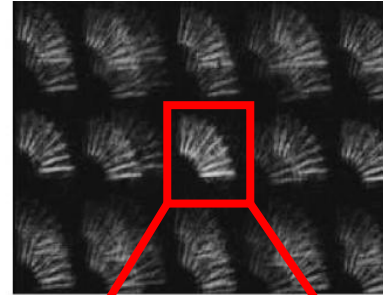


(a)

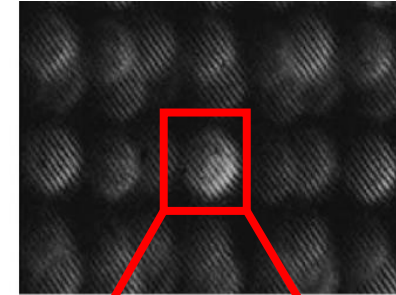


(b)

Closed aperture



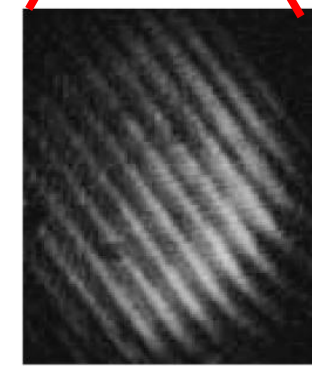
(a)



(b)



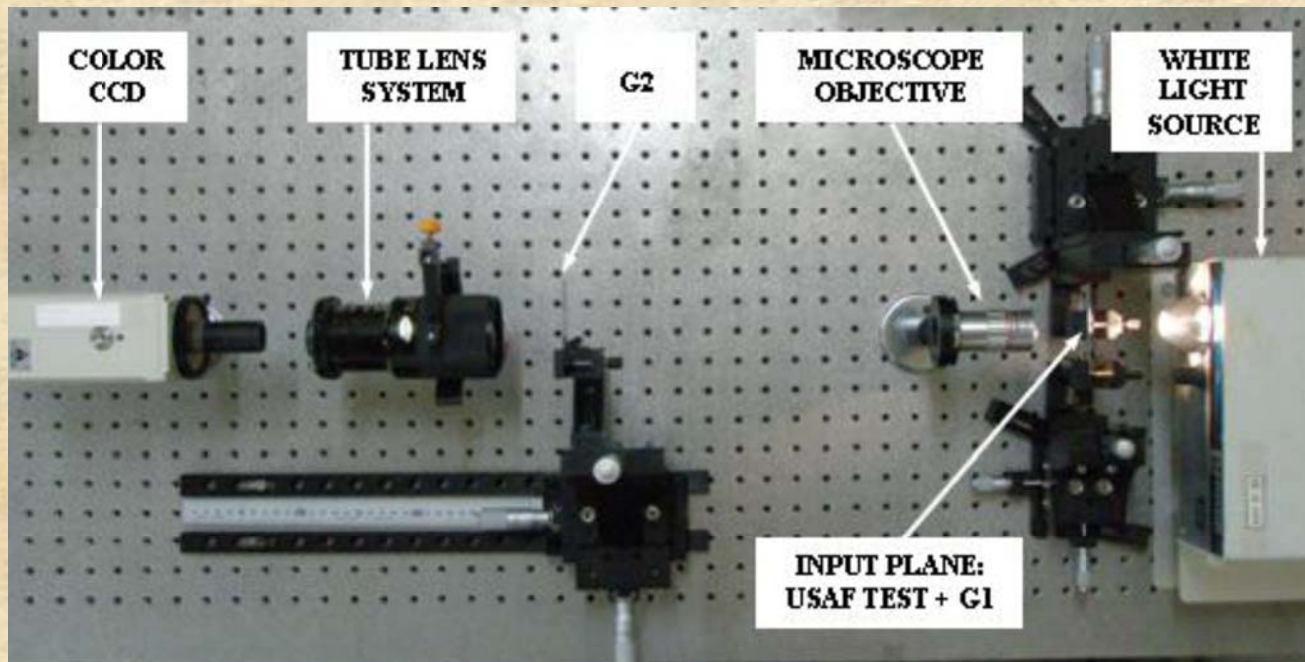
(c)



(d)

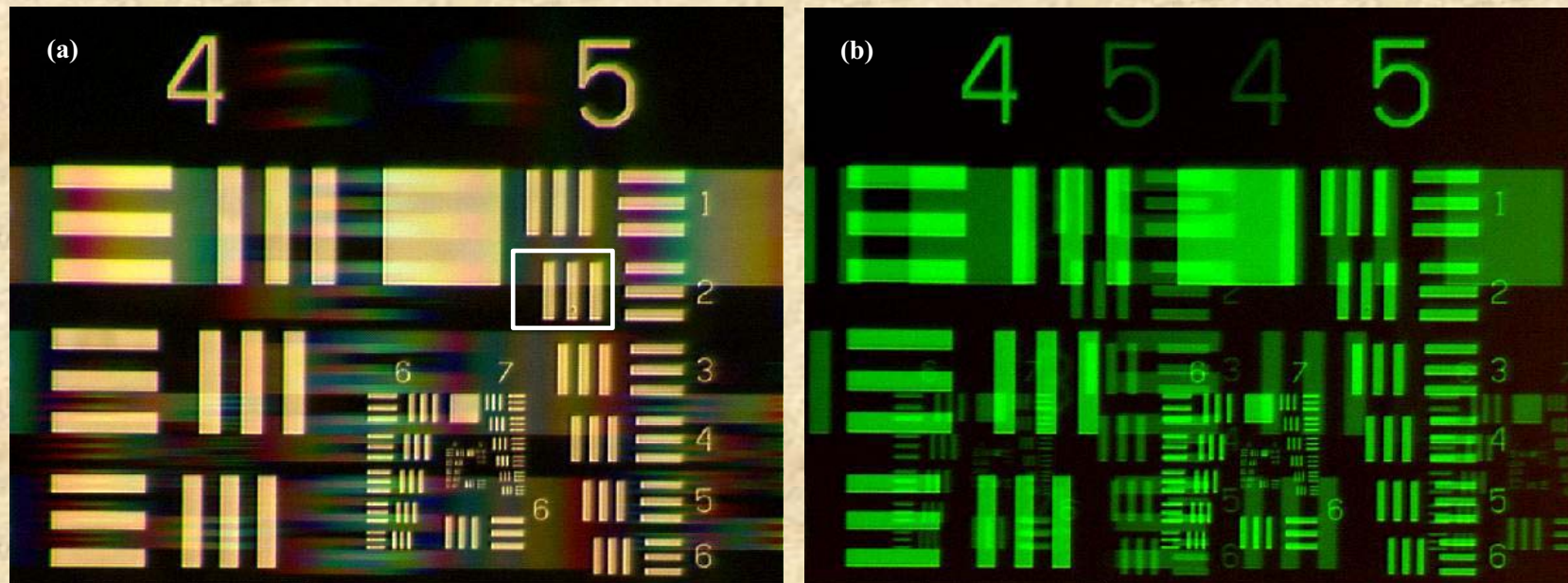
Super Resolution

White light experiments



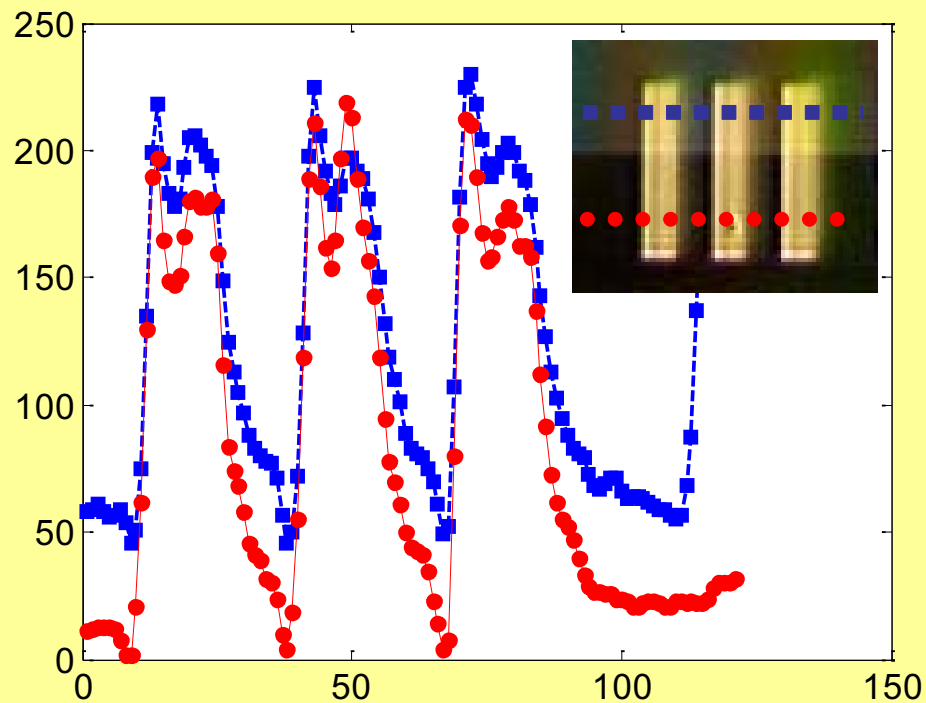
- G1 and G2 have periods of $p_1=600$ lp/mm and $p_2=80$ lp/mm.
- Mitutoyo microscope lens with 0.14NA .
- White light source: halogen lamp.

White light experiments- cont.



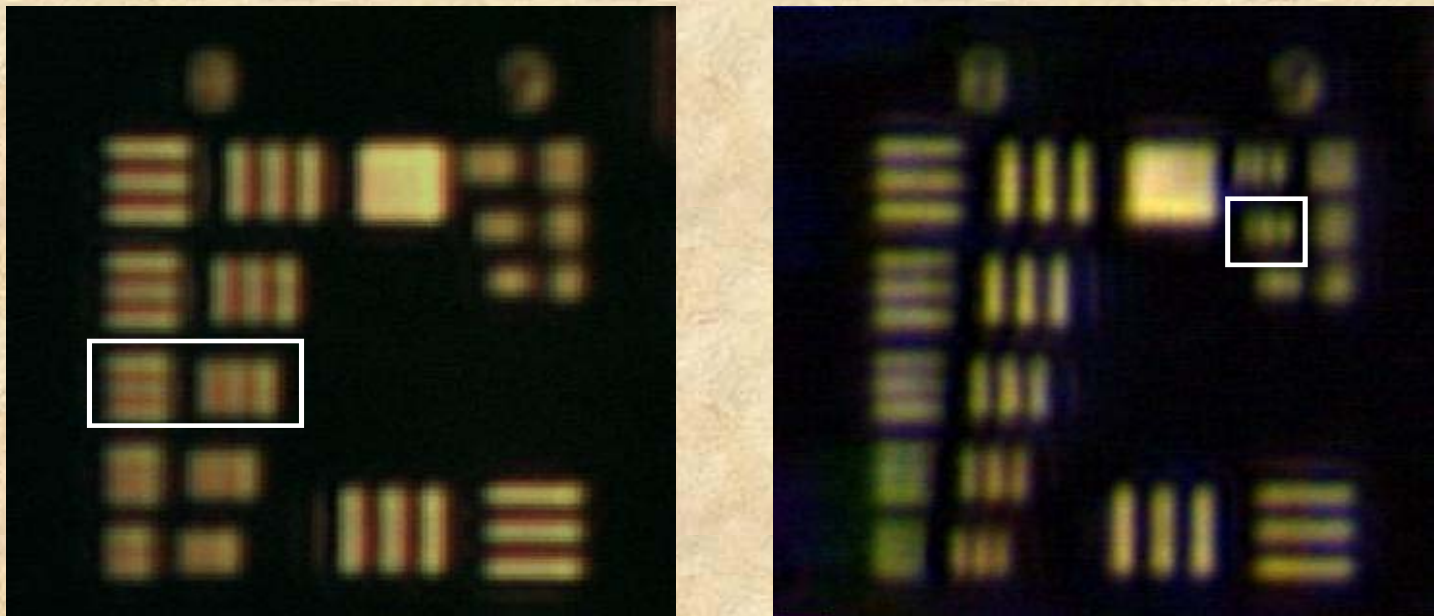
(a) The full field of view super resolved image obtained using the presented approach, and (b) The full field of view image with monochromatic illumination (Bachl and Lukosz approach).

White light experiments- cont.

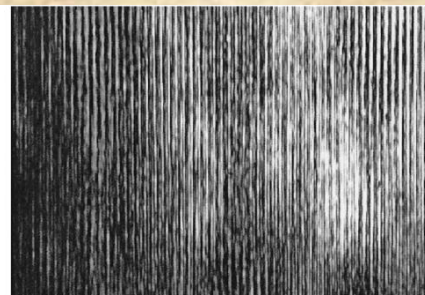
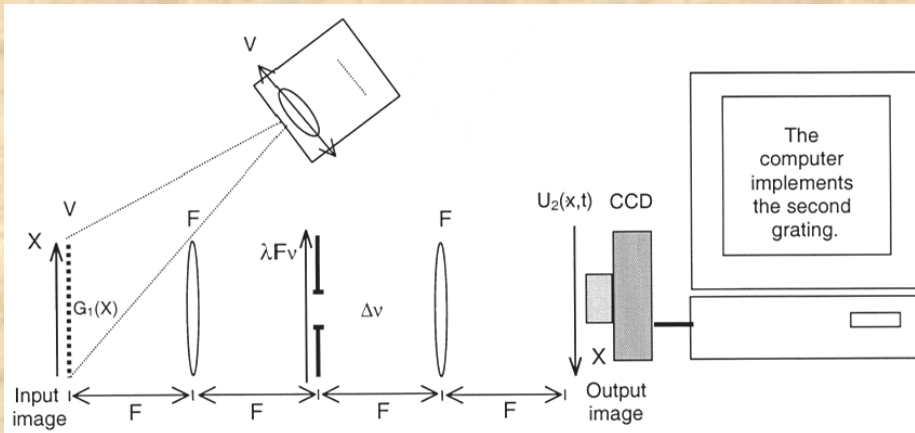


Cross section of Fig. 4(a) for purpose of computing the reduction in contrast.

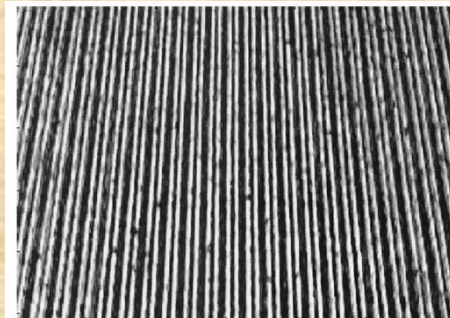
White light experiments- cont.



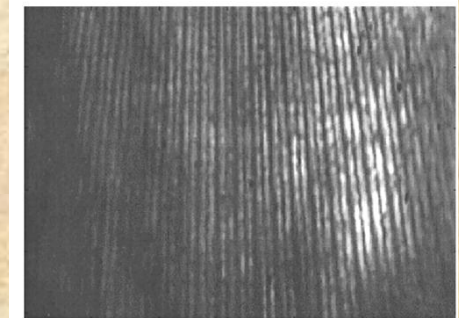
Experimental results showing the high resolution region of interest. The reference image is obtained (a) without the gratings, and (b) with the gratings installed and using the presented super-resolution approach. White squares mark the resolution limit.



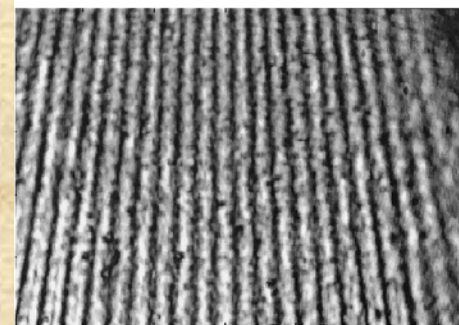
Projected grating



Open aperture

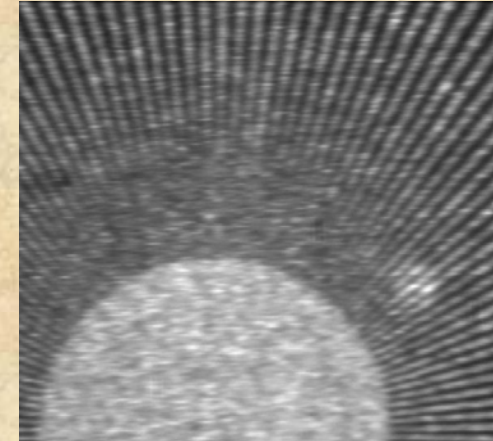
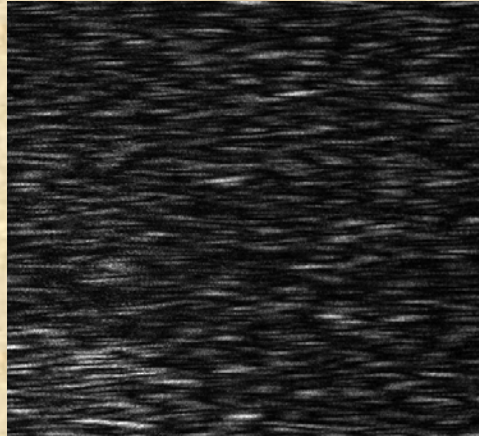


Reconstruction

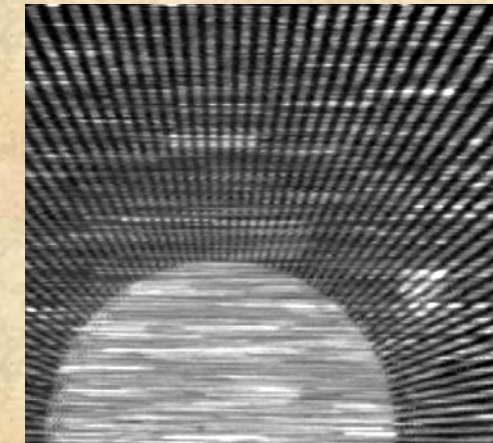
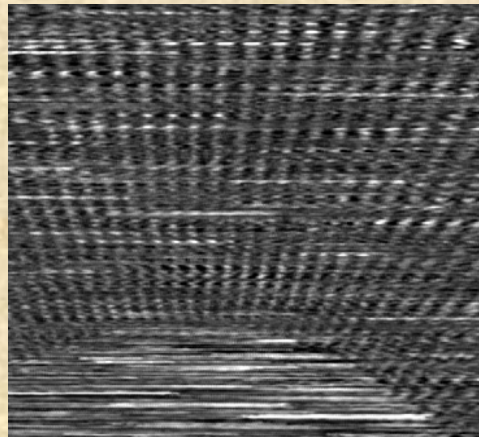


Closed aperture

Closed aperture

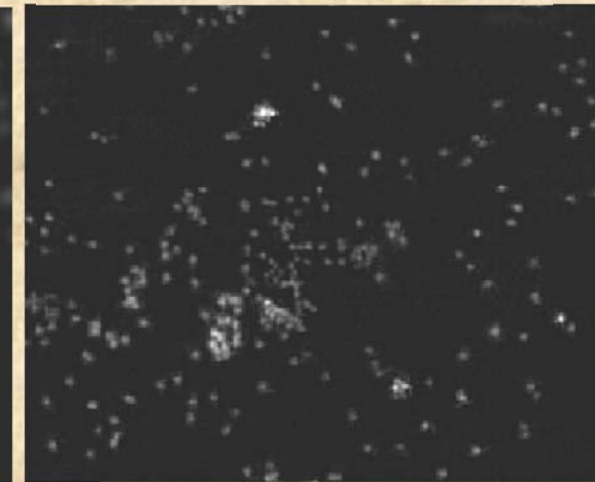
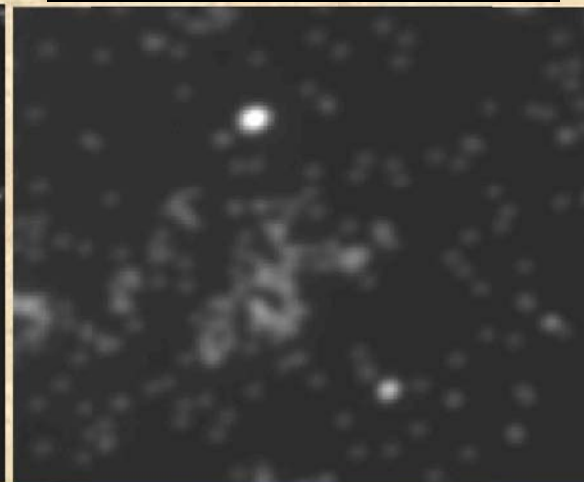
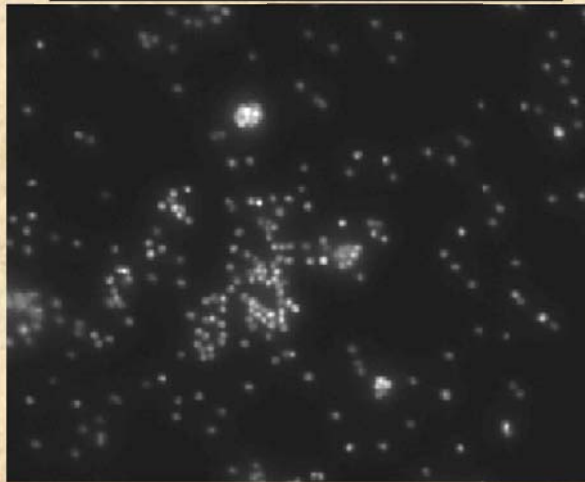
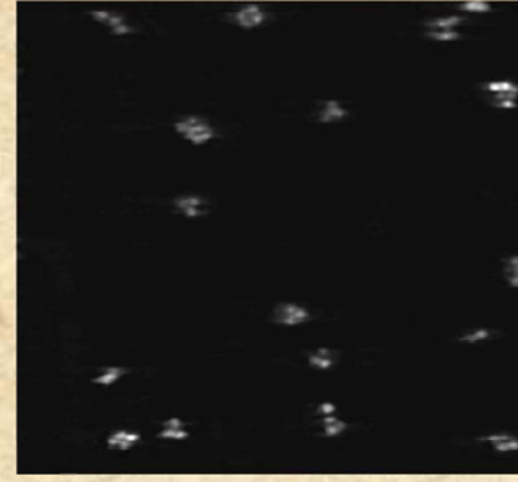
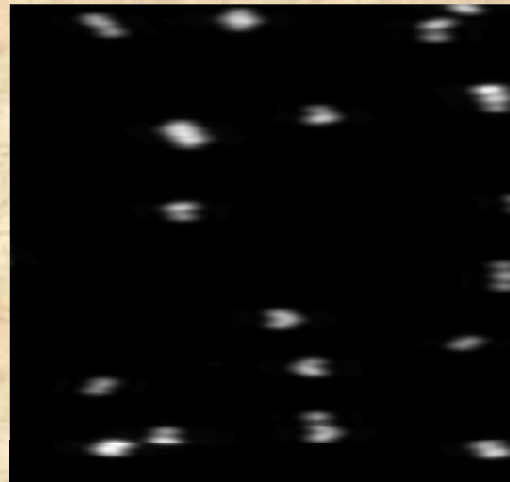


Reconstruction



Coherent

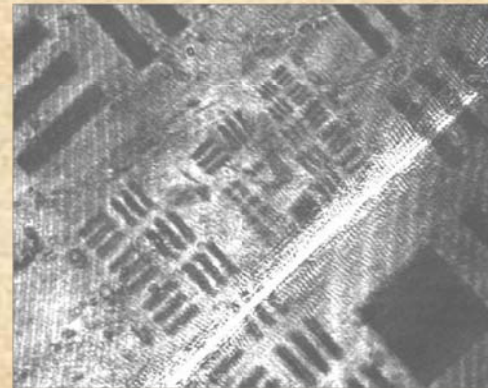
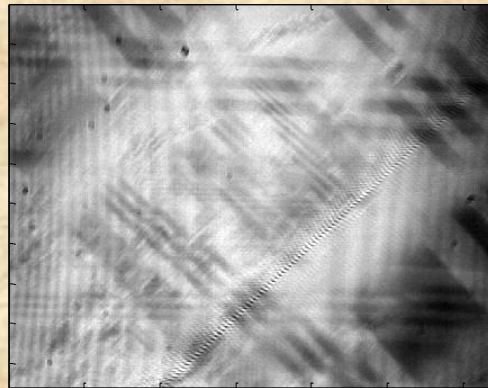
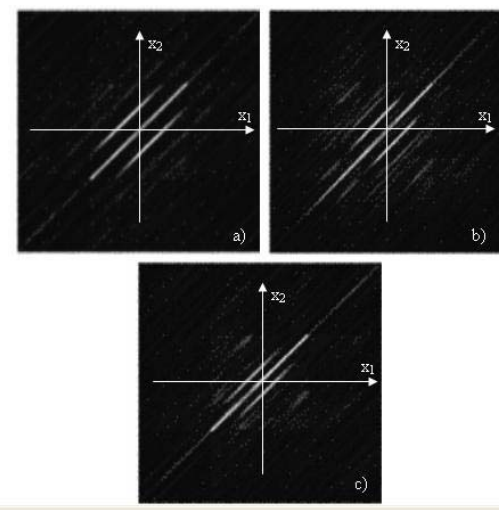
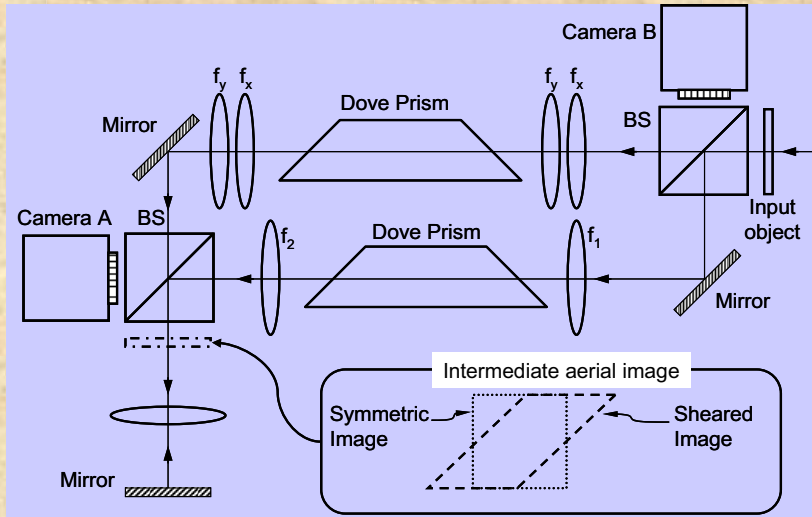
Incoherent



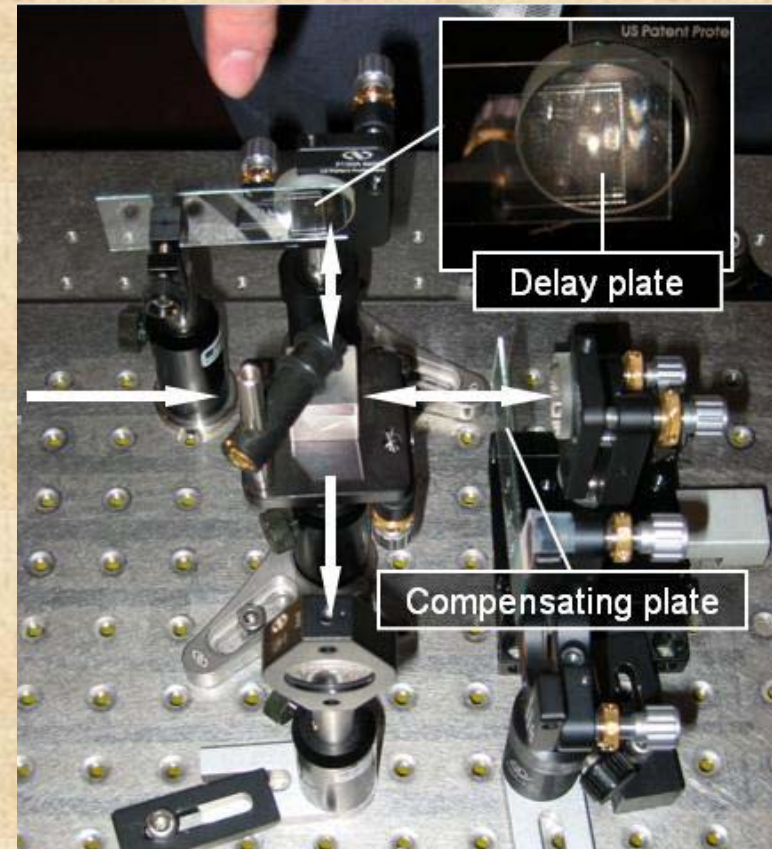
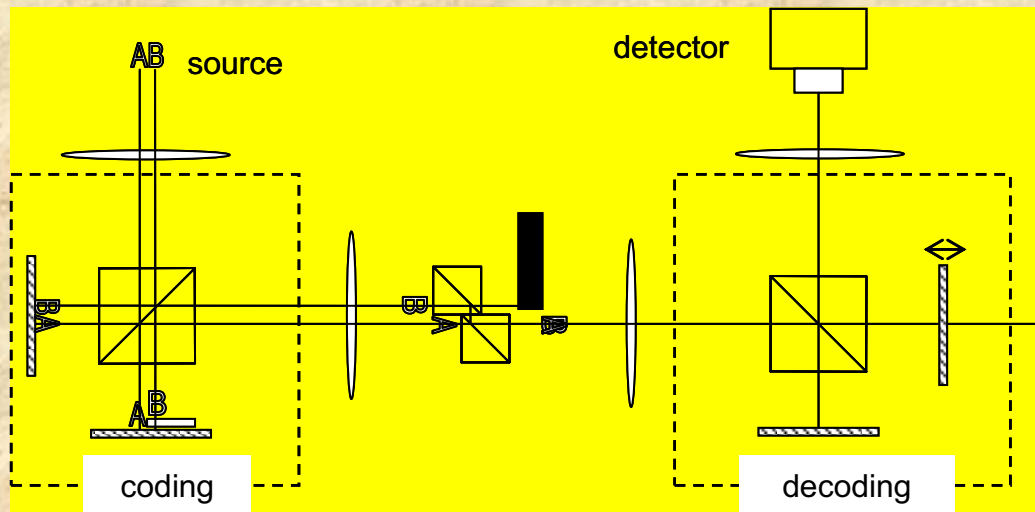
Open aperture

Closed aperture

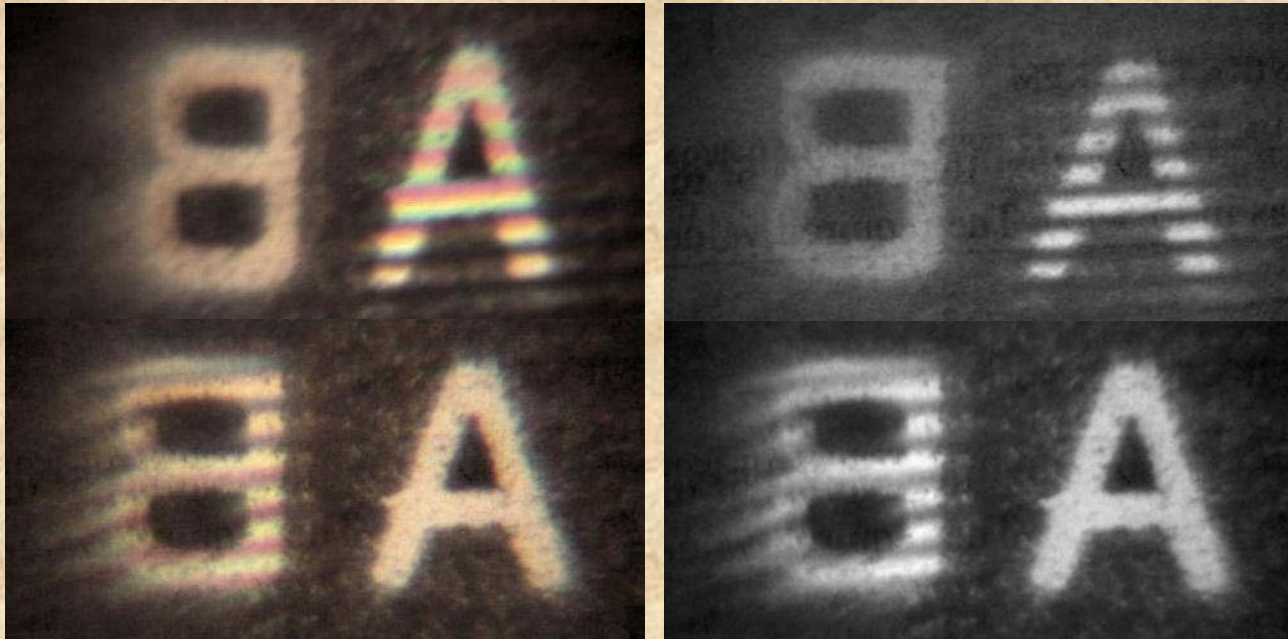
Reconstruction



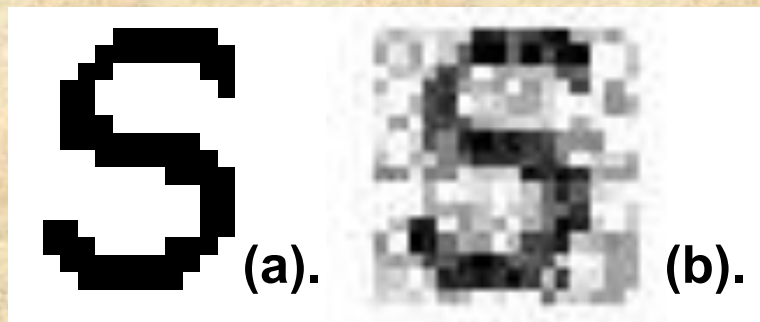
Diff. SR- Axial Coherence Coding



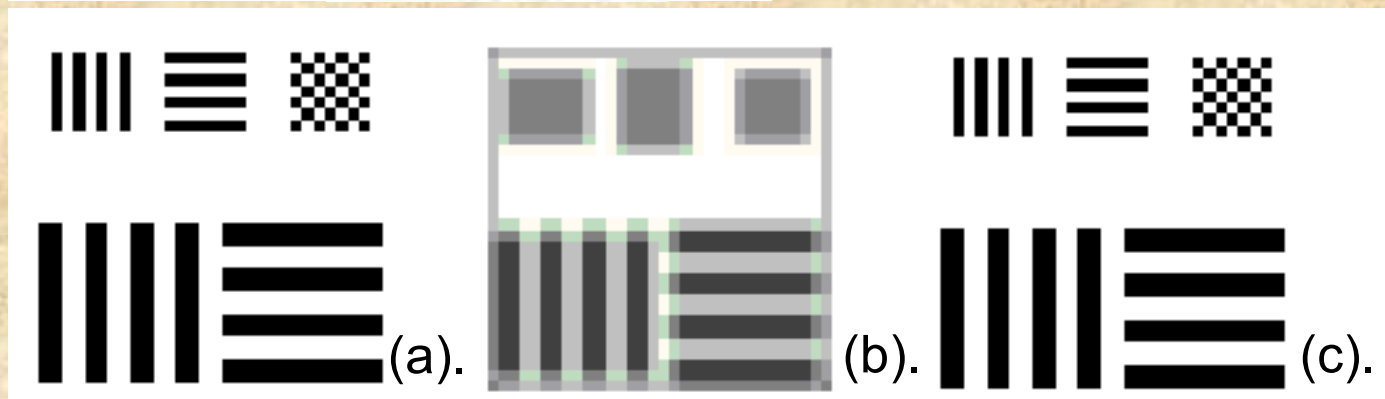
Diff. SR- Axial Coherence Coding



Numerical Simulations- I

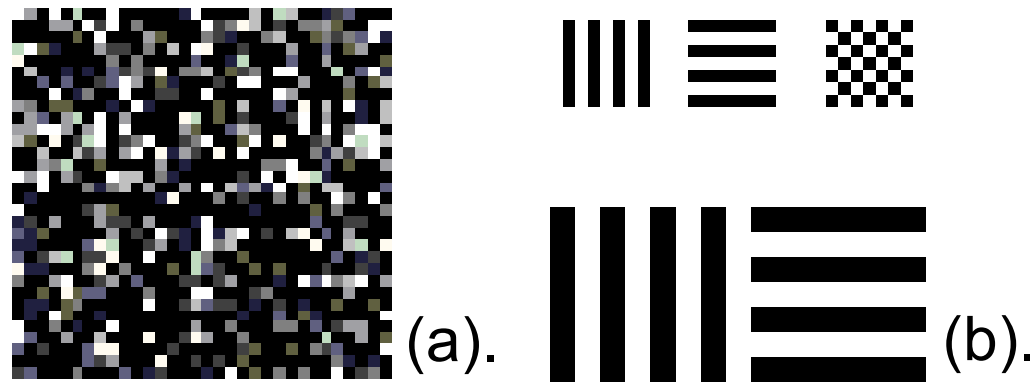


Single pixel transmission:
(a). The original object.
(b). The obtained reconstruction.



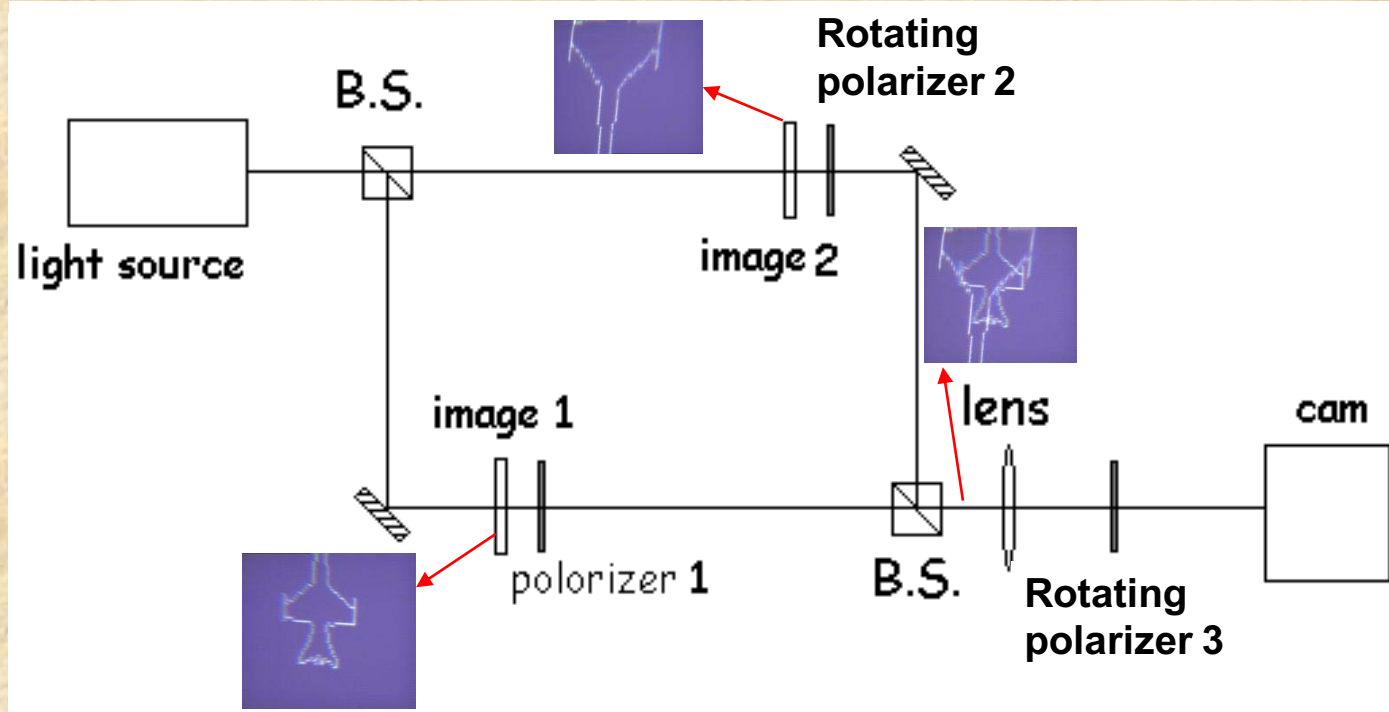
Blurred image reconstruction: (a). The original object. (b). The low resolution transmitted 2-D information. (c). The obtained reconstruction.

Numerical Simulations- II



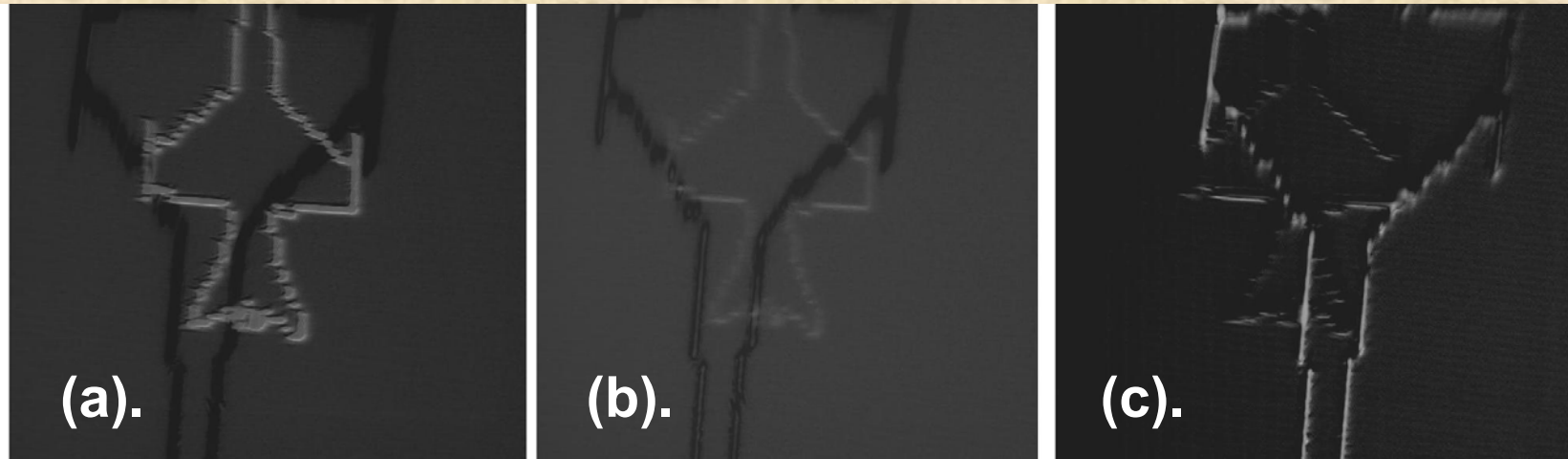
The effect of noise: (a). The blurred image of previous figure after the addition of zero mean white Gaussian noise with two sigma equal to 1. (b). The obtained reconstruction.

Experimental setup- I



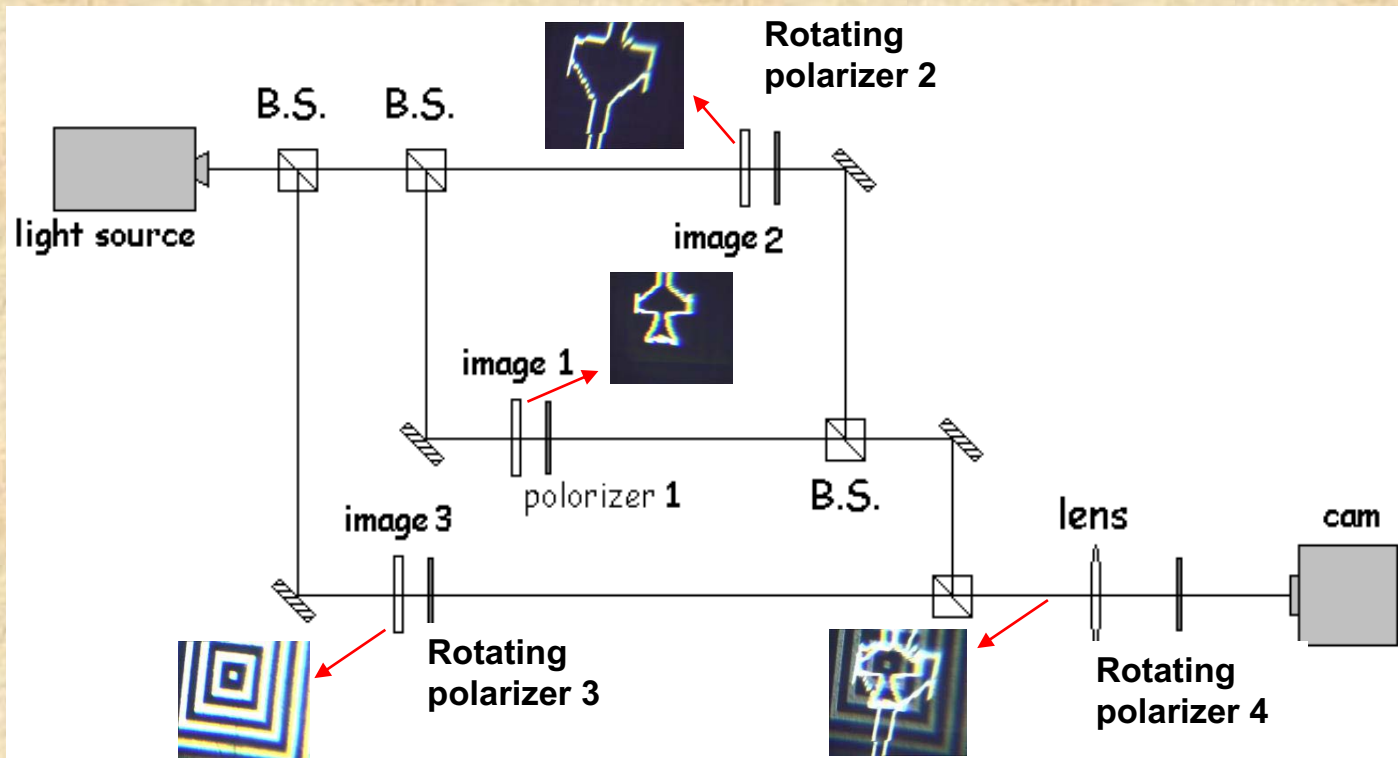
The experimental setup with two regions coding.

Experimental results- I



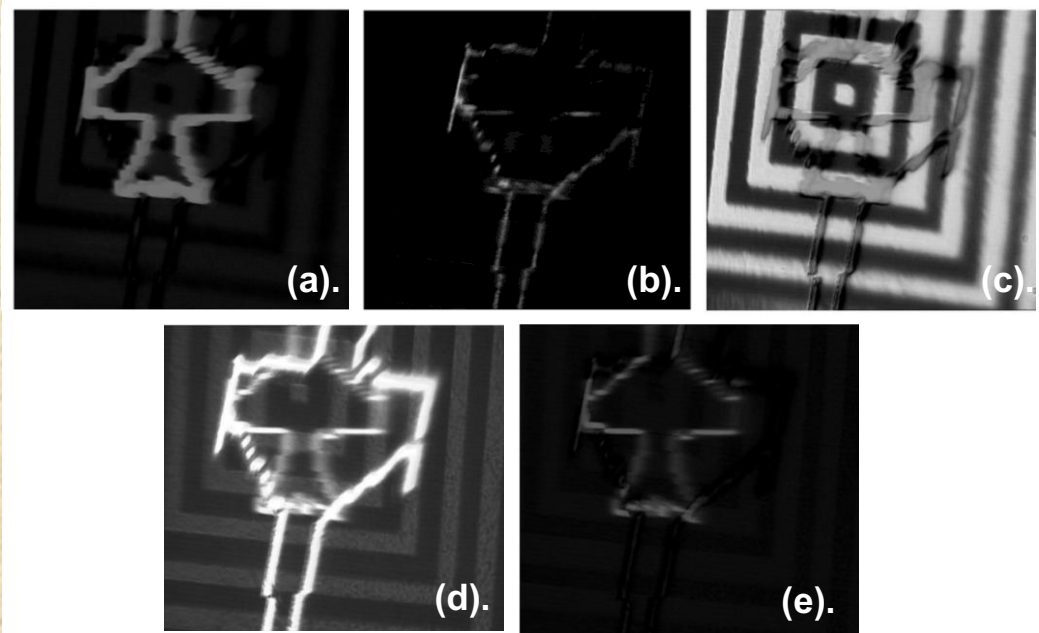
Experimental results. (a). Reconstruction of image from branch 1.
(b). Reconstruction of image from branch 1 even when it is 5 times more attenuated than the original image of branch 2. (c). Reconstruction of image from branch 2.

Experimental setup- II



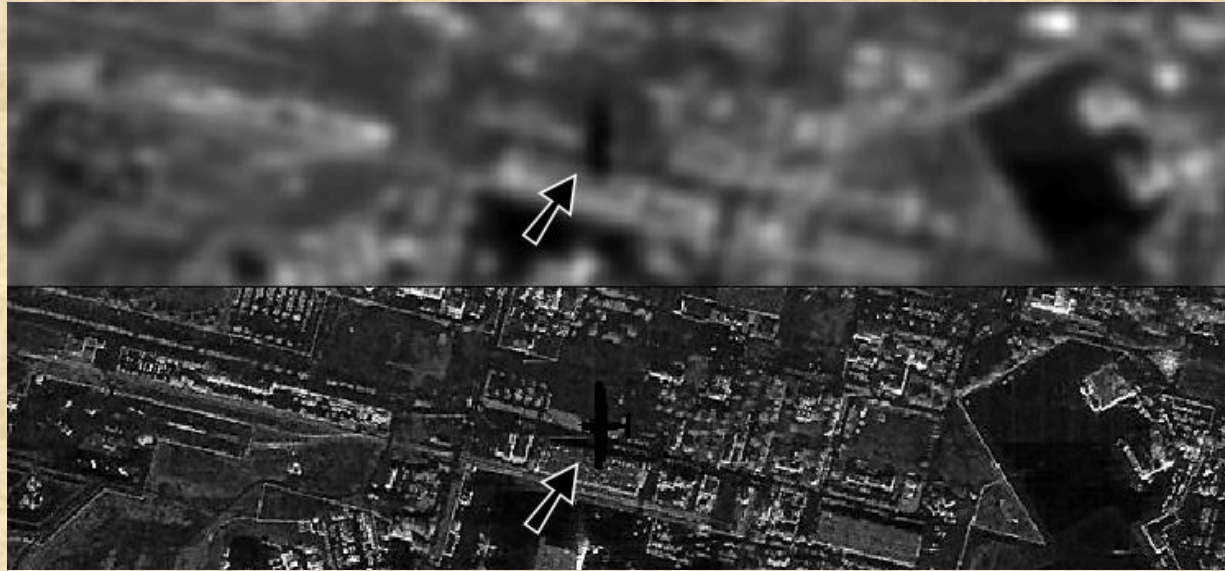
The experimental setup with three regions coding.

Experimental results- II

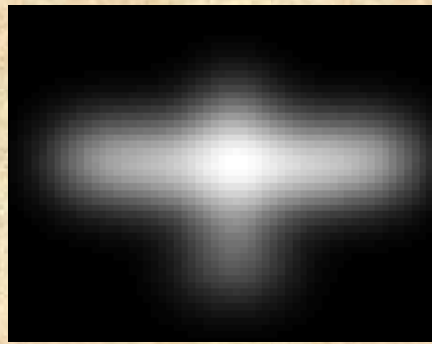


Experimental results. (a). Reconstruction of image from branch 1. (b). Reconstruction of image from branch 2. (c). Reconstruction of image from branch 3. (d). The case when the input image from branch 2 is four times stronger than the rest of the images. (e). The reconstruction of image from branch 1 for in the input case of figure (d).

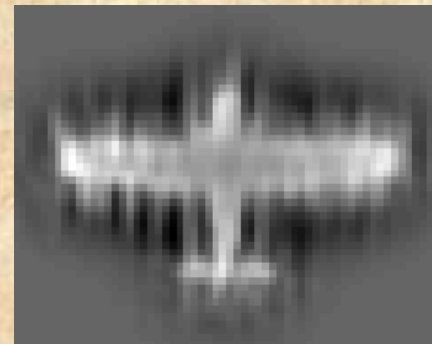
Remote Diff. SR- via Background



Open aperture



Closed aperture



Reconstruction

***Remote Diff. SR- via background,
cont.***



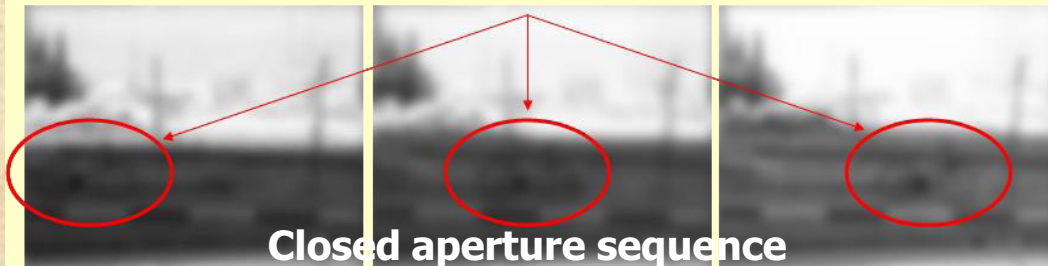
Super resolved moving target

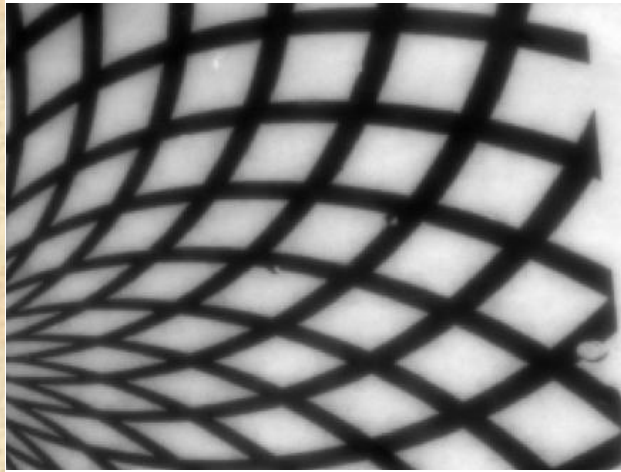


Closed aperture

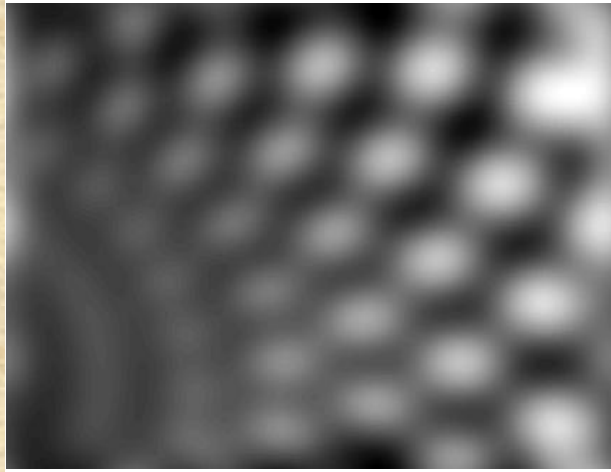
Reconstruction

Low resolution sequence of moving target

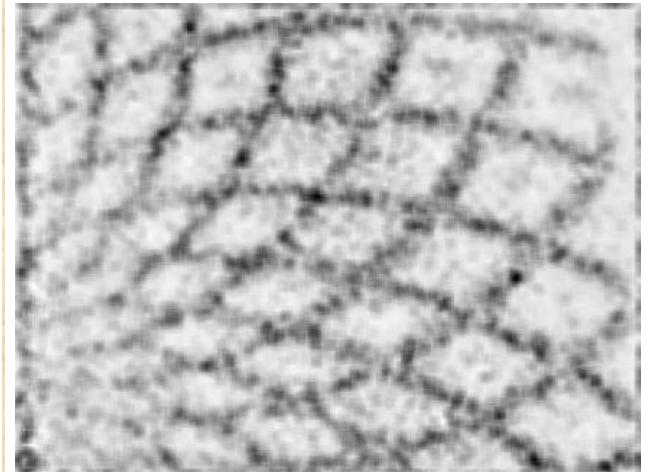




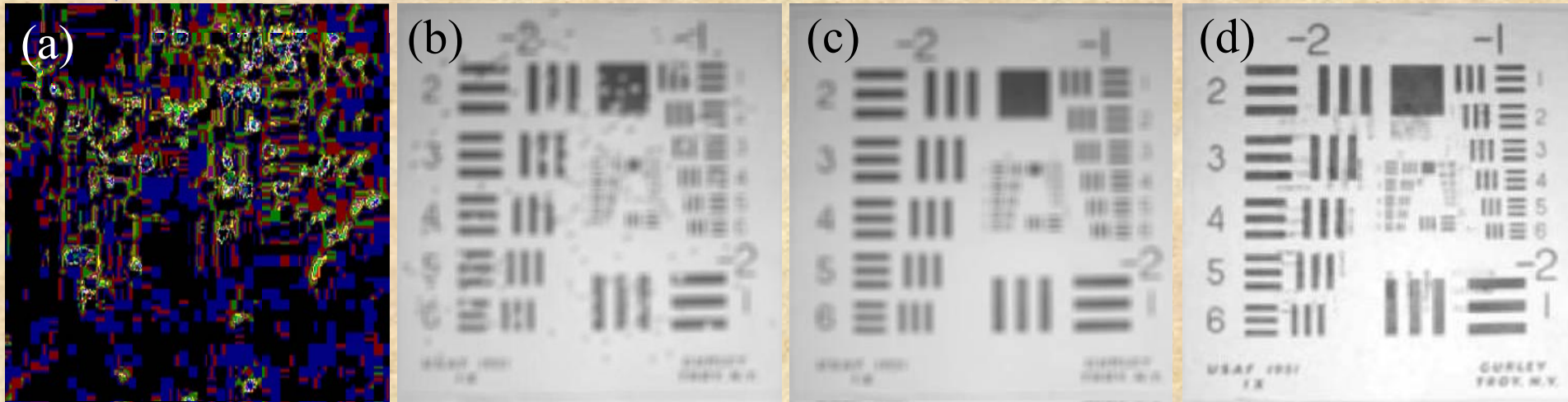
Open aperture



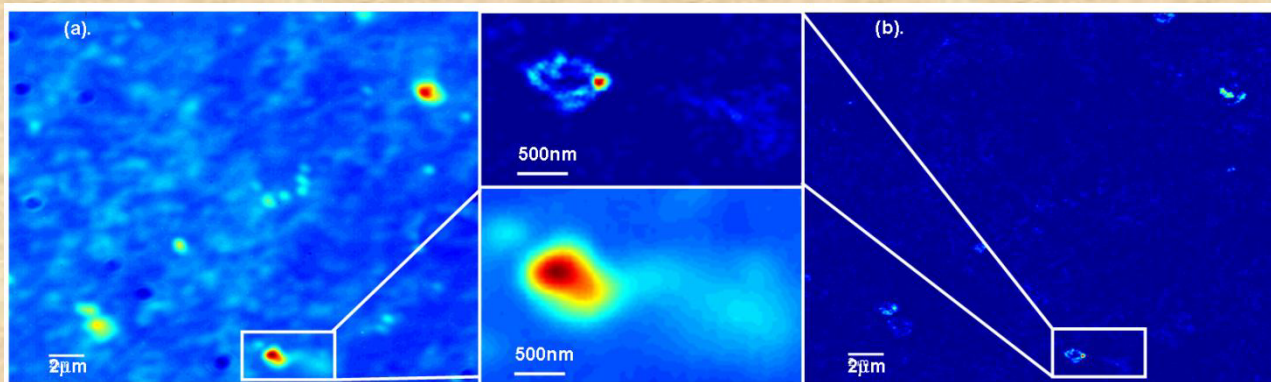
Closed aperture

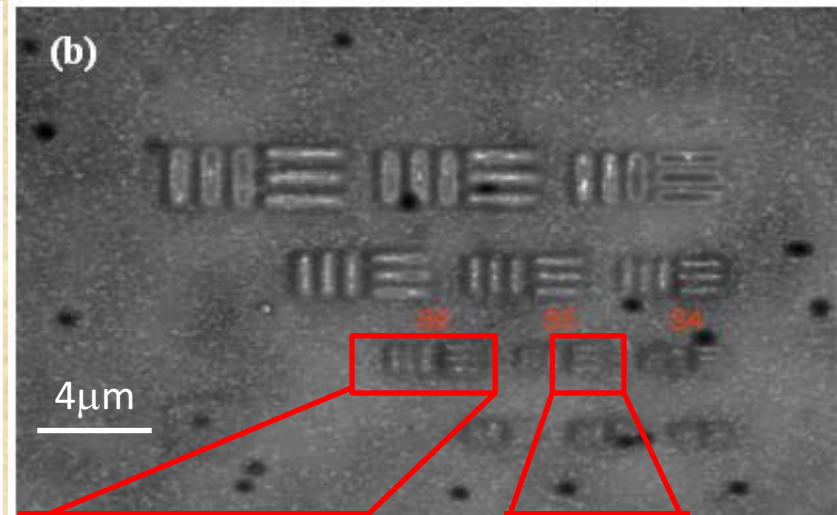
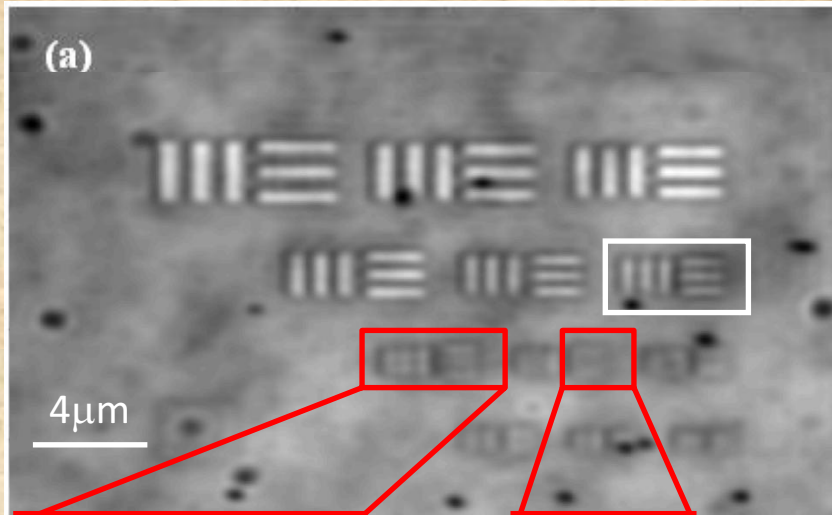


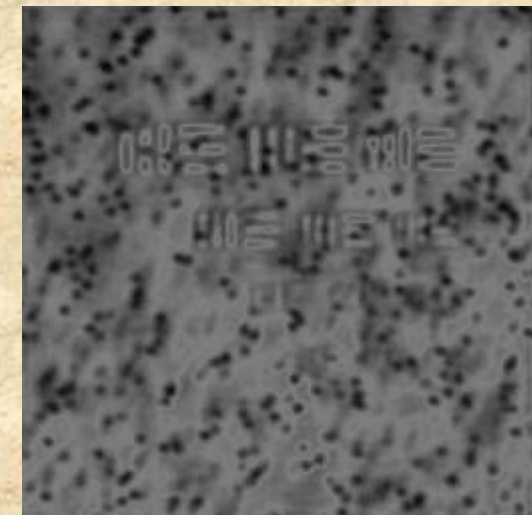
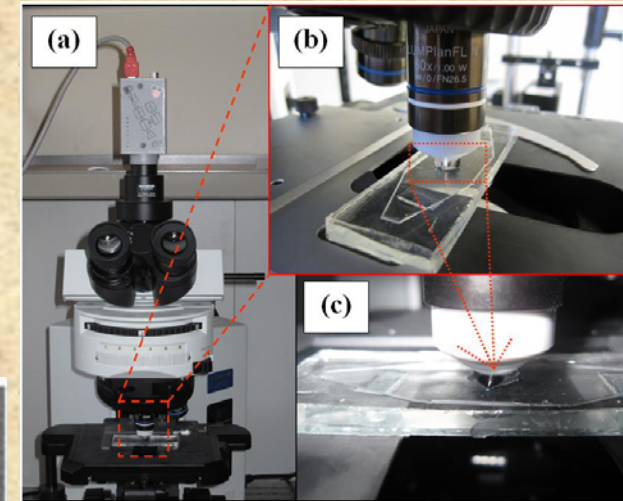
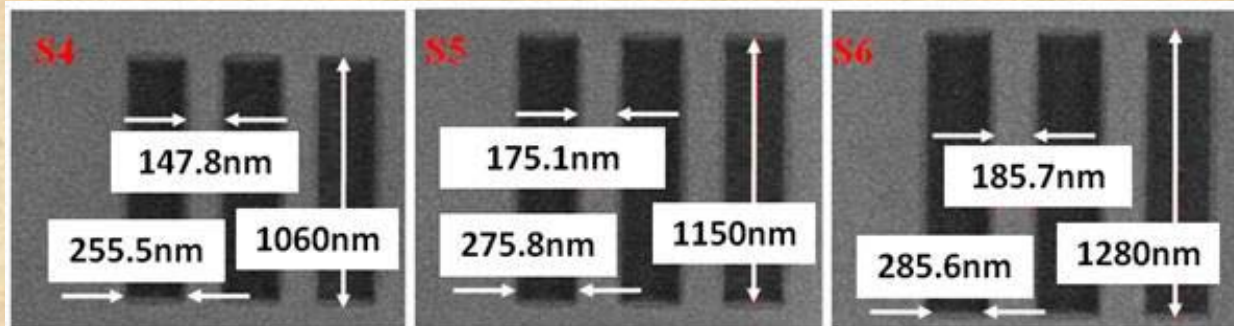
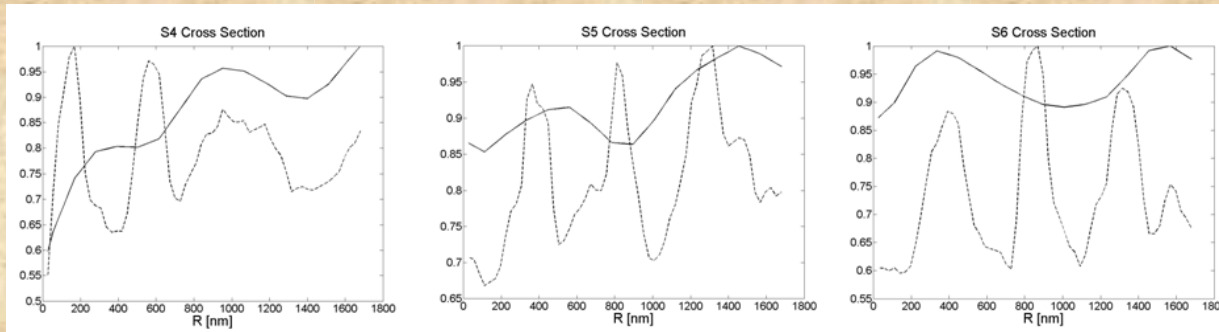
Reconstruction



Experimental results. (a) Low resolution image of only the particles. (b) One low resolution USAF image out of the sequence captured by the camera (with particles). (c) Low resolution image captured by the camera (without particles). (d) The super resolved reconstruction.







Remote Diff. SR- via turbulence¹

a).

Bar Ilan University
School of engineering
Graduates students 2006/2007

d).



b).

Bar Ilan University
School of engineering
Graduates students 2006/2007

e).

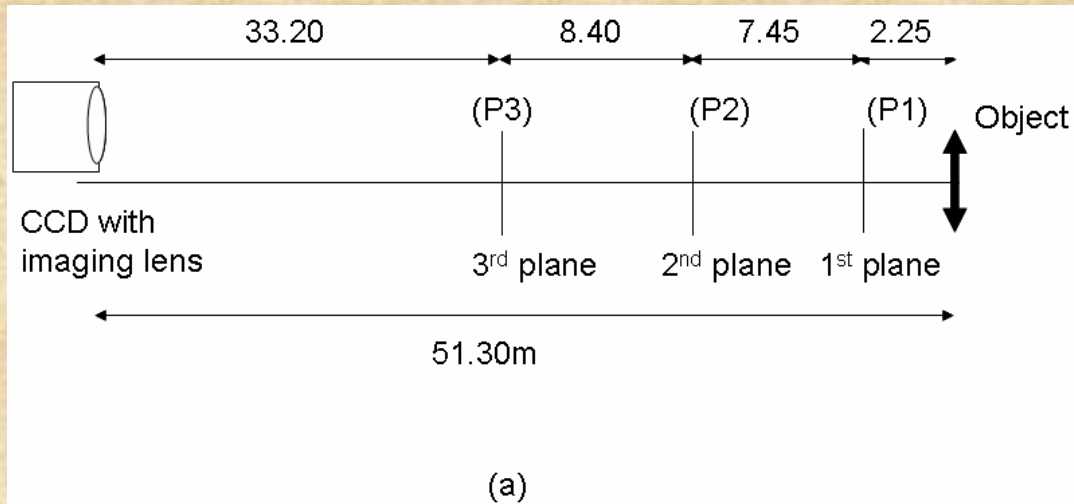
Bar Ilan University
School of engineering
Graduates students 2006/2007

c).

Bar Ilan University
School of engineering
Graduates students 2006/2007

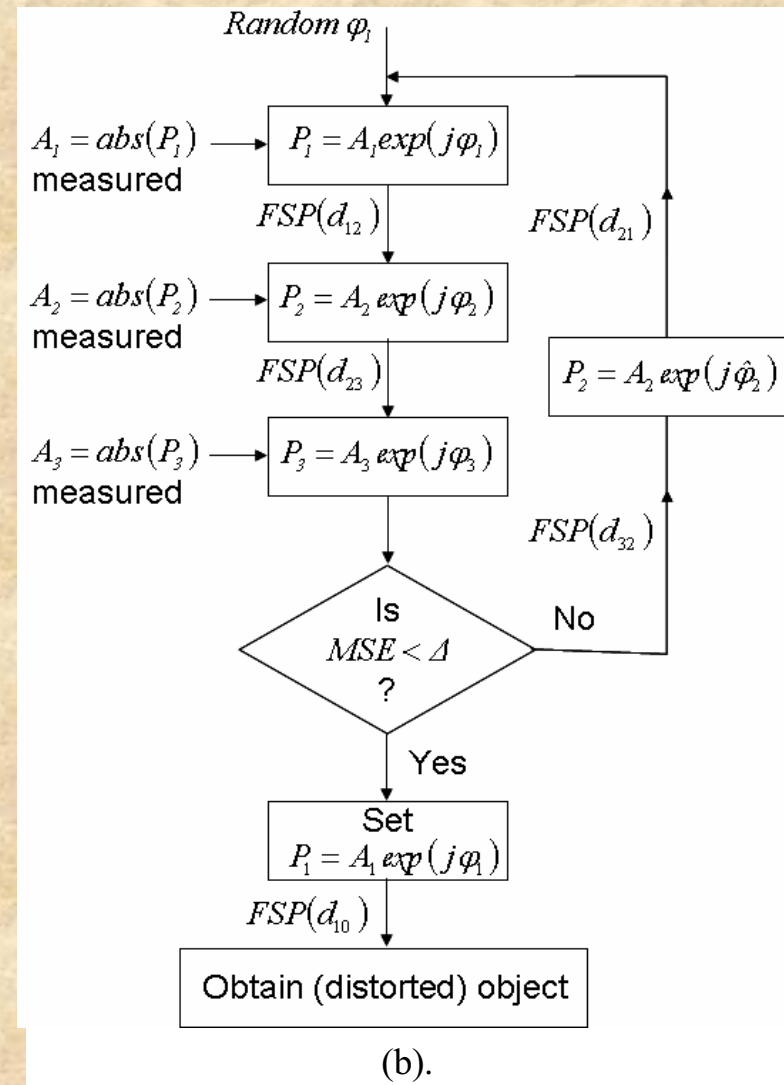
- a). **Open aperture**
- b).-c). **Regular imaging sequence**
- d). **The turbulence**
- e). **SR reconstruction**

Experiments



(a). The experimental setup.

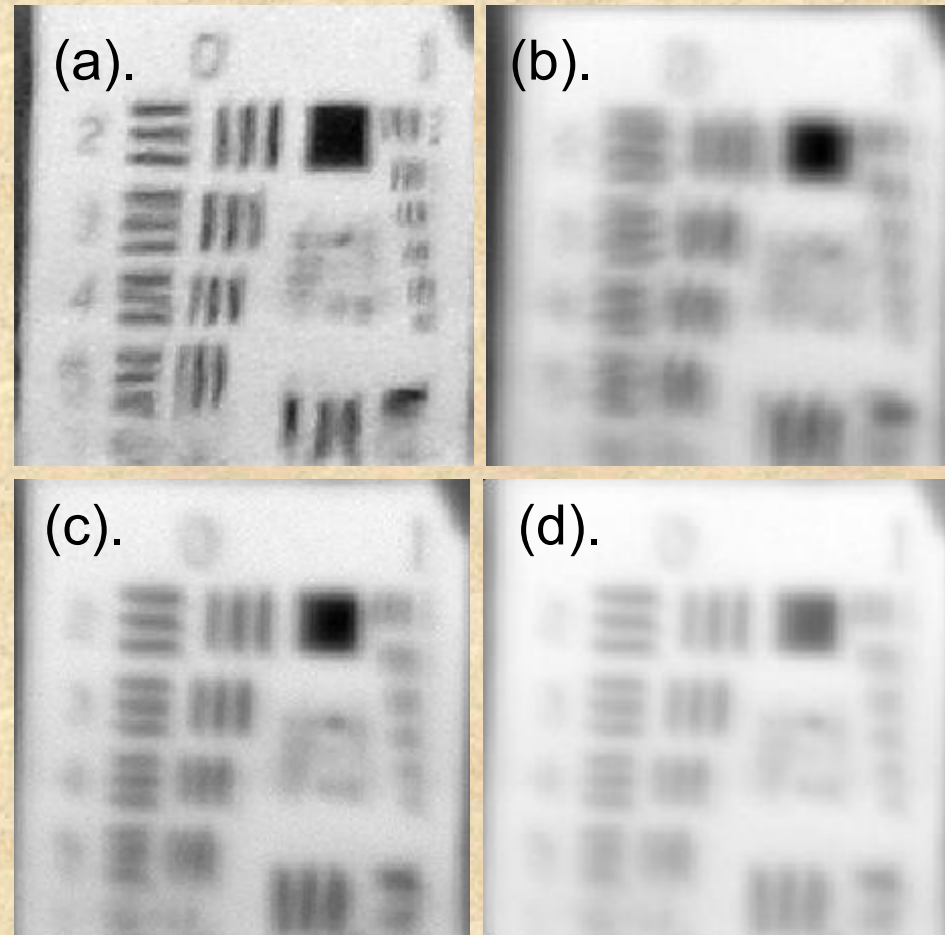
(b). Schematic sketch of the proposed iterative image reconstruction algorithm.



Remote Diff. SR- via turbulence2

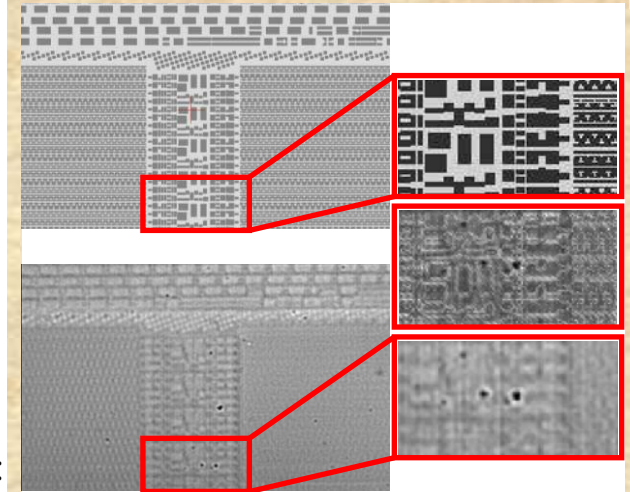
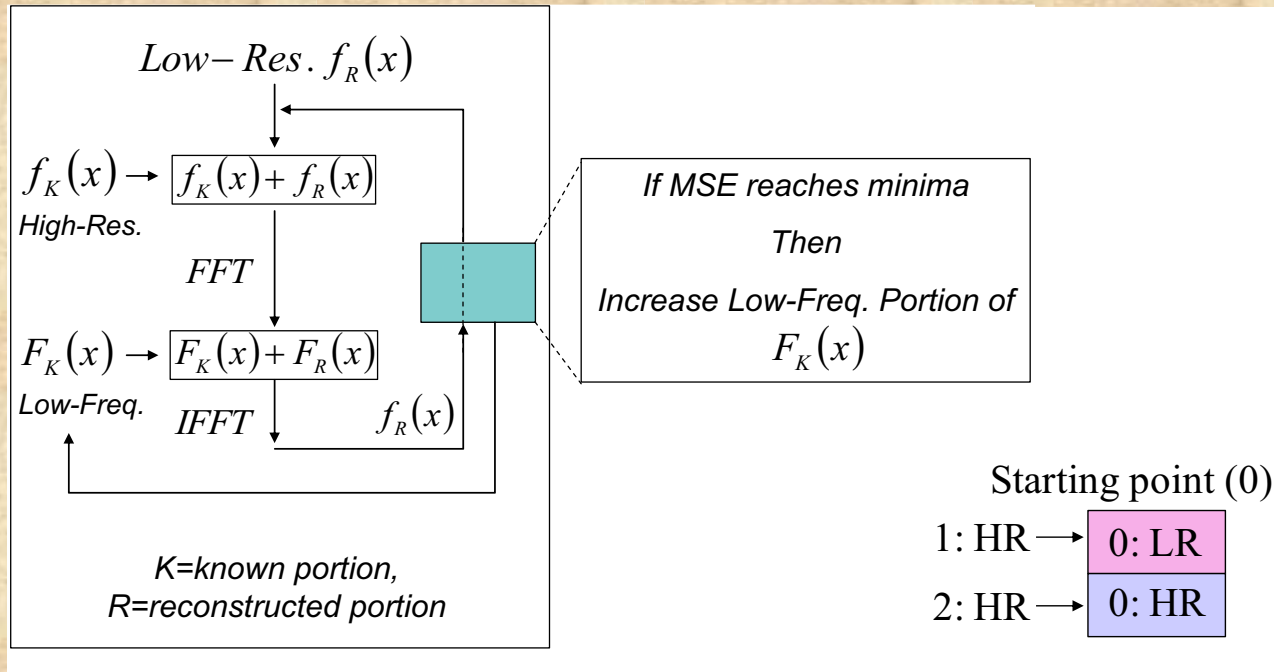


An example of one captured image. The resolution target is positioned at the center of the image.

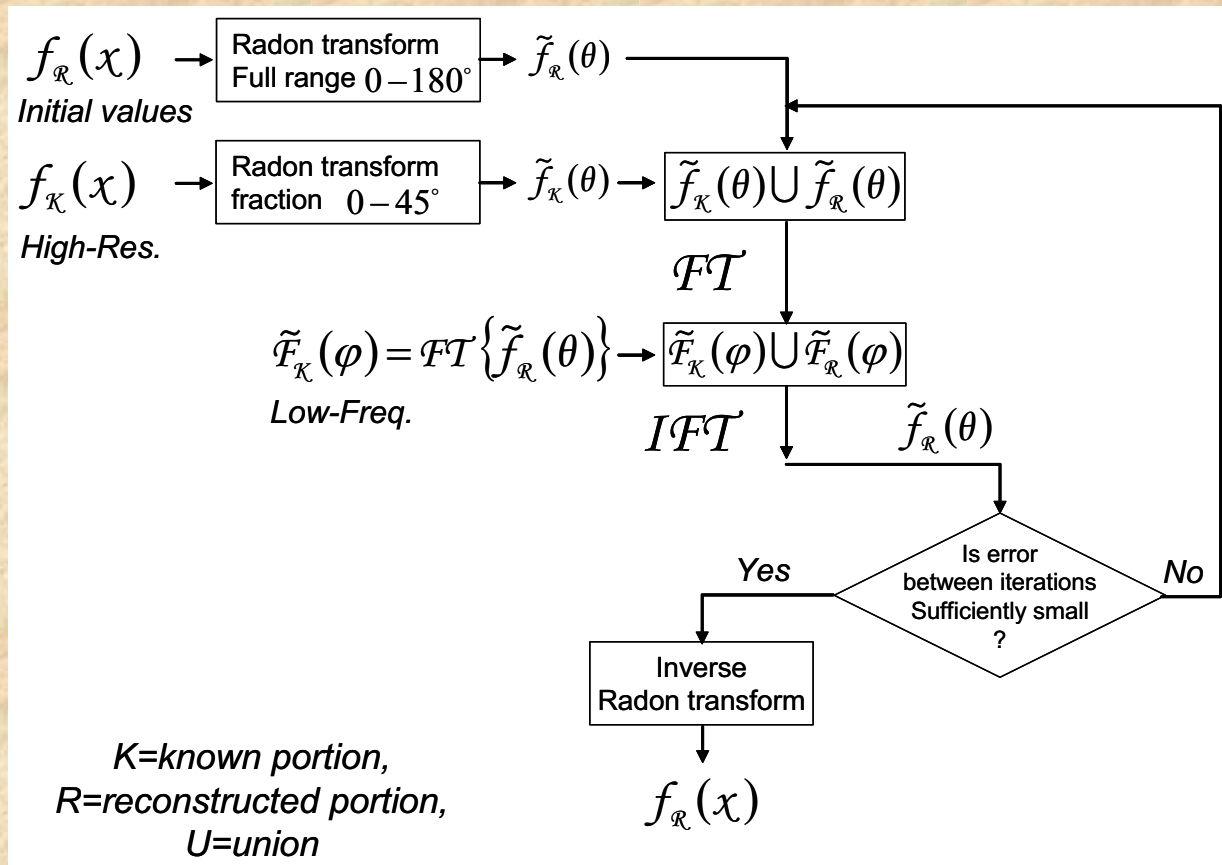


(a). High resolution image captured at short exposure (reduced turbulence distortion).
(b). Image blurred due to turbulence (long exposure). (c). Reconstructed image. (d).
Enhanced reconstruction with post filtering.

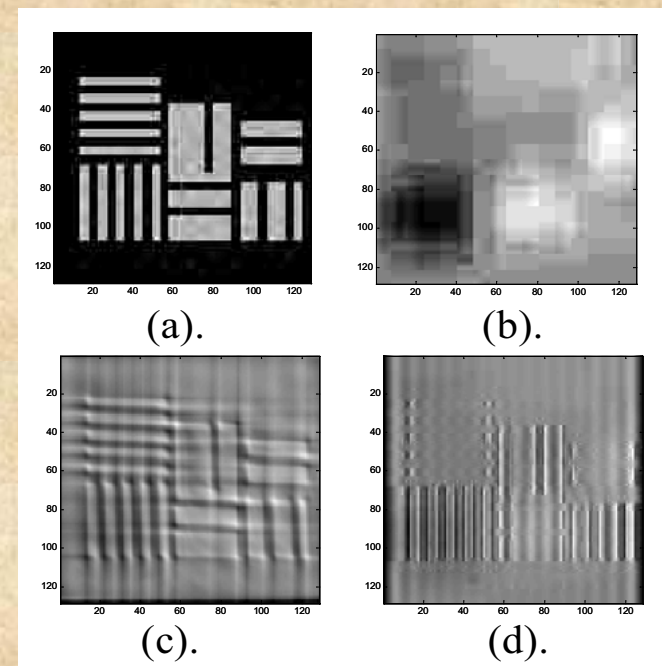
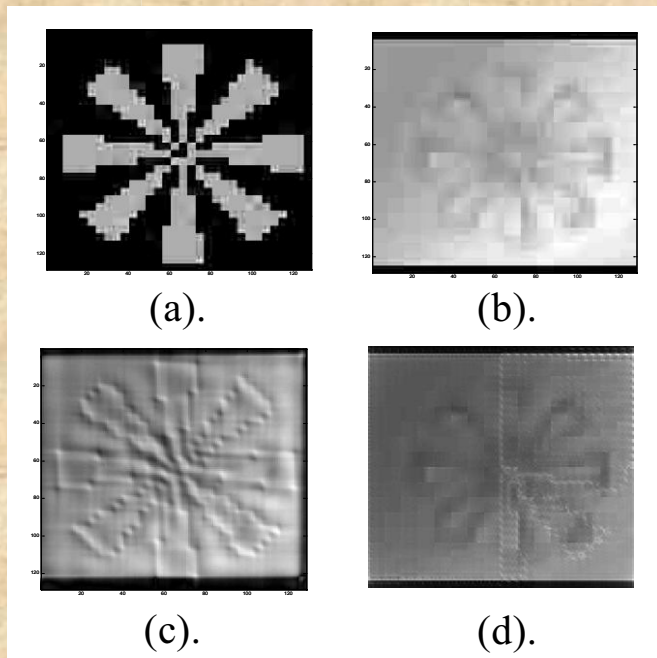
Digital SR for failure analysis of ULSI chips- 1



The layout and the experimentally acquired image with solid immersion lens from 45nm process, showing the resolution limit. On the right zoomed-in parts we present also the image obtained using the proposed algorithm (in the middle).



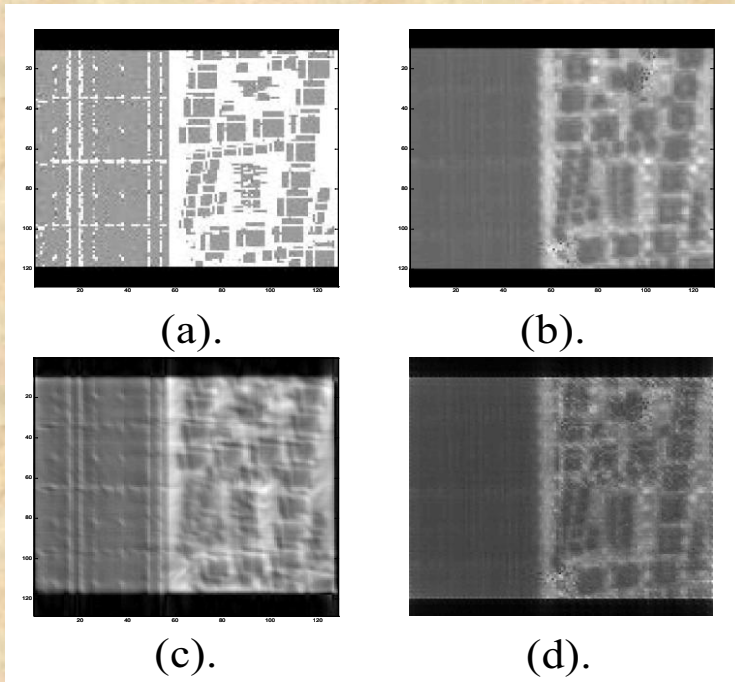
$$R(r, \theta)\{f(x, y)\} = \int_{-\infty}^{\infty} \int_{-\infty}^{\infty} f(x, y) \delta(r - x \cos \theta - y \sin \theta) dx dy$$



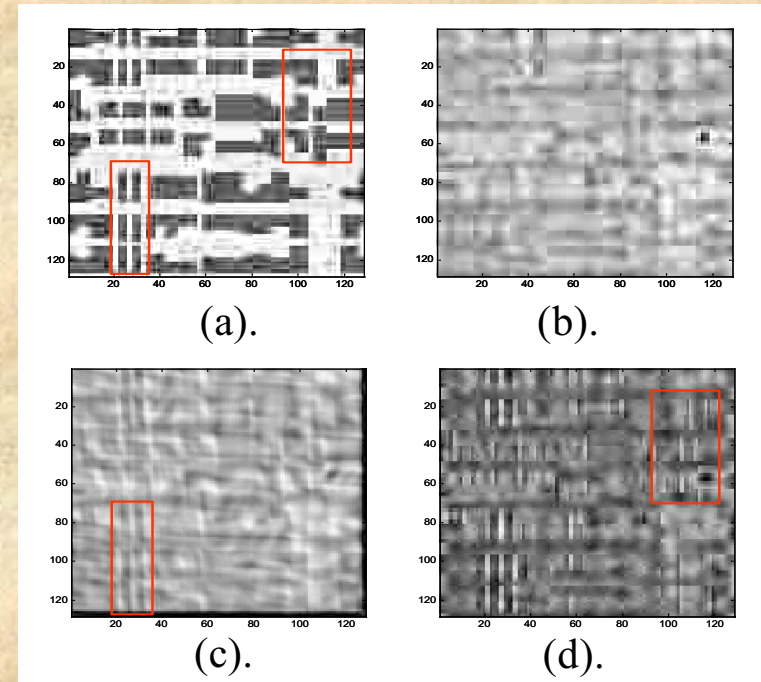
(a). High resolution reference layout image of a resolution target. (b). Experimentally imaged object (right side) captured by infra red microscope (LSM). (c). The result obtained after applying Radon-based super resolving algorithm (93.6% correlation with (a)). (d). The result obtained after applying dynamic Gerchberg-Papoulis algorithm (53.1% correlation with (a)).

(a). High resolution reference layout image of a resolution target. (b). Experimentally imaged object captured by infra red microscope (LSM). (c). The result obtained after applying Radon-based super resolving algorithm (91.7% correlation with (a)). (d). The result obtained after applying the Gerchberg-Papoulis algorithm (41.3% correlation with (a)).

Digital SR for 45nm micro-electronics process

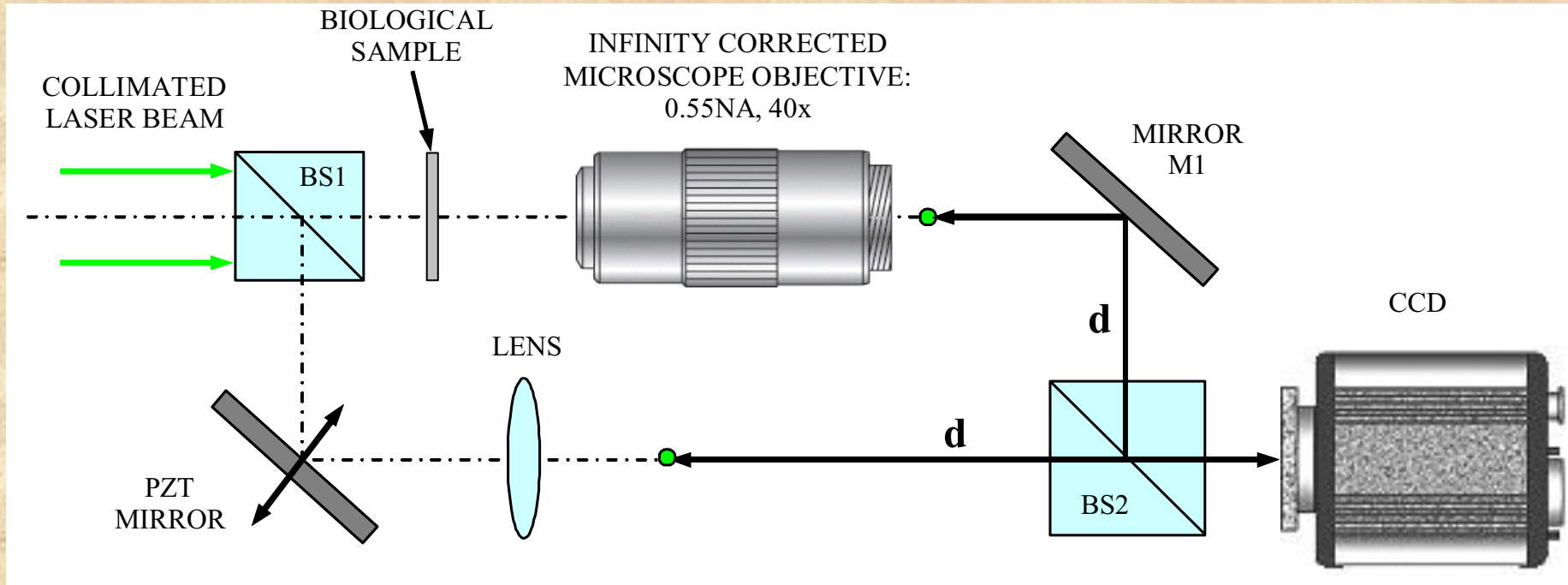


(a). The layout image of a 45nm process chip. (b). The experimentally acquired image with solid immersion lens, showing the resolution limit. (c). The image obtained after applying the Radon-based image processing approach (99.8% correlation with (a)). (d). The result obtained after applying dynamic Gerchberg-Papoulis algorithm (95.8% correlation with (a)).

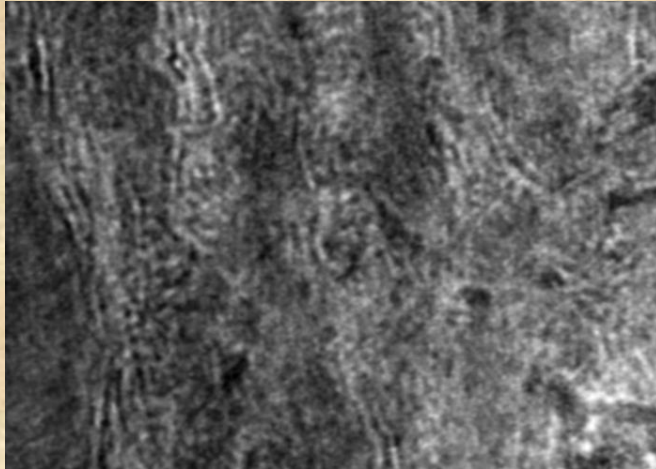


Layout with only active diffusion. (a). The layout image of a 45nm process chip. (b). The experimentally acquired image with solid immersion lens, showing the resolution limit. (c). The result obtained after applying Radon-based super resolving algorithm (99.8% correlation with (a)). (d). The result obtained after applying dynamic Gerchberg-Papoulis algorithm (92.6% correlation with (a)).

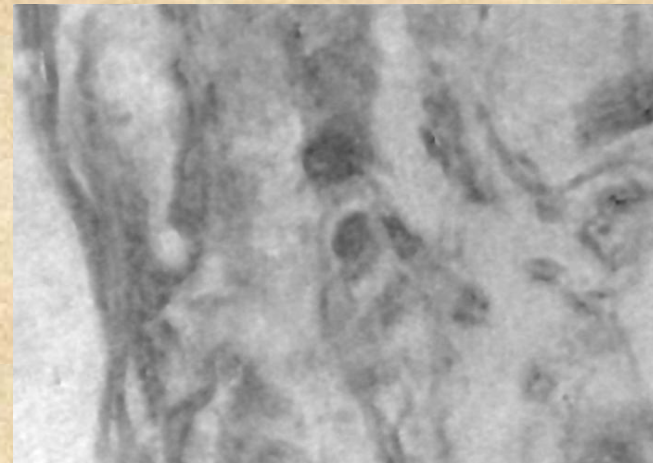
Phase Shifting and Axial Super Resolution



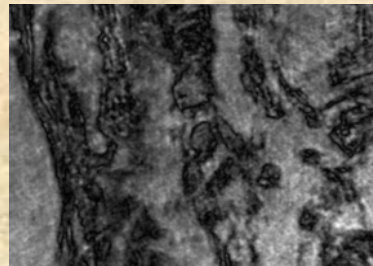
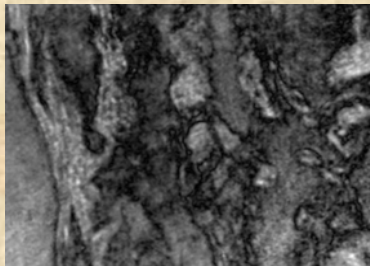
Experimental setup



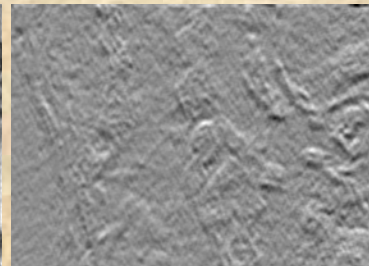
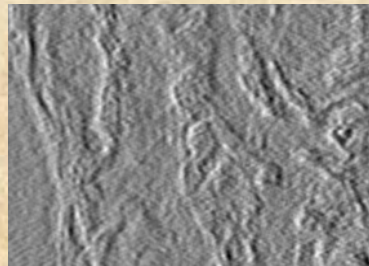
Amplitude



Extracted phase



Phase contrast for π and $\pi/2$

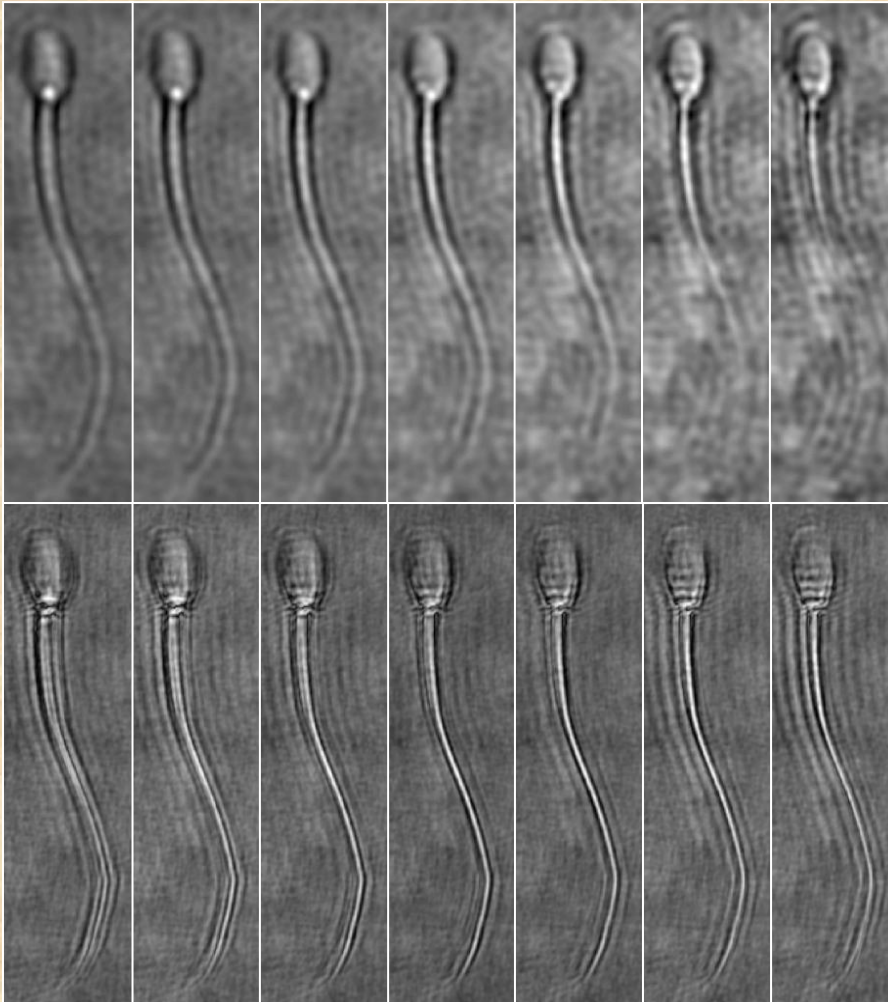


**Differential interference contrast for
horizontal and vertical shearing**

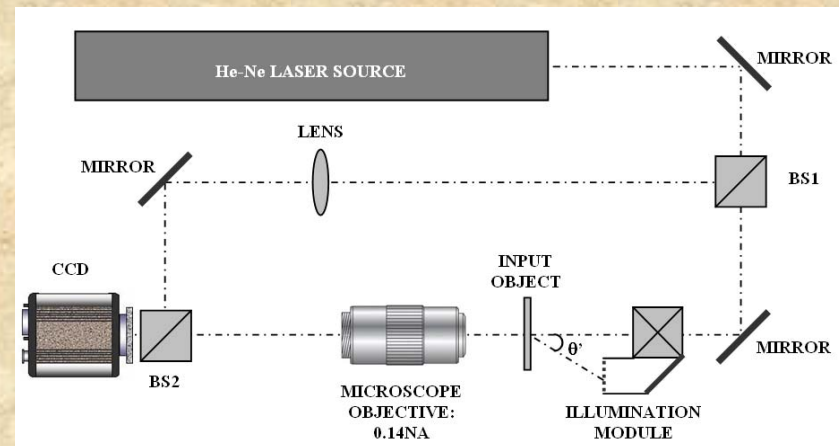


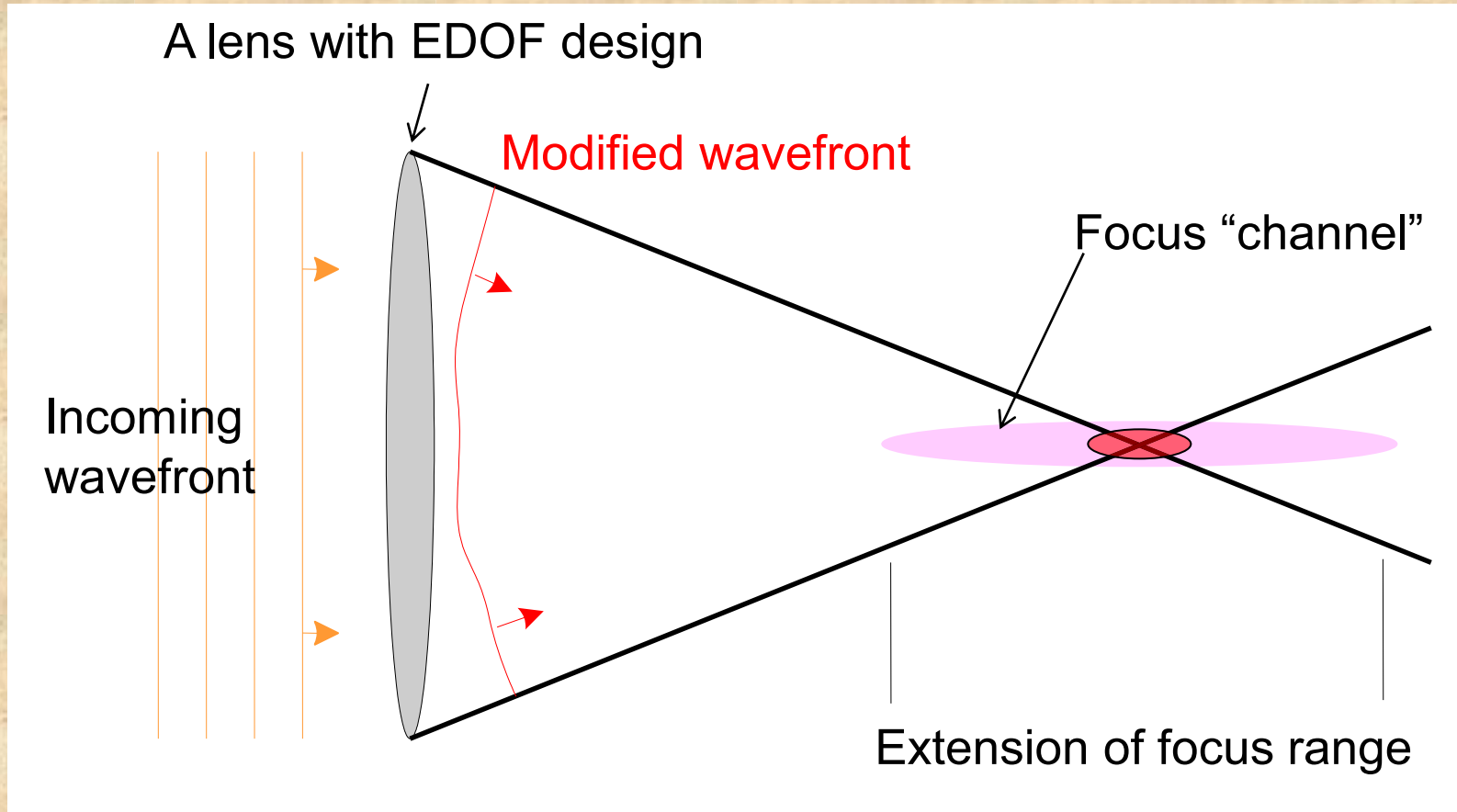
Dark field image

Phase visualization techniques

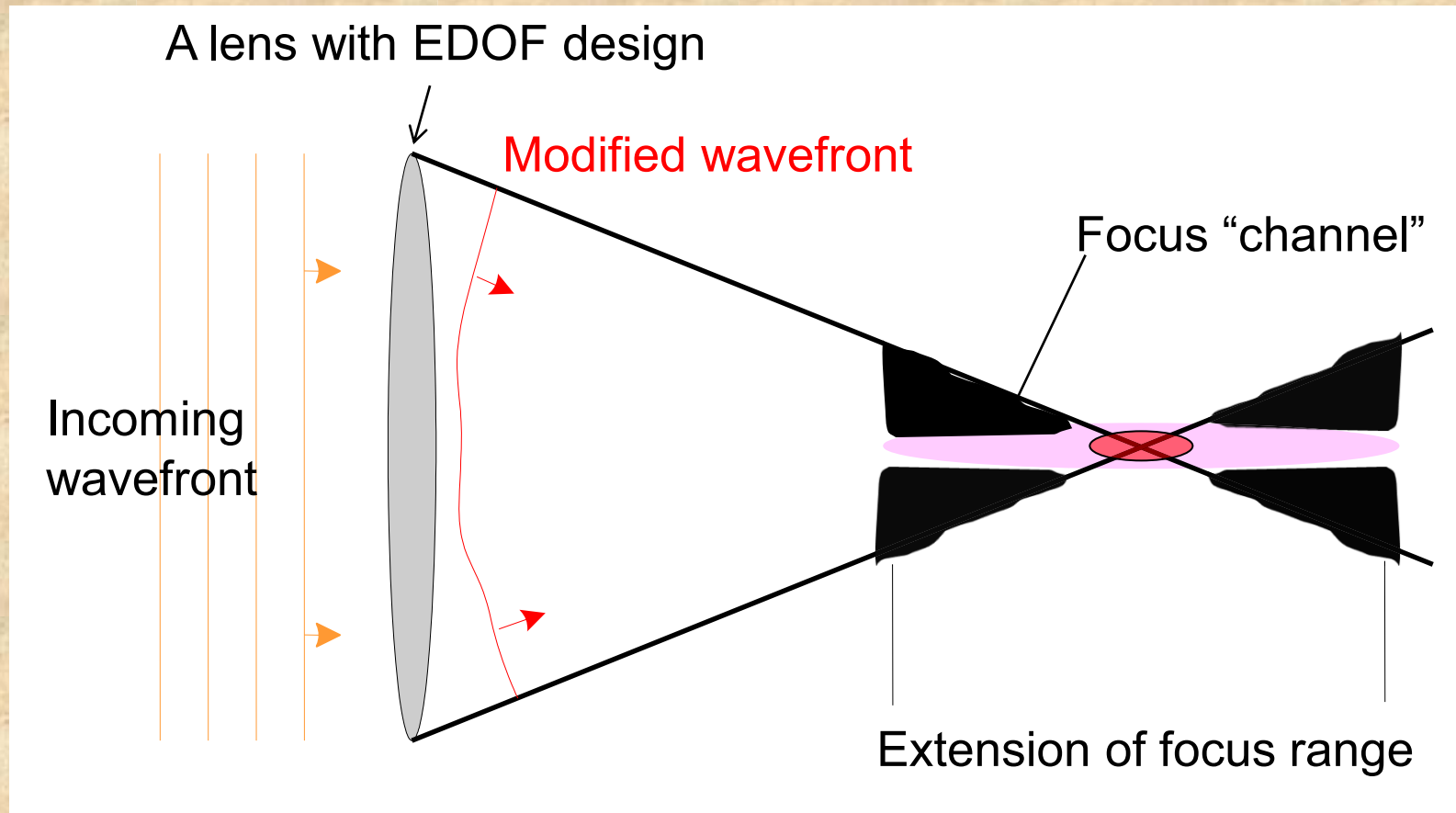


A set of refocused images at different axial distances without (upper row) and with (lower row) applying the axial synthetic aperture generation.





EDOF=Extended Depth Of Focus

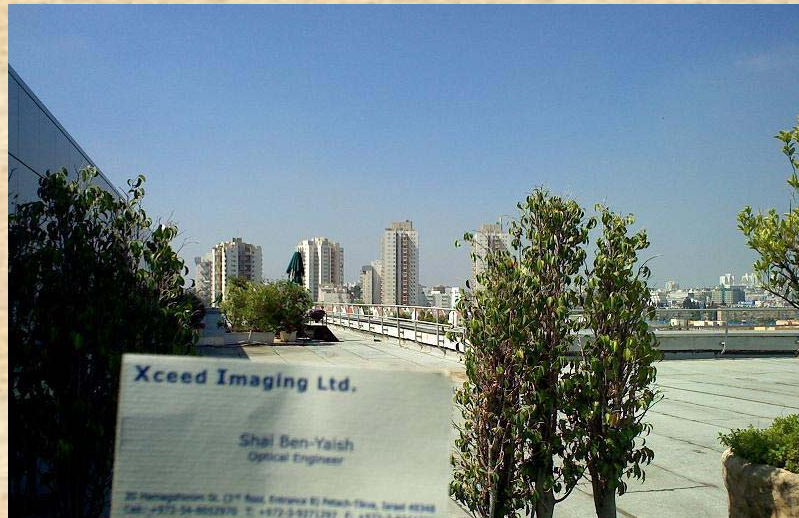




SR- Extended Depth Of Focus

Regular fixed lens (equal to 1 D presbyopia)

With Xceed EDOF element



Zoomed Region

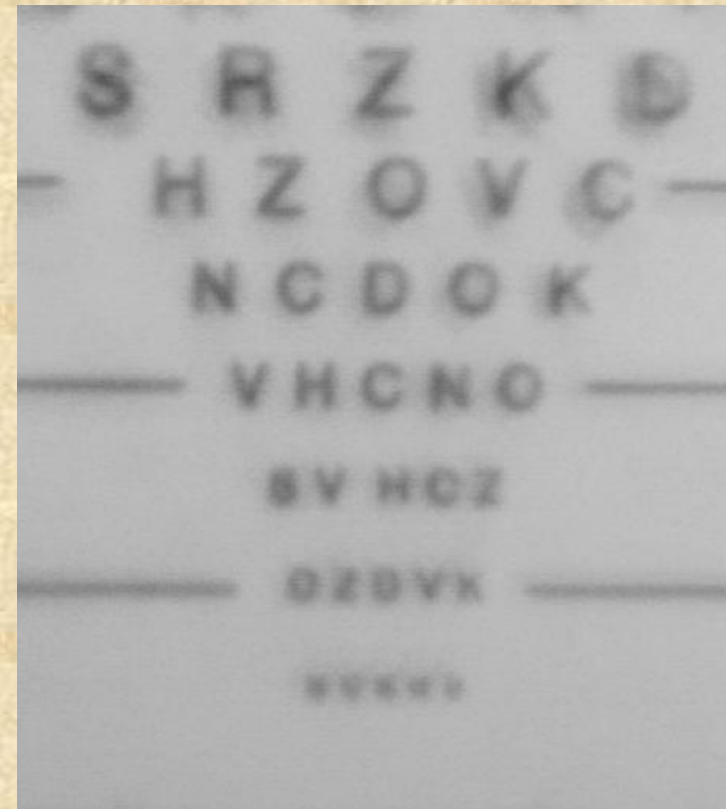


Zoomed Region

Experimental demonstration for 1.75D

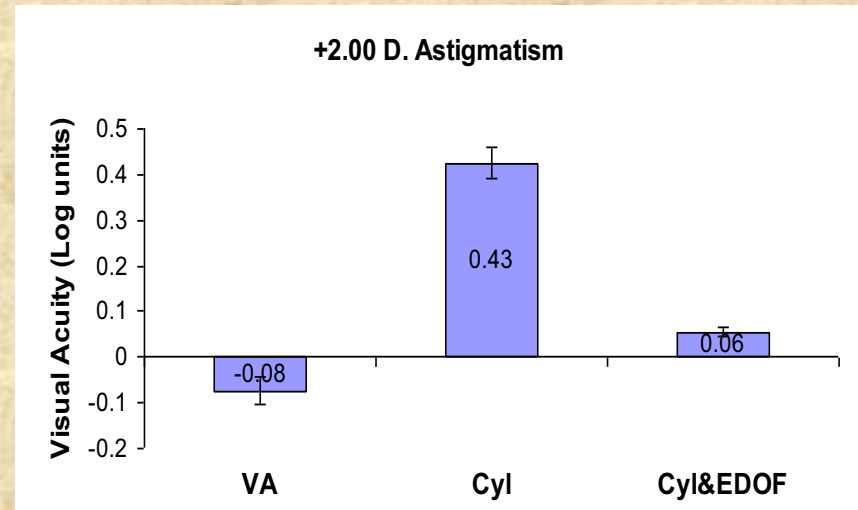
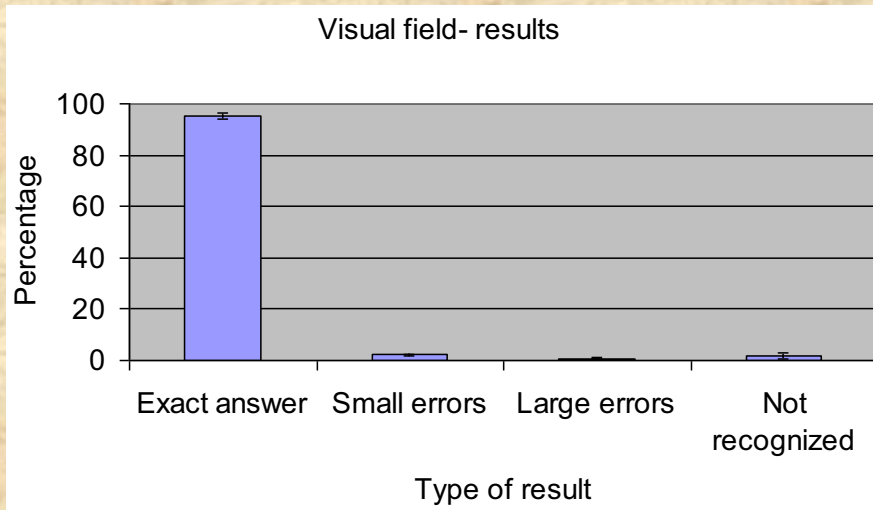
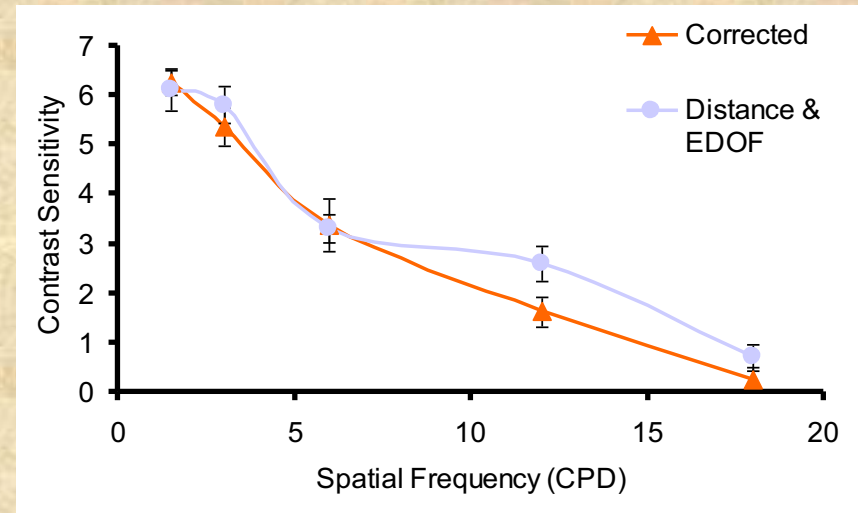
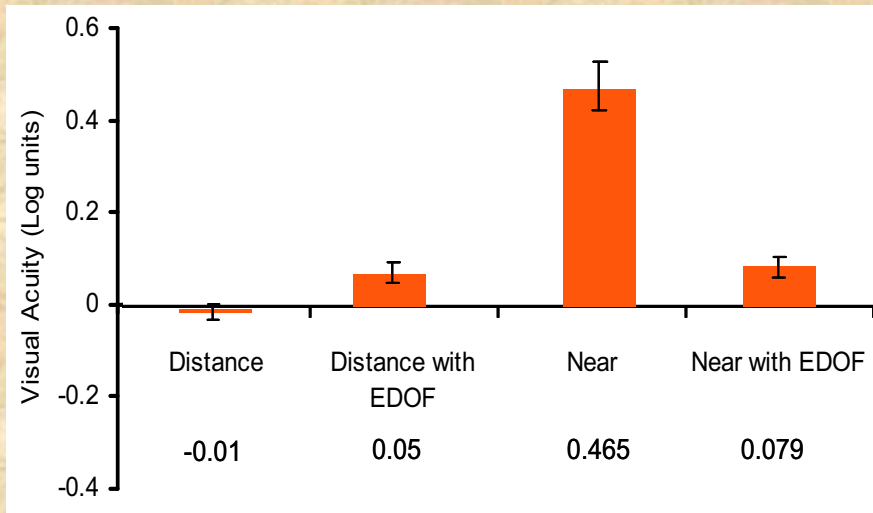


(1) Without EDOF element.

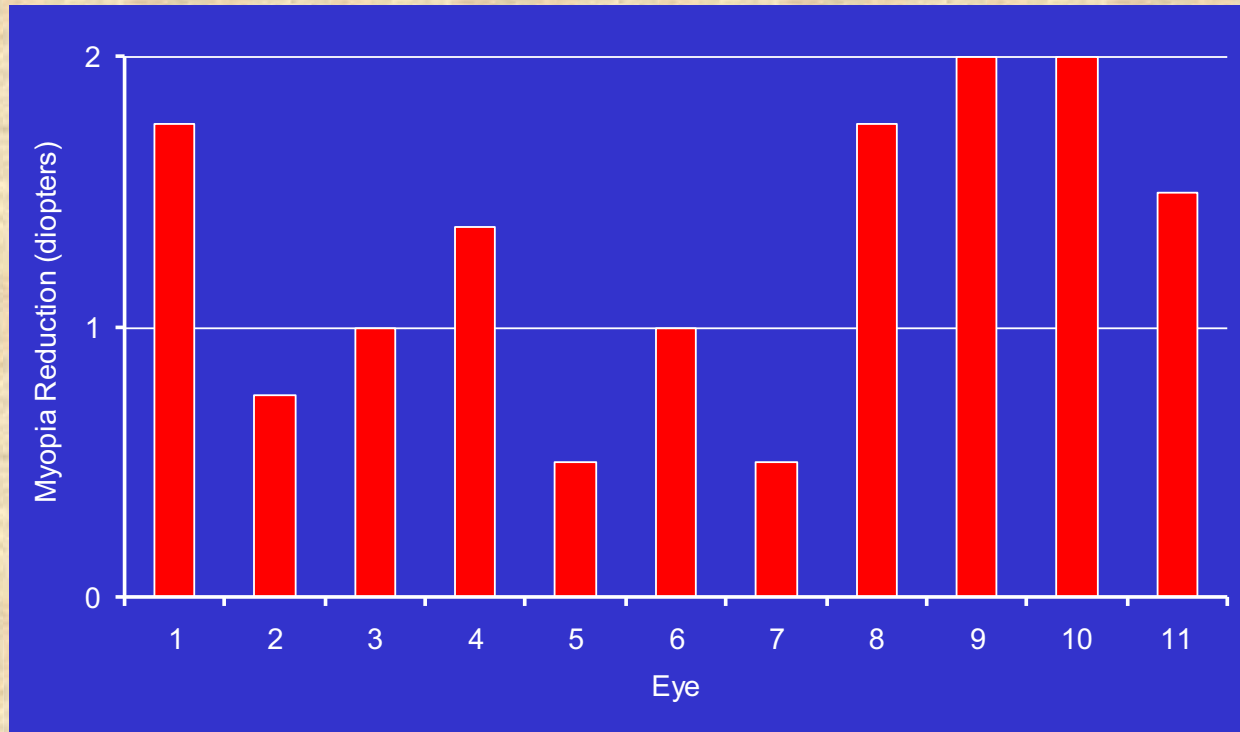


(2) With EDOF element.

SR- Extended Depth Of Focus: spectacles- presbyopia, visual field and astigmatism

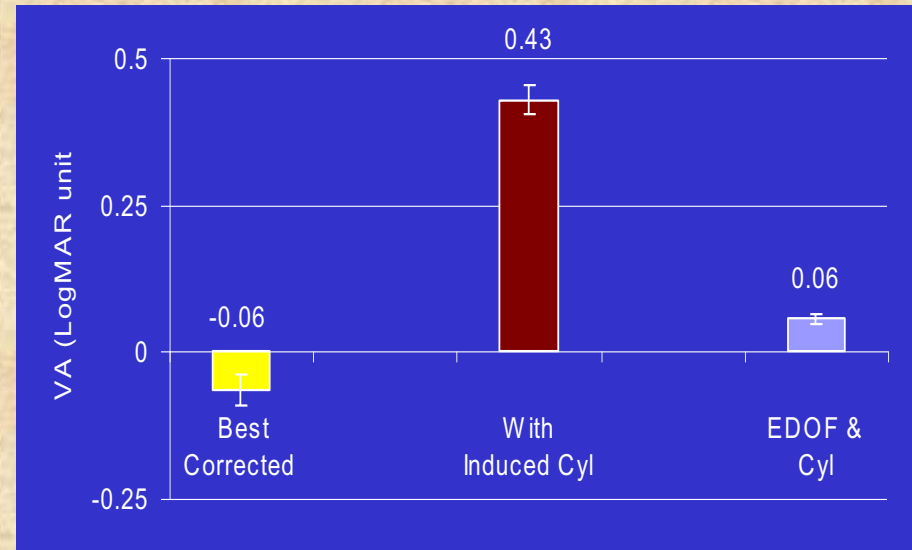
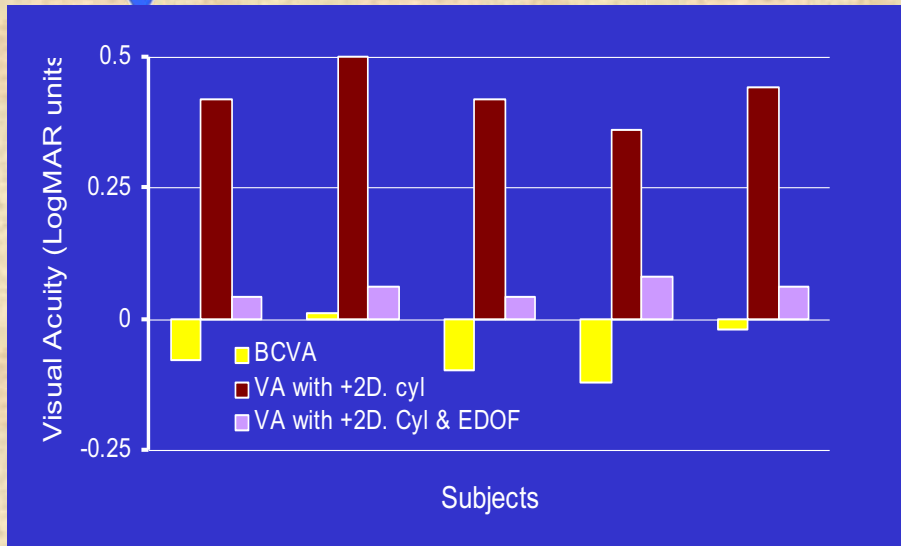


***SR- Extended Depth Of Focus:
contact lenses- myopia***



Compensation for myopic correction: The amount of negative correction the EDOF pattern reduced from the far field correction in each subject while maintaining VA of 6/6 is shown. The EDOF pattern compensated for minus correction of between 0.50 and 2.00 D. [Mean - 1.28 ± 0.56 Diopters]

SR- Extended Depth Of Focus: contact lenses- astigmatism



yellow - best corrected distance VA

brown - VA with induced astigmatism

purple - VA with induced astigmatism and the EDOF element.

• The mean distance VA in Log units:

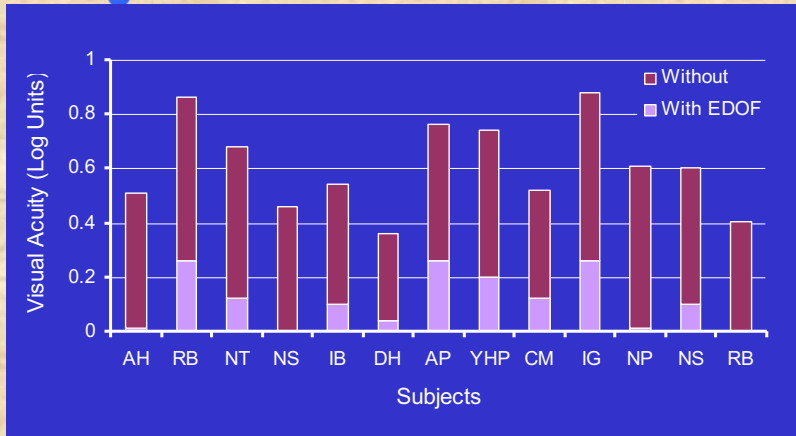
• -0.06±0.03

• 0.43±0.02 with the +2.00 D cylinder

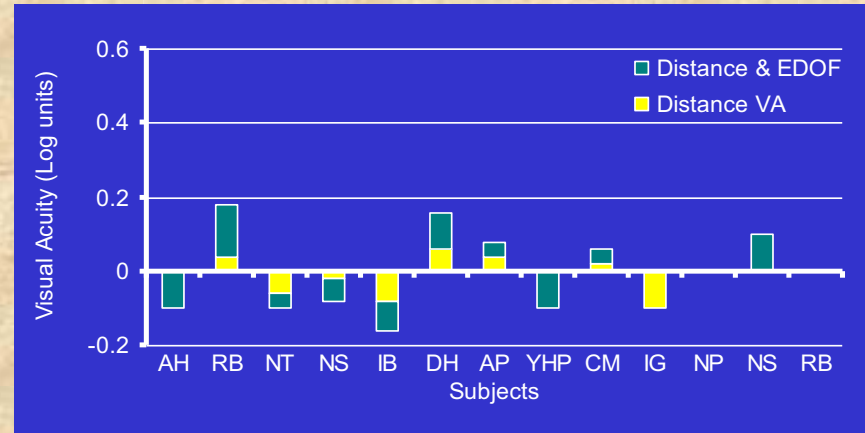
• 0.05±0.01 with the cylinder and the EDOF element

• **The EDOF element improved the VA significantly** (by 0.5±0.09 Log units, $P < 0.0005$, paired t-test)

SR- Extended Depth Of Focus: contact lenses- presbyopia



Near VA with vs. without EDOF with distance correction

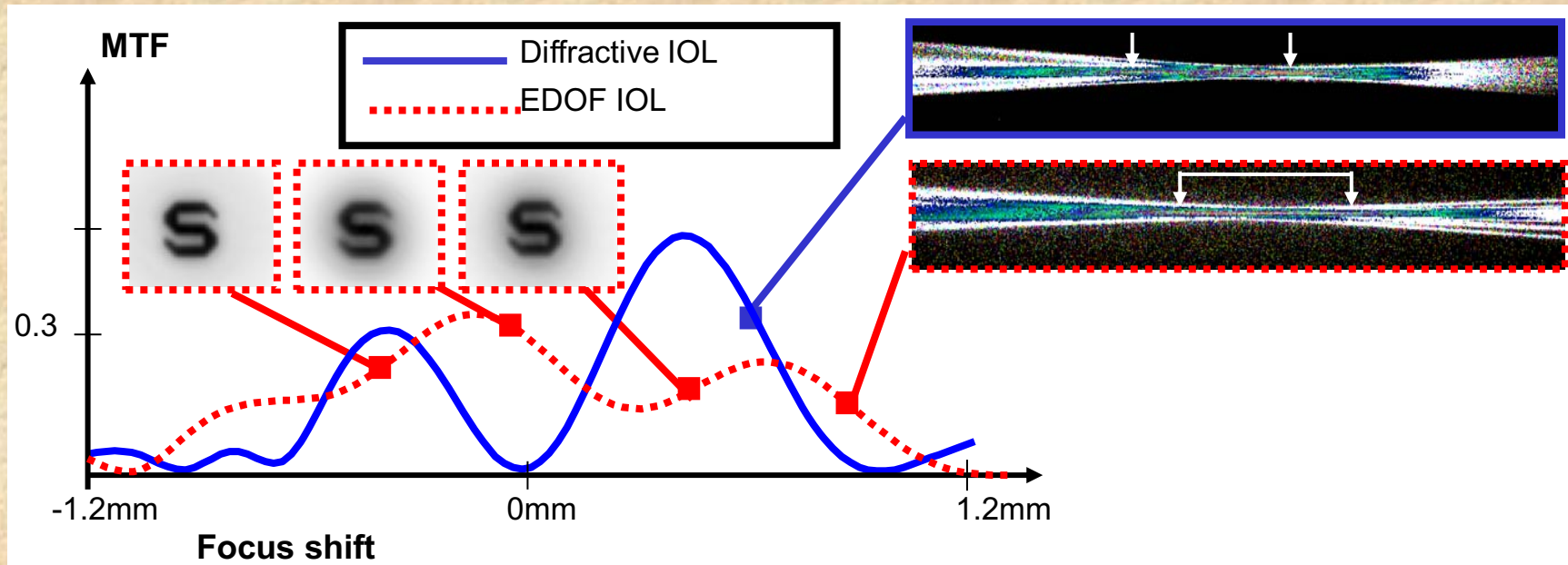
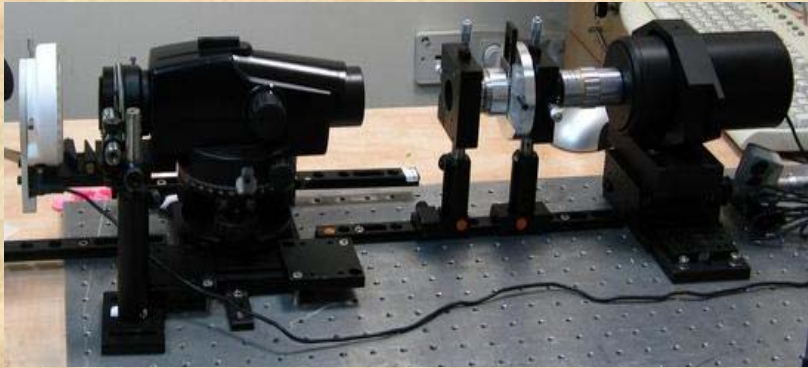


Distance VA with vs. without EDOF



Mean visual acuity in all patients

- **The difference between the near VA with and without EDOF was significant** (0.11 ± 0.03 vs. 0.495 ± 0.02 Log units respectively, $P < 0.005$, paired t-test)
- **The difference between the distance VA with and without EDOF was not significant** (0.003 ± 0.02 vs. -0.007 ± 0.01 Log units respectively, $P > 0.5$, paired t-test)



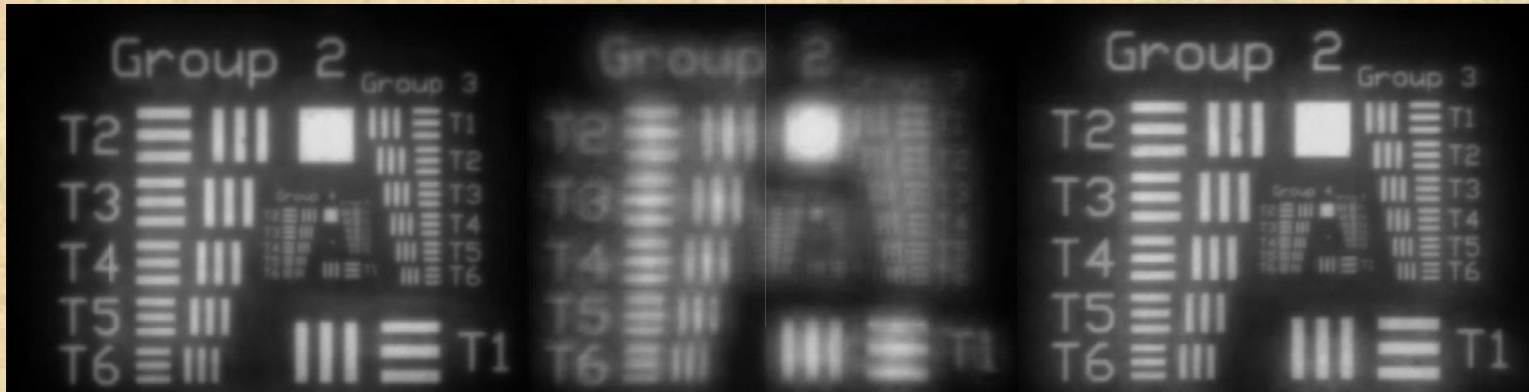
SR- Extended Depth Of Focus: IOL

Best image - Far

Worst Intermediate

Best image - Near

EDOF

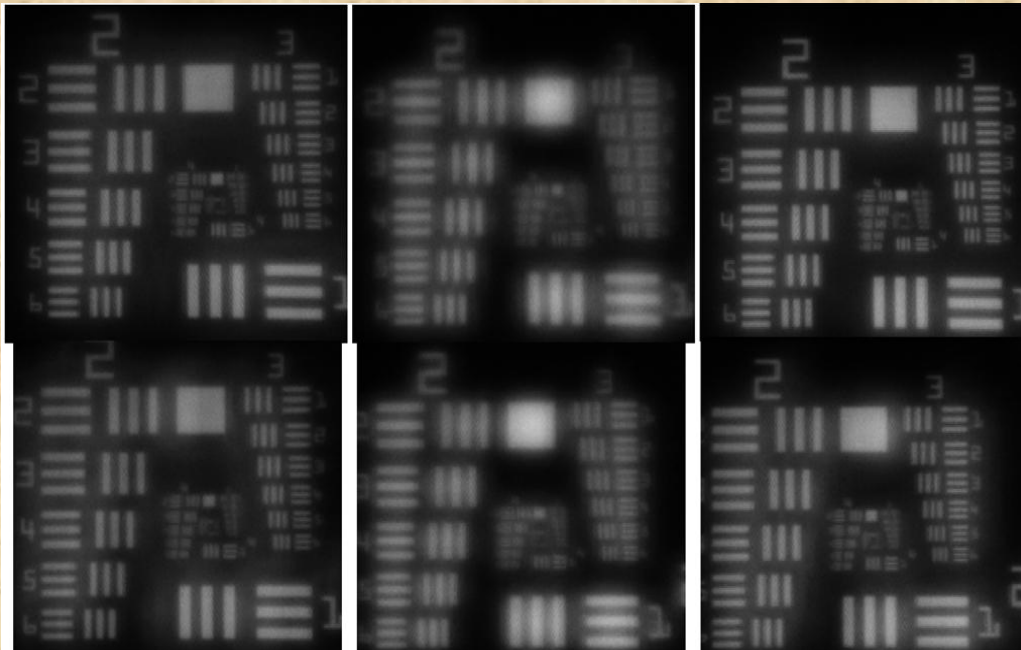


ReStore

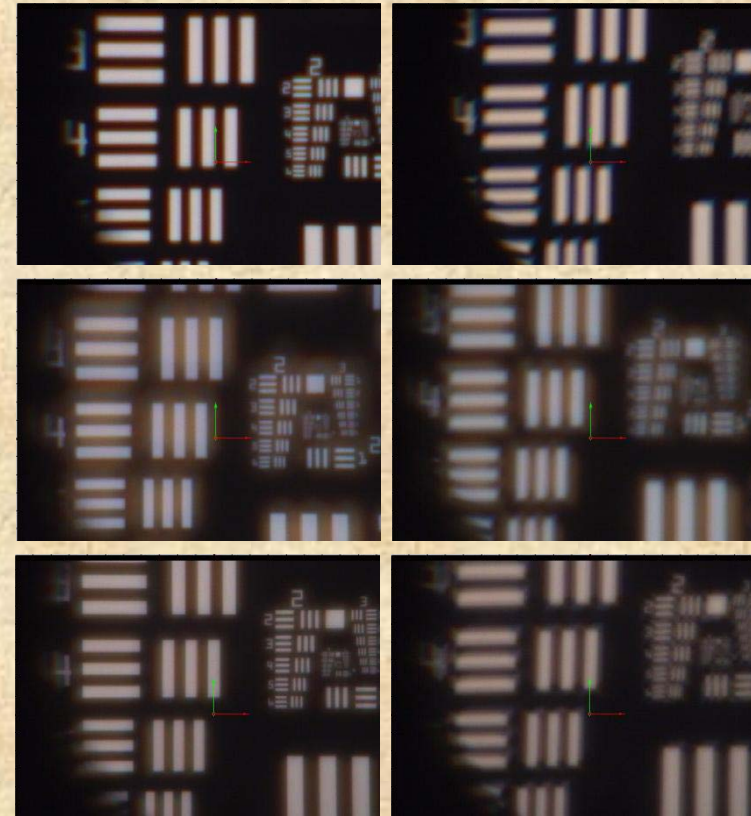


3mm pupil

SR- Extended Depth Of Focus: IOL

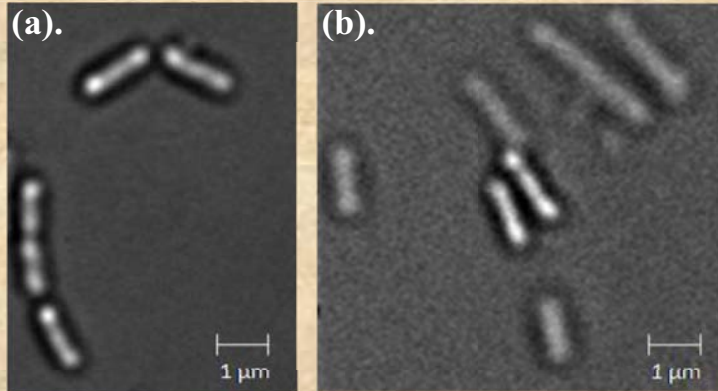


Tolerance to decentration. Experimental results obtained for the EDOF IOL with pupil size of 3mm. Upper row centered results and lower row - 0.75mm decentrated results: far image (left column), intermediate image (middle column) and near image (right column).

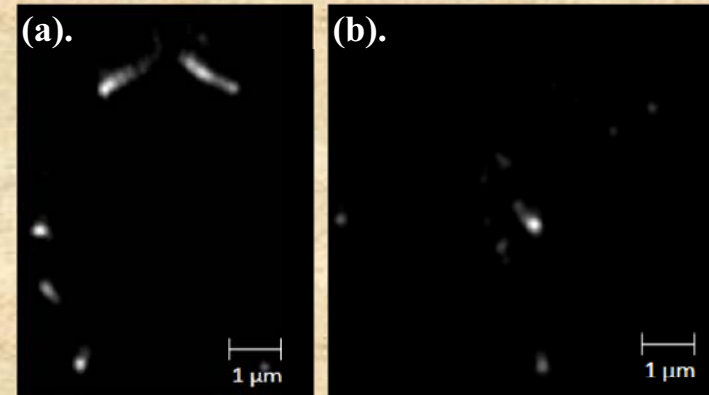


Tolerance to astigmatism aberrations. Experimental results of far field without (left column) and with (right column) 1.00 D of astigmatism aberration for mono focal lens (upper row), ReStor lens (middle row) and EDOF lens (lower row).

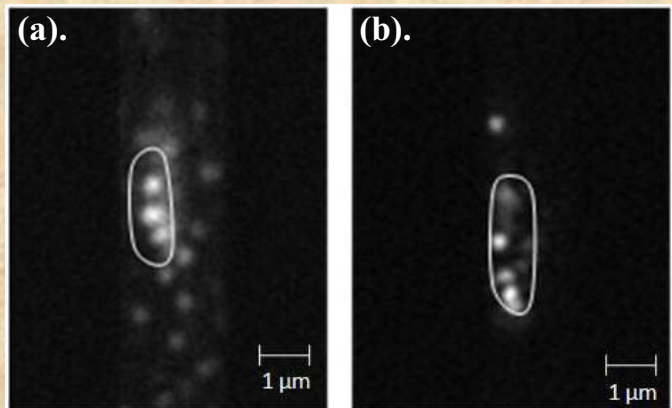
Single Molecule Imaging- EDOF



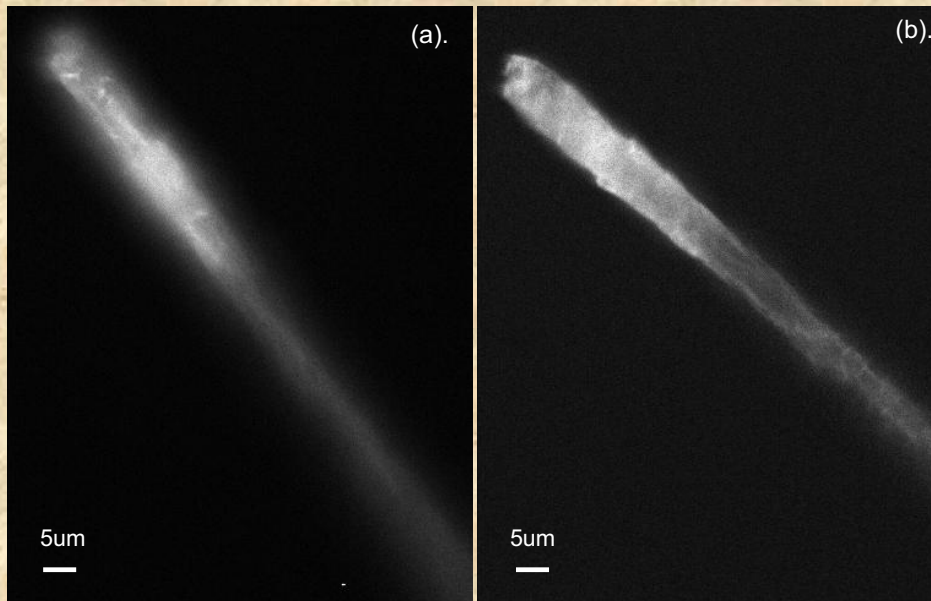
Samples including a few E. coli cells: (a). Transmission image with the EDOF element. (b). Transmission image without the EDOF element.



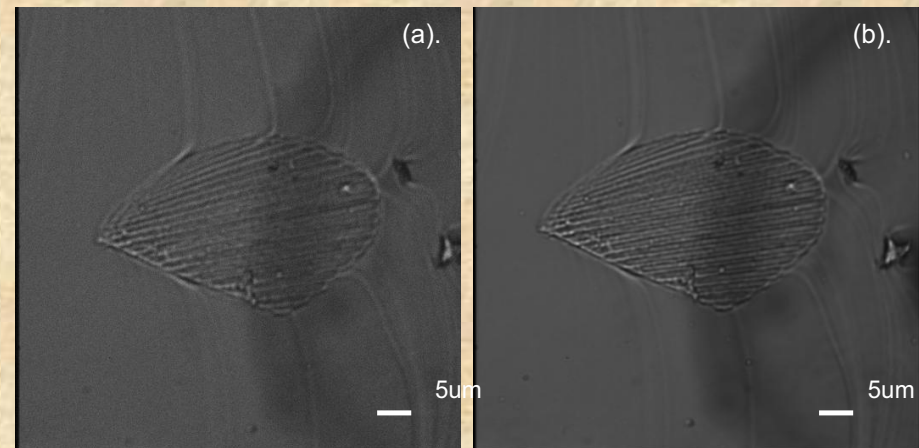
Single molecules imaging: (a). Transmission image with the EDOF element. (b). Transmission image without the EDOF element.



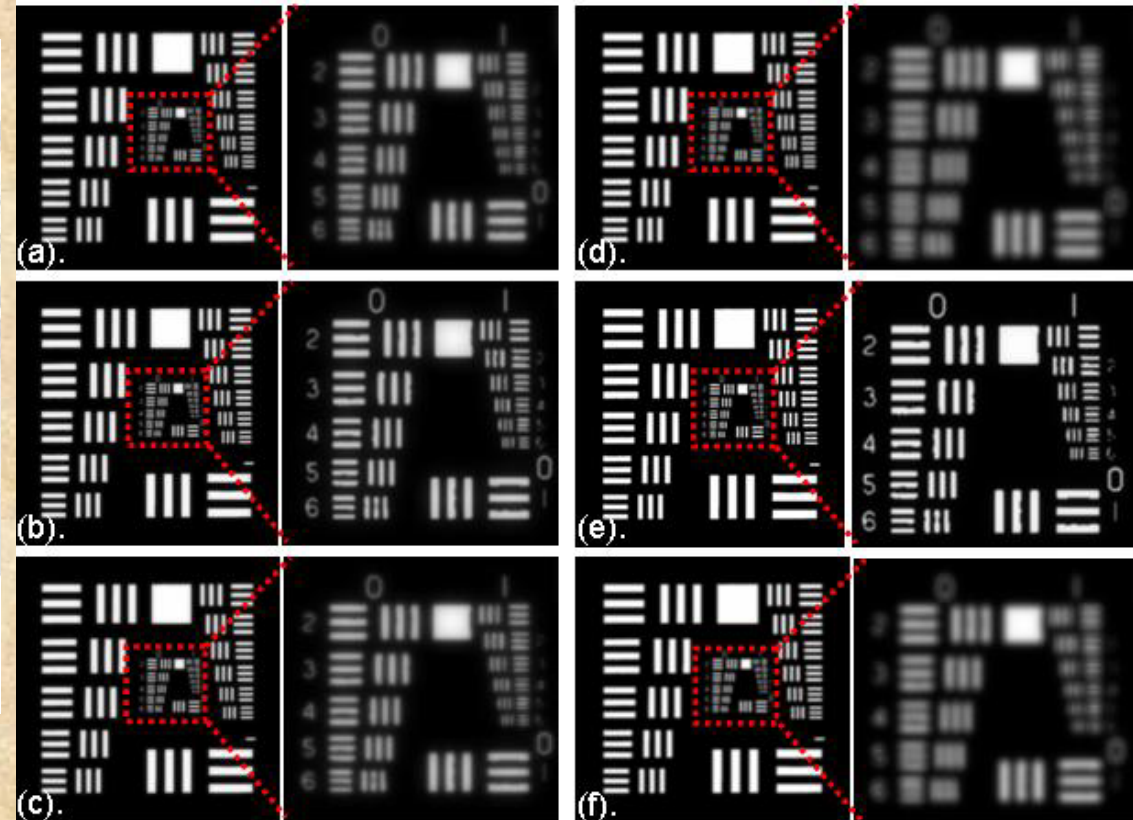
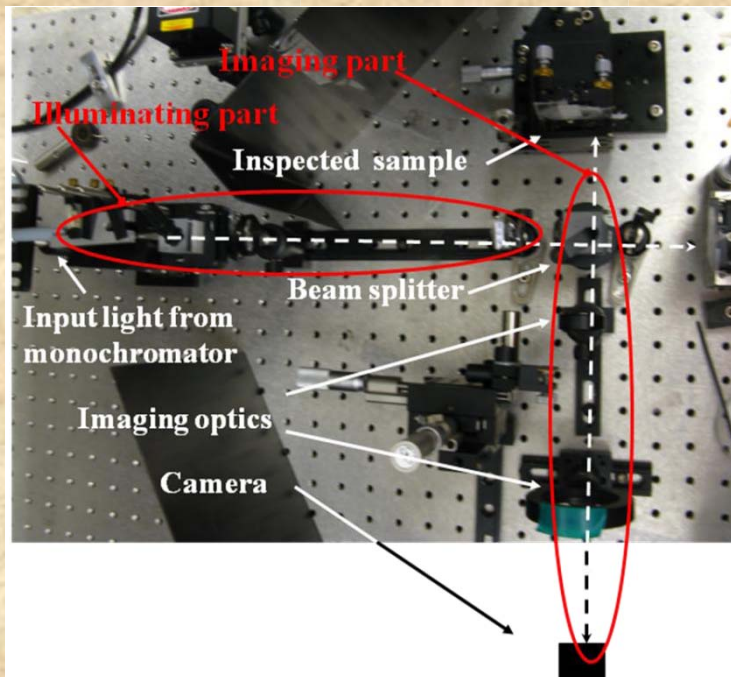
Single molecules "in cell" imaging (a). Fluorescence image with the EDOF element. (b). Fluorescence image without the EDOF element. White line borders the cell shape.



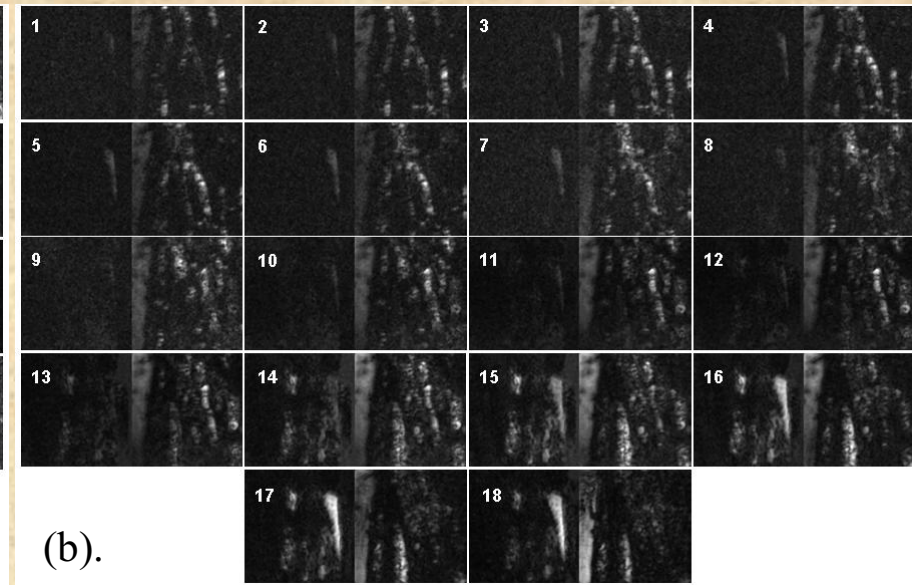
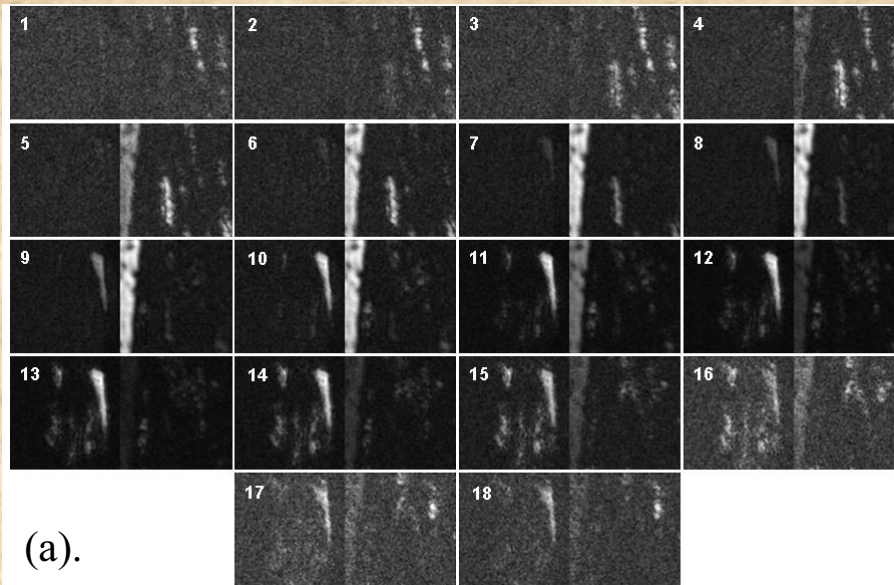
Chlorophyll fluorescence image of moss (*Ceratodon purpureus*) fragment. (a). Without the EDOF mask. (b). With the EDOF mask.



Transmission image of flake-like crystal structure of PVA. (a). Without EDOF mask. (b). With the EDOF mask.

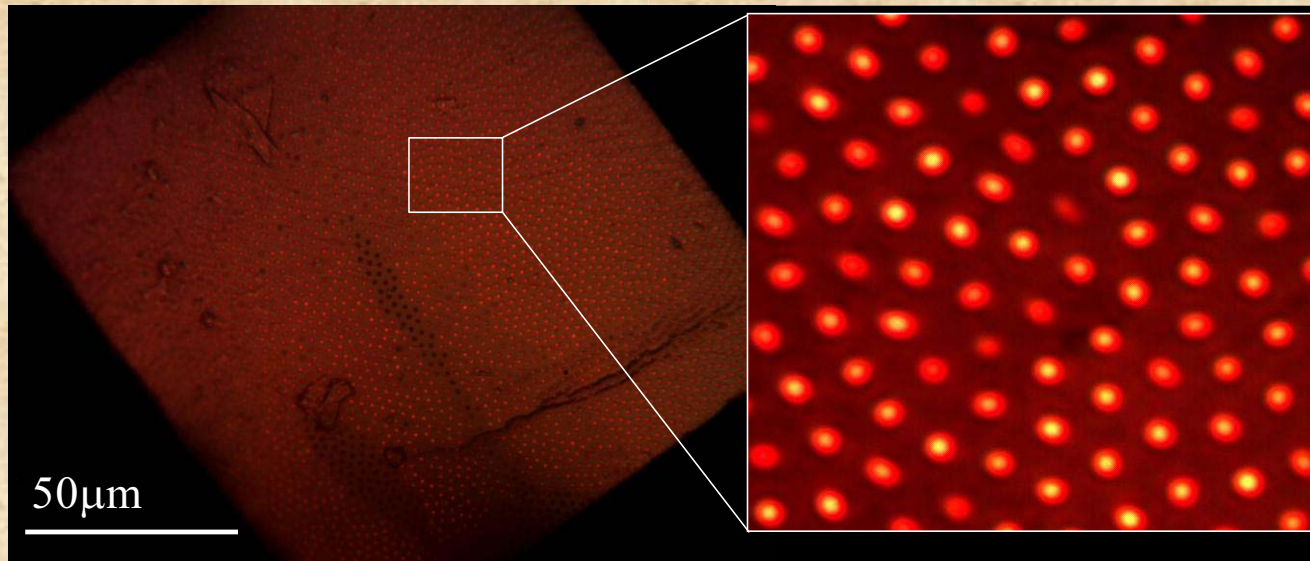


(a)-(c) USAF with EDOF. (d)-(f). USAF without EDOF. (a). and (d). are at axial position of $-130\mu\text{m}$, (b). and (e). are at best focus position and (c). and (f). are at axial position of $+130\mu\text{m}$. The largest USAF bars correspond to 15 cyc/mm. The smallest bars correspond to 200 cyc/mm.

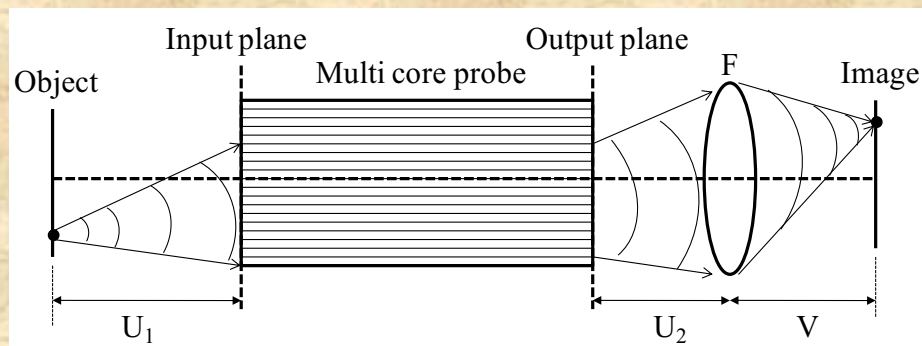


Experimental results of the full field OCT configuration. The reconstructed images correspond to axial distance separation of 900nm. In each image the horizontal size is 520 μ m and the vertical is 260 μ m. (a). Without the EDOF. (b). With the EDOF.

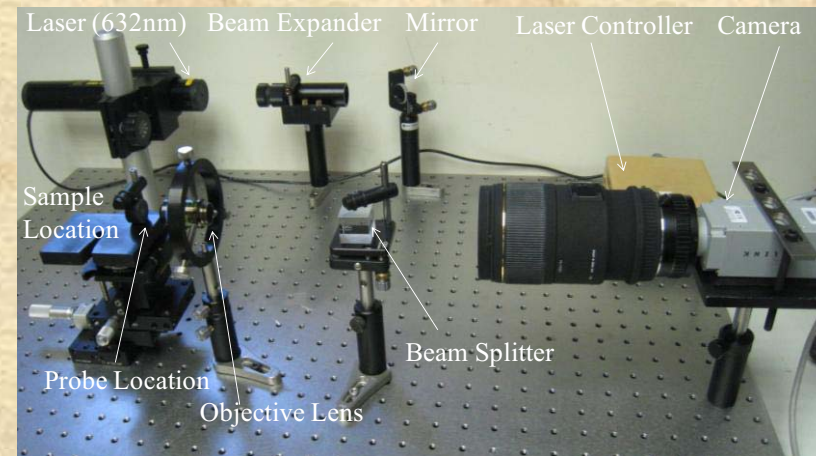
Multi-Functional Probe

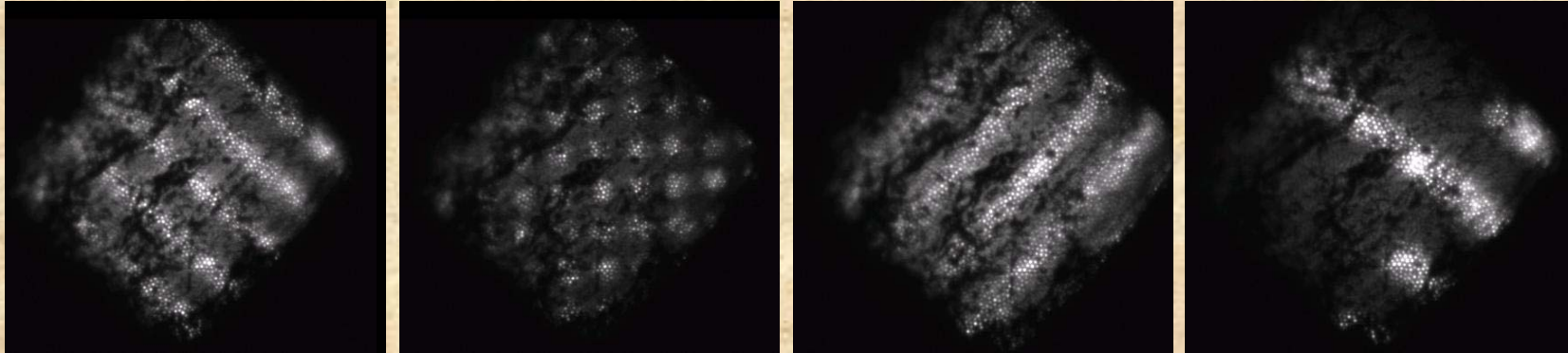


The edge of the fabricated micro probe having approximately 5,000 cores while each one of them is being used as light transmitting channel (each core is a single pixel in the formed image). In this image each core transmits red channel of light at wavelength of 632nm.

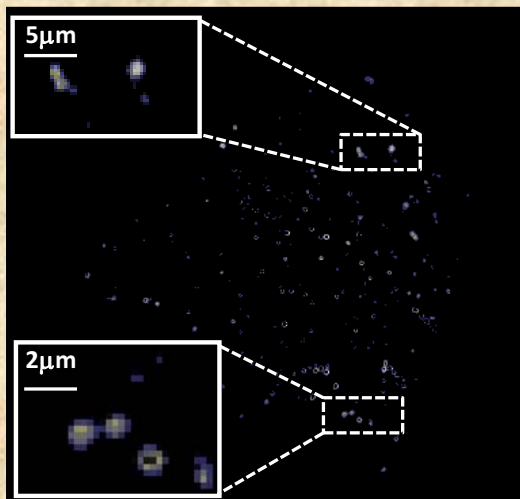


$$\frac{1}{U_1 + U_2} + \frac{1}{V} = \frac{1}{F}$$





Experimental results of images transmitted backwards by the proposed micro probe. The scanned objects are as follows; From left to right: black vertical lines, black rectangles, horizontal black lines, black lines and black rectangle appearing in the left side of the backwards transmitted image.



Experimental results of images with Fe beads having diameter of $1\mu\text{m}$ imaged through an agar solution.

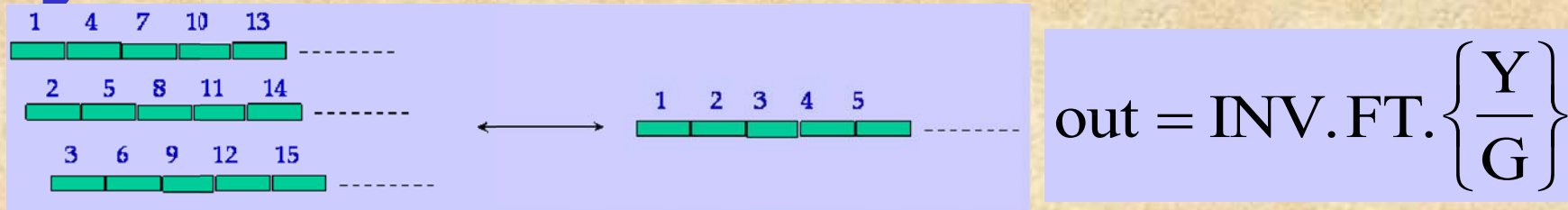


Outline

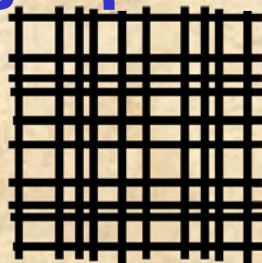
- Introduction
- The “SW Adaptation” Process
- Diffractive type Super Resolution
- Geometrical type Super Resolution
- Hearing with light
- Conclusions

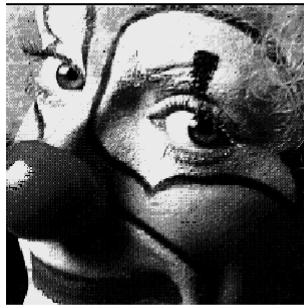
Geometrical SR:

- A sub pixeling algorithm similar to the Gabor transform is applied in order to obtain sub pixel geometrical S.R.

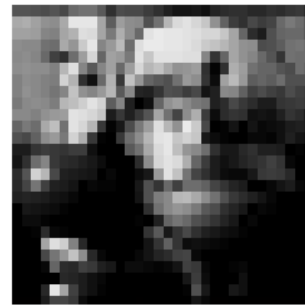


- Special DOE is attached to the detector plane in order to obtain high quality reconstruction of images.

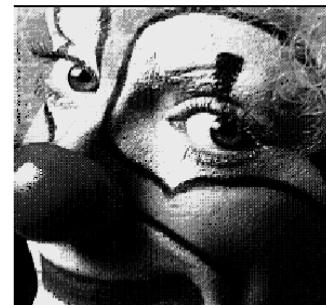




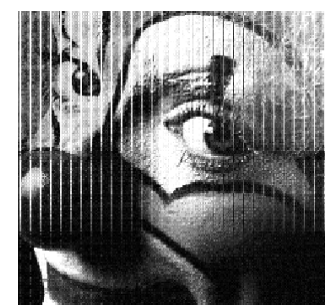
Input Image



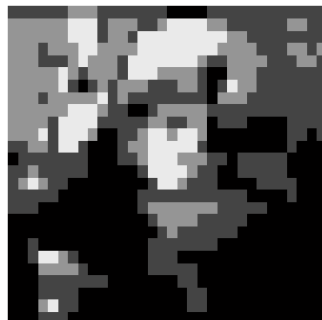
8 times resolution
reduction



Reconstruction



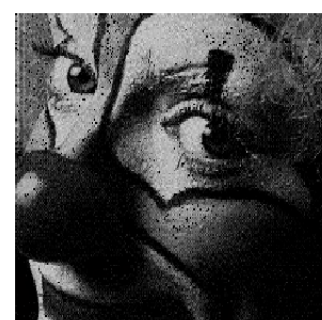
Without masking



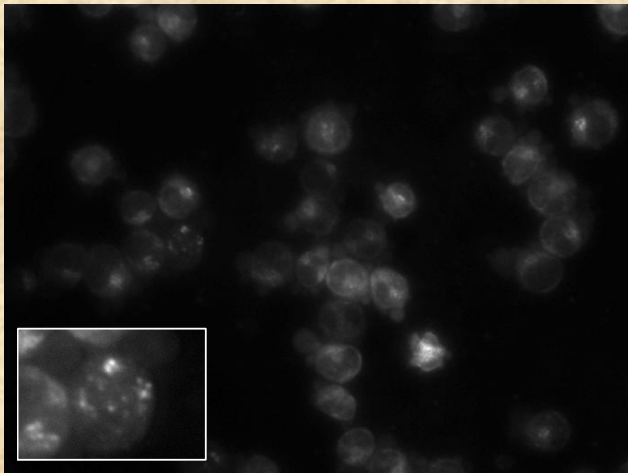
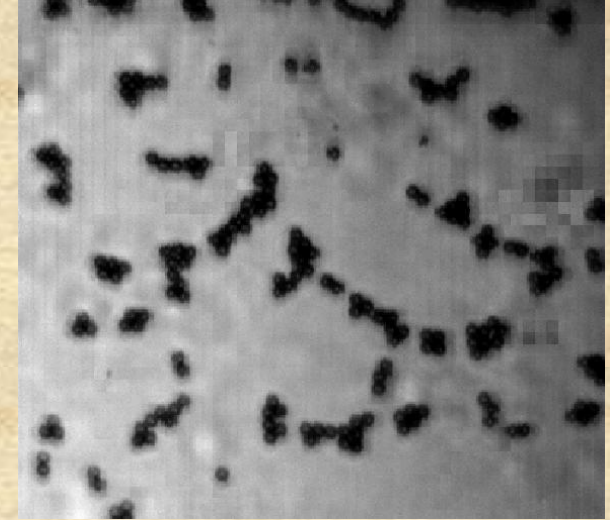
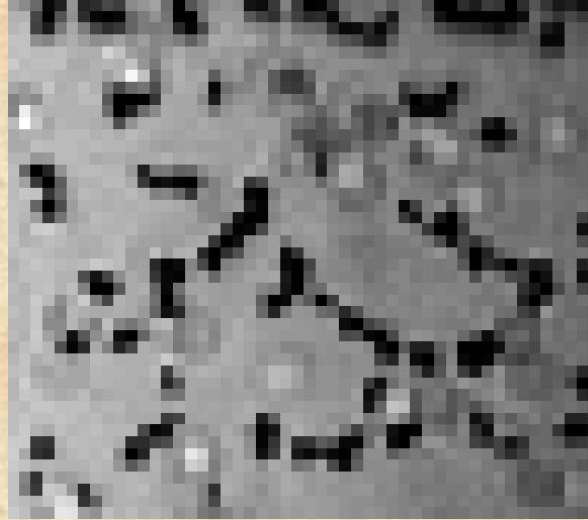
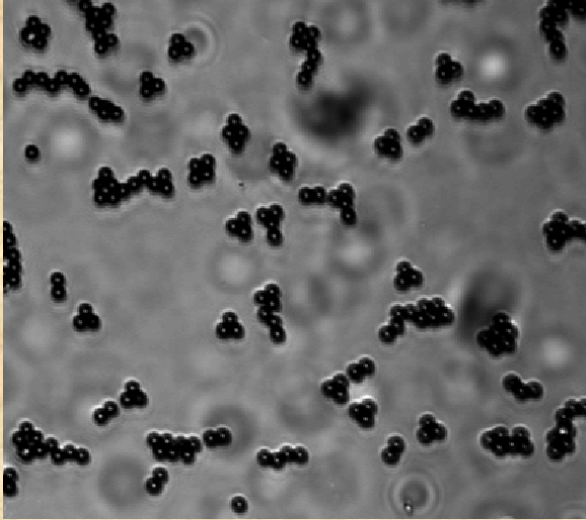
2 bits camera



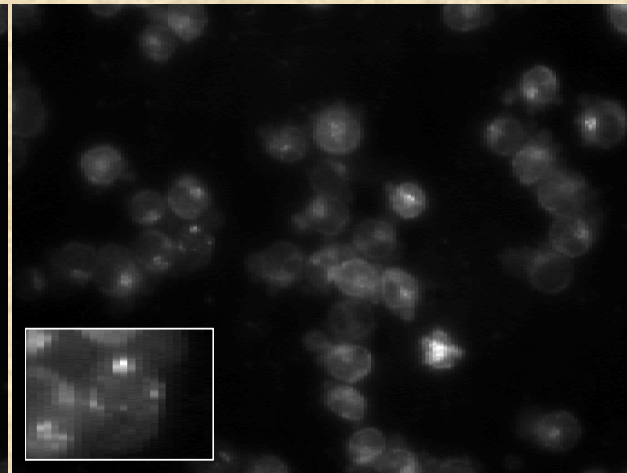
Reconstruction



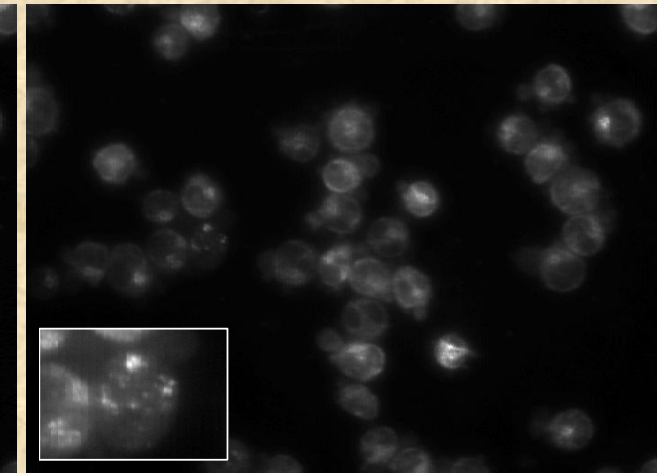
Reconstruction
for 4 bits camera



Open aperture

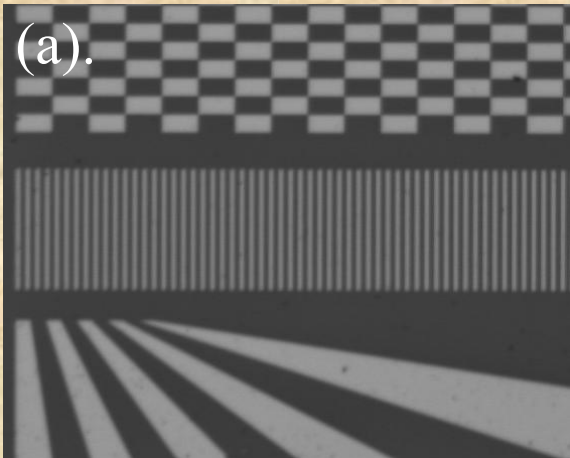


Closed aperture



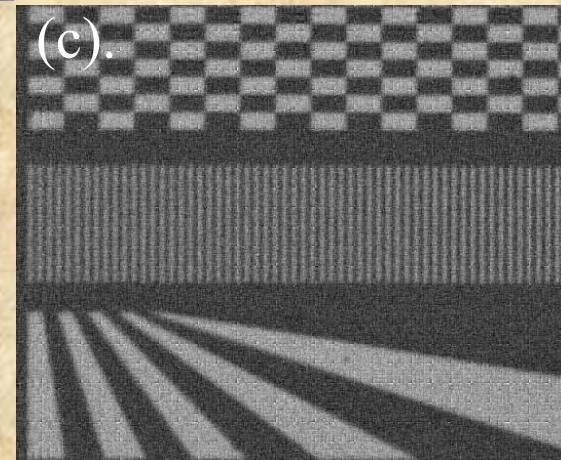
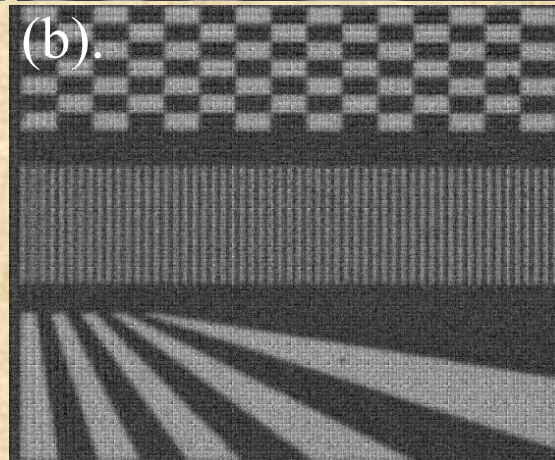
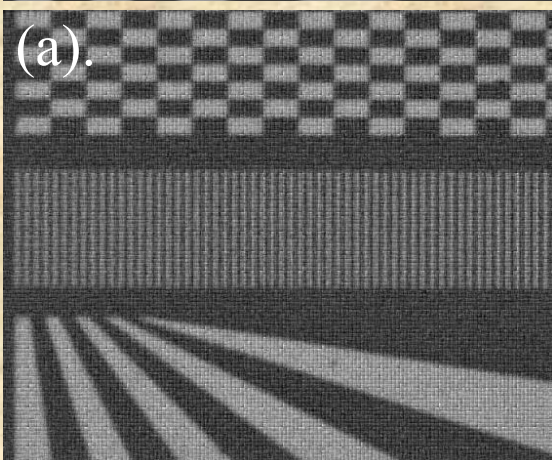
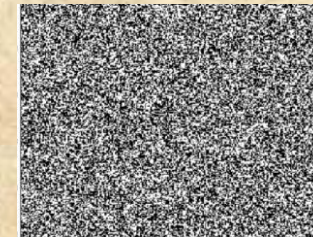
Reconstruction

Geometrical SR- Intermediate plane mask



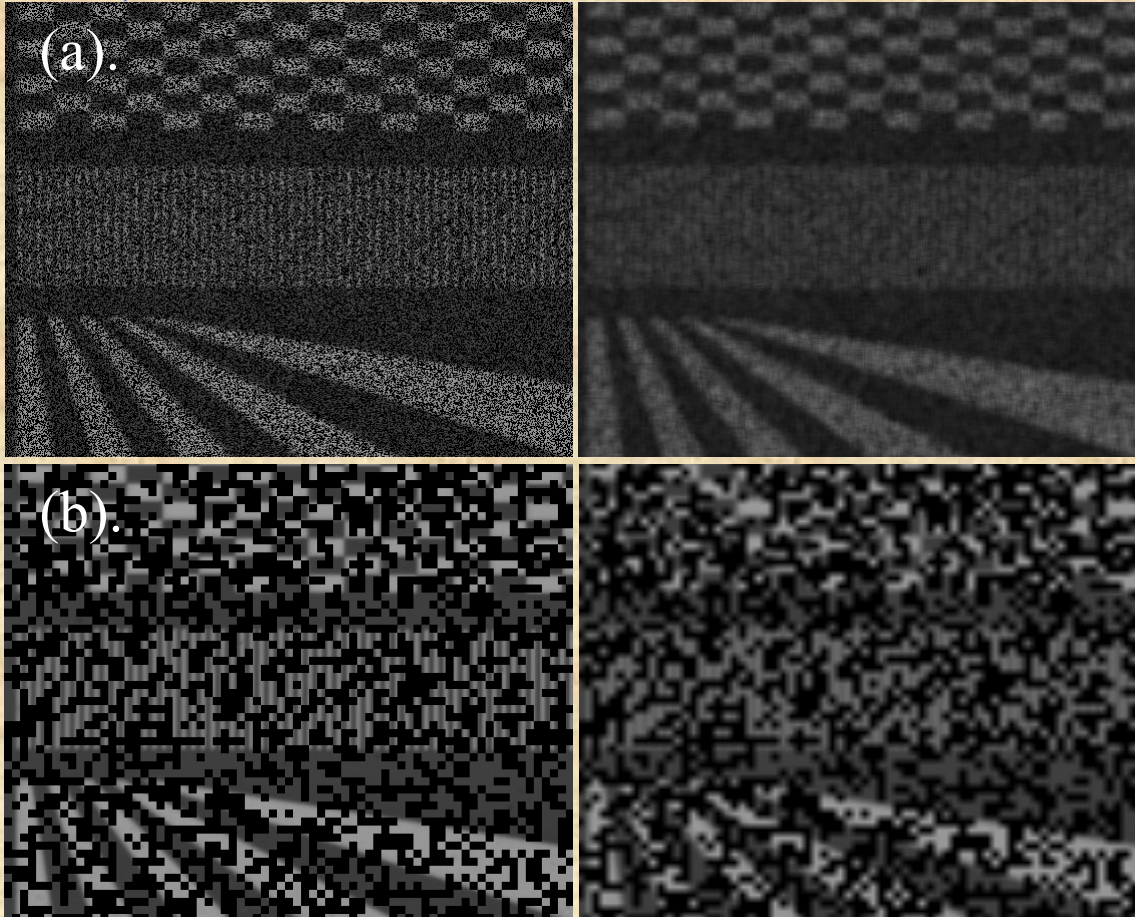
(a). High resolution ref.

(b). Low resolution image
without SR



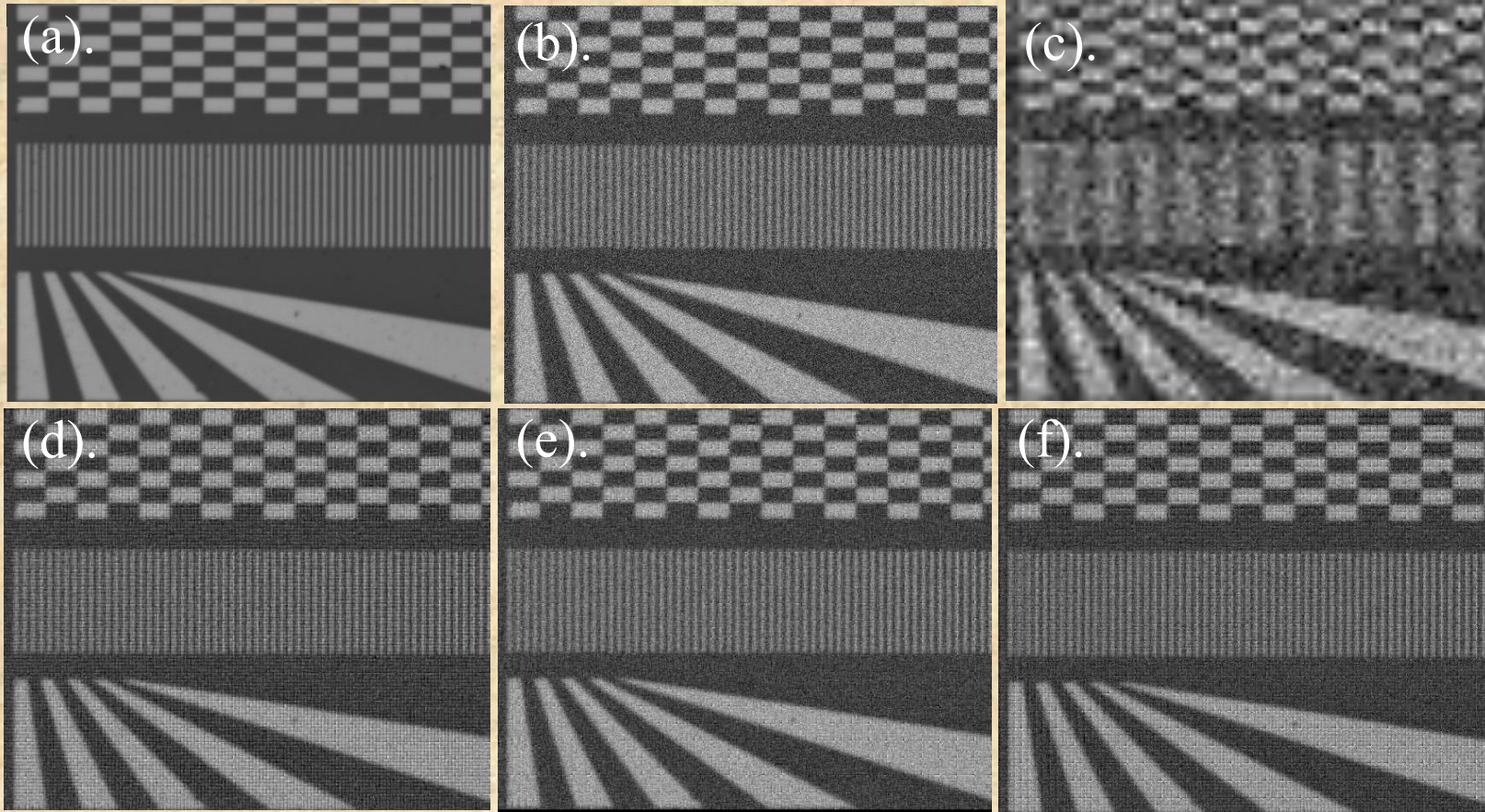
Reconstruction: (a). Field of view border condition. (b). High resolution mask in the intermediate image plane. (c). Low resolution mask in the intermediate image plane.

Geometrical SR- Intermediate plane mask



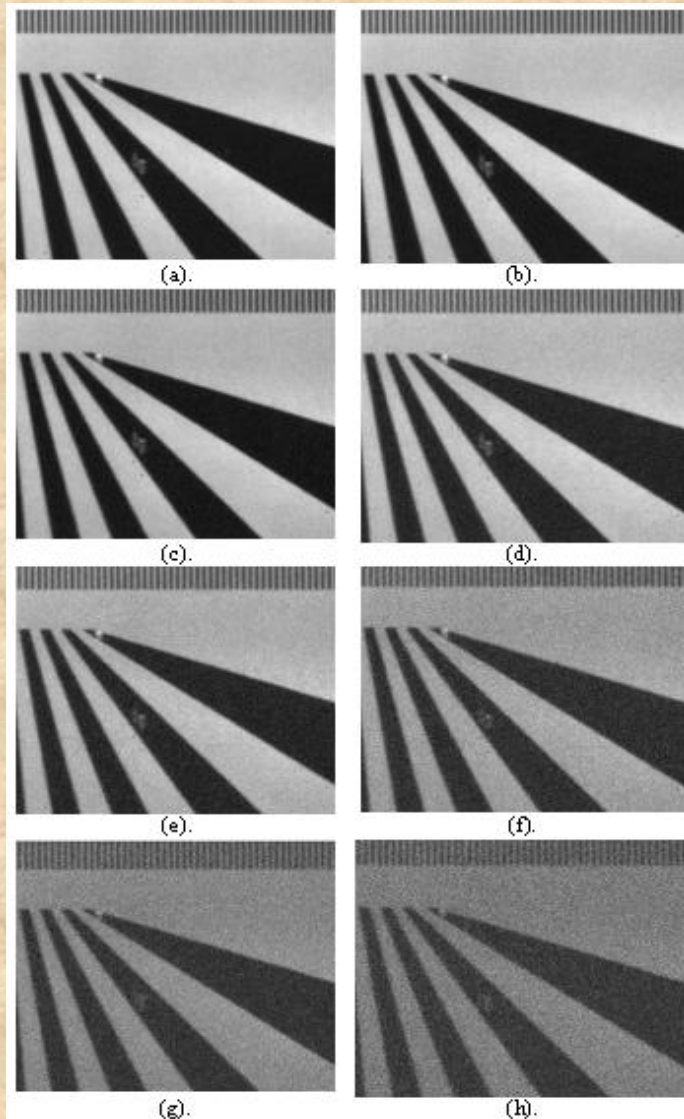
Masked image (left) and blurred masked image (right) for: (a). High resolution mask in the intermediate image plane. (b). Low resolution mask in the intermediate image plane.

Geometrical SR- Intermediate plane mask: with noise



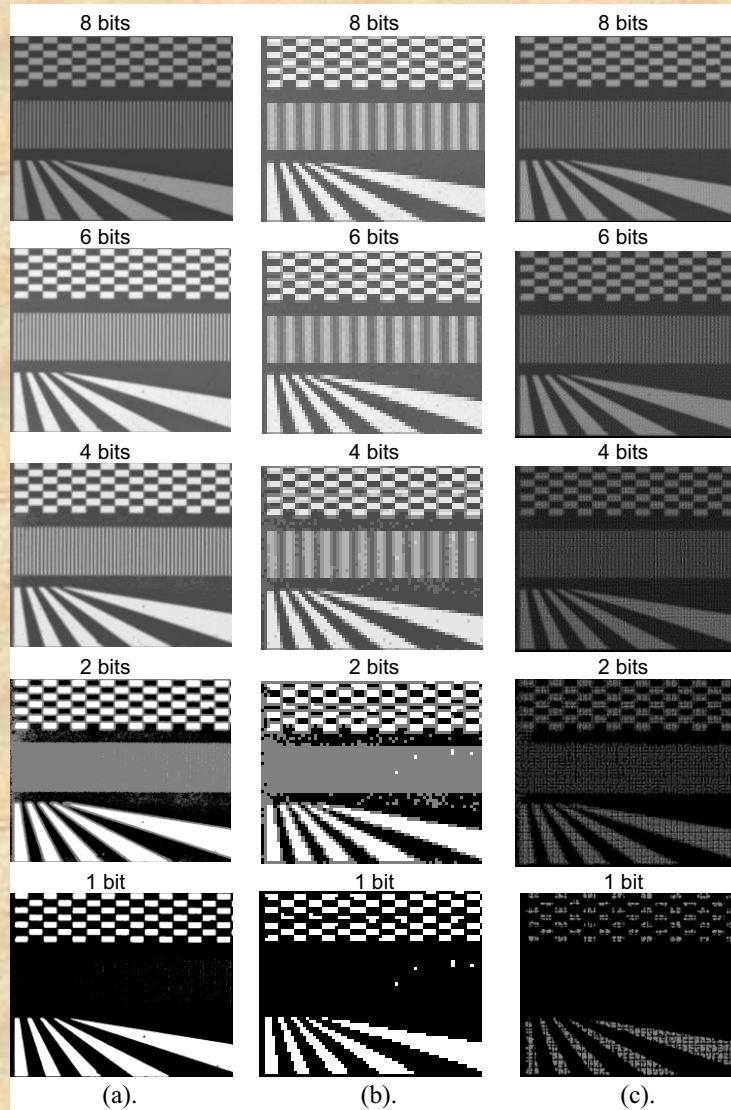
(a). High resolution reference. (b). High resolution reference embedded with noise with standard deviation of 20 gray levels. (c). The low resolution image after blurring by a factor of 8 in every axis. (d). The reconstruction with mask, that is, blocking the edges of the field of view. (e). The same as in (d) but with applying random binary mask with large pixels. (f). The same as in (d) but with applying random binary mask with small pixels.

Geometrical SR- Intermediate plane mask: tolerance to noise



Sensitivity to Gaussian noise (with zero average). The noise level is described by its variance in normalized dynamic range of 0 to 1. The noise variance we applied was: (a). 0.0001 (b). 0.0002 (c). 0.0005 (d). 0.001 (e). 0.002 (f). 0.005 (g). 0.01 (h). 0.02

Geometrical SR- Intermediate plane mask: effect of quantization



Computer simulations that examine the sensitivity of the suggested technique to the number of quantization bits of the camera: (a). Reference images captured by a CMOS detector with varied number of quantization bits, (b). Low resolution images, (c). The reconstructed images.



Outline

- Introduction
- The “SW Adaptation” Process
- Diffractive type Super Resolution
- Geometrical type Super Resolution
- Hearing with light
- Conclusions

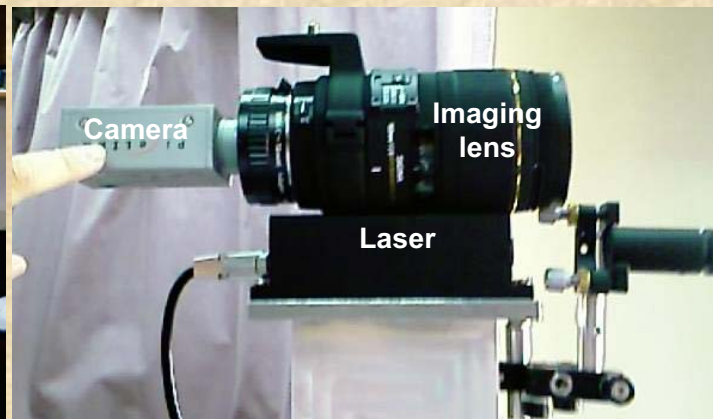
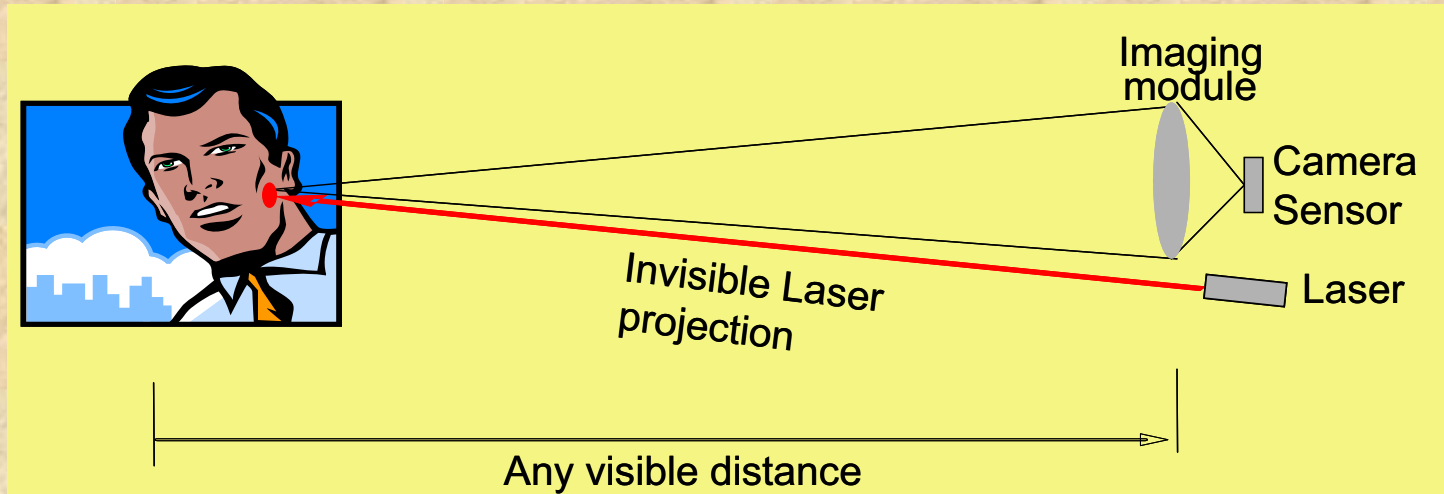
Hearing with Light: Features

- **The ultimate voice recognition system compatible to “hear” human speech from any point of view (even from behind).**
- **There is no restriction on the position of the system in regards to the position of the sound source.**
- **Capable of hearing heart beats and knowing physical conditions without physical contact for measuring.**

Features- cont.


- **Works clearly in noisy surroundings and even through vacuum.**
- **Allows separation between plurality of speakers and sounds sources.**
- **Works through glass window.**
- **Simple and robust system (does not include interferometer in the detection phase).**

Opto-Phone: Hearing with Light



Let's listen...from 80m



Cell phone 

Counting...1,2,3,4,5,6



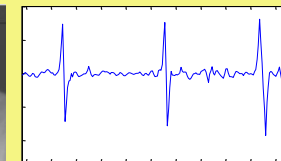
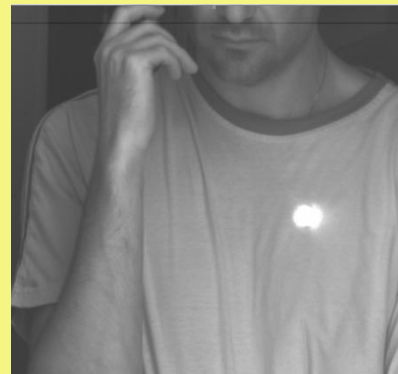
Back part of neck 

Counting...5,6,7



Face (profile) 

Counting...5,6

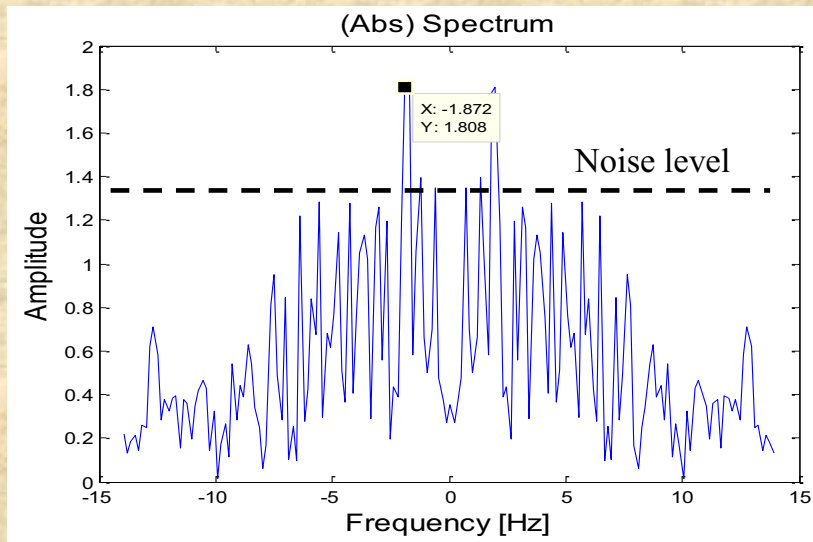
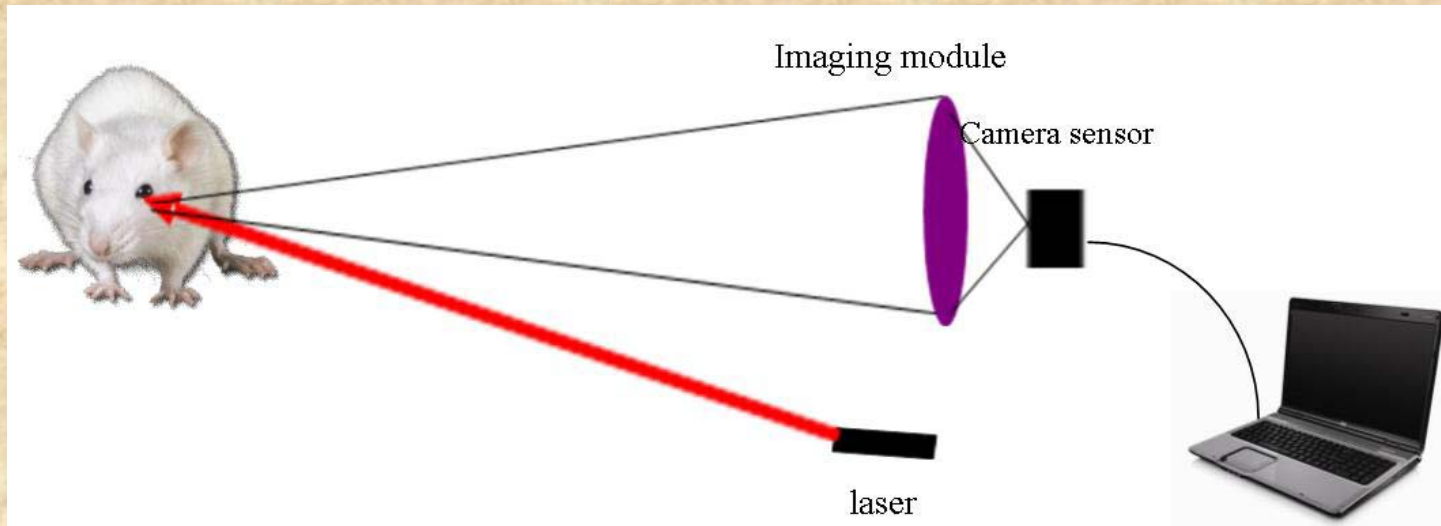


**Heart beat pulse
taken from a throat**

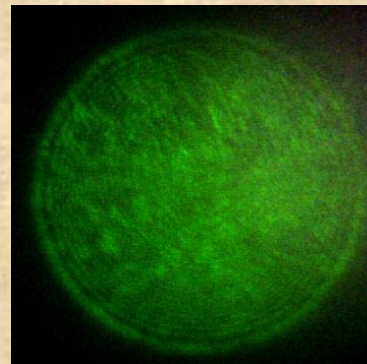


All recordings were done in a very noisy constriction site at distance of more than 80m.

Measuring of breathing from rat's cornea reflections

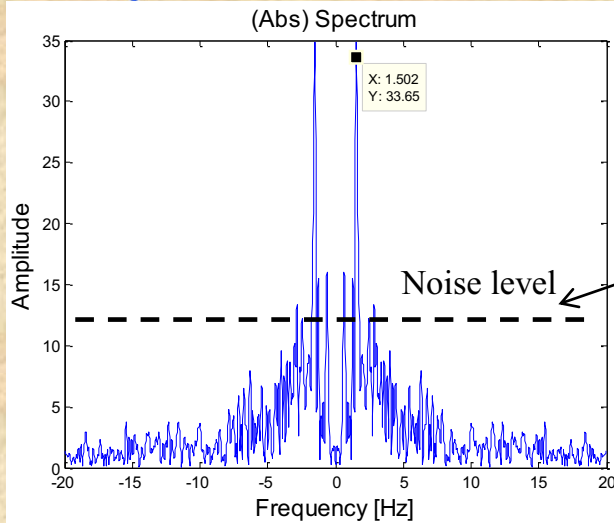


Detected rat's breathing beating at frequency around 1.87Hz.

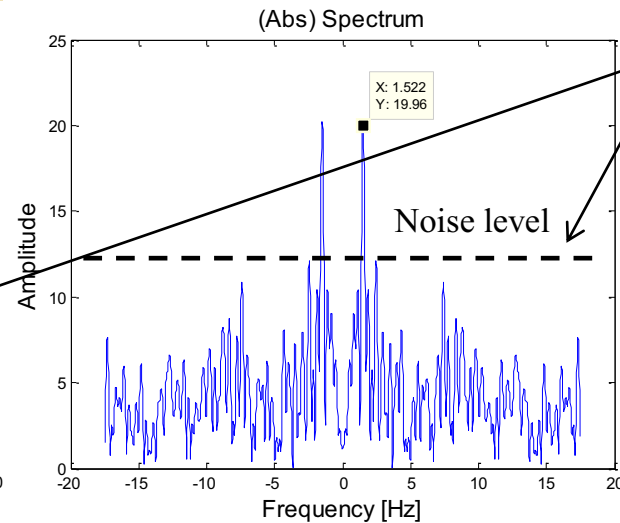


Reflected speckle pattern.

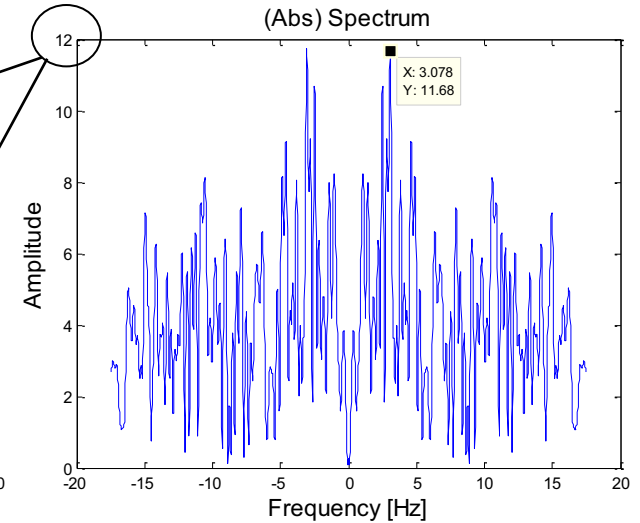
Measuring of heart beating from human's cornea reflections



Subject #1 (measurement taken while subject was holding his breath)

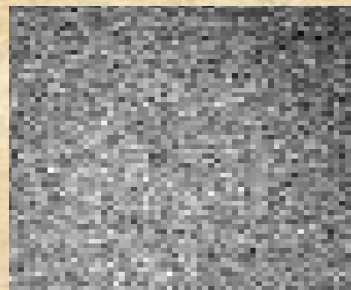


Subject #2 (measurement taken while subject was holding his breath)

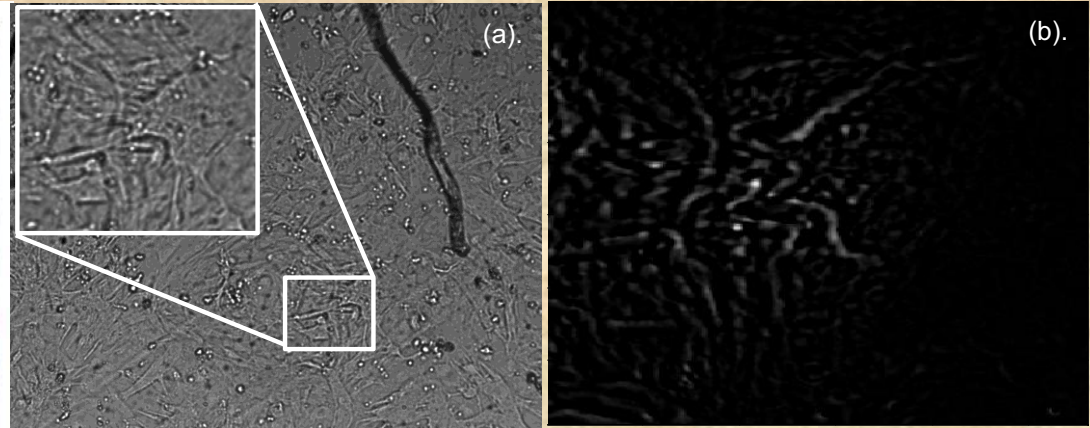
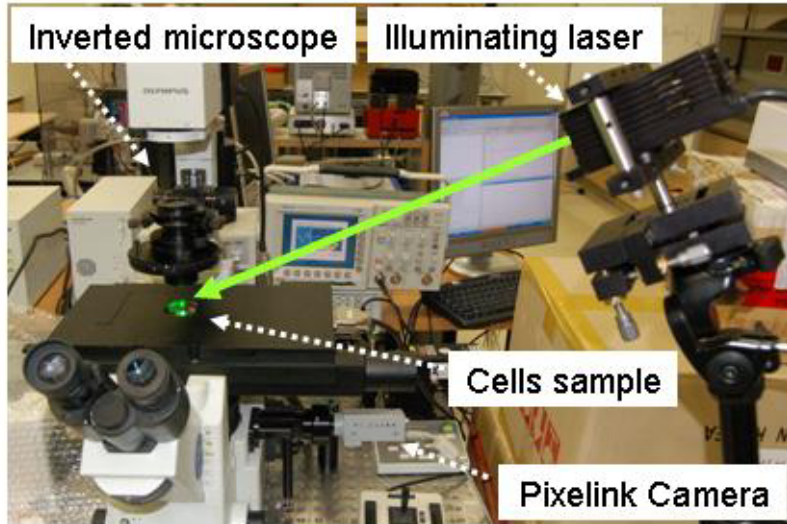


Reference noise level (detected reflection from a wall)

Detected heart beating of humans at frequency of around 1.5Hz.

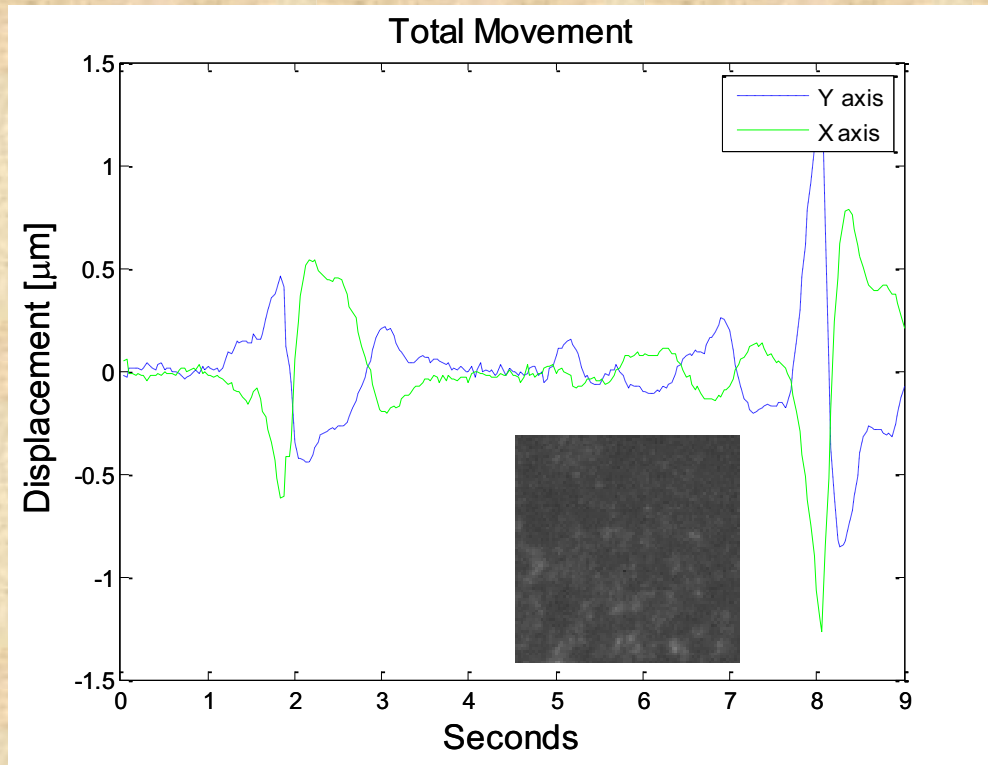


Reflected speckles pattern.

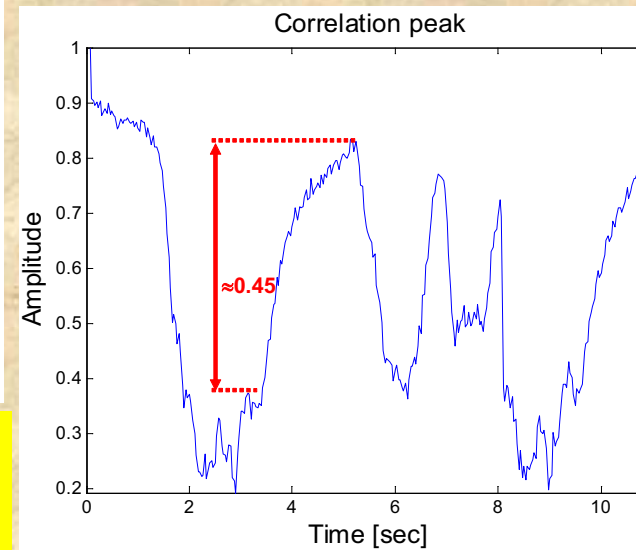
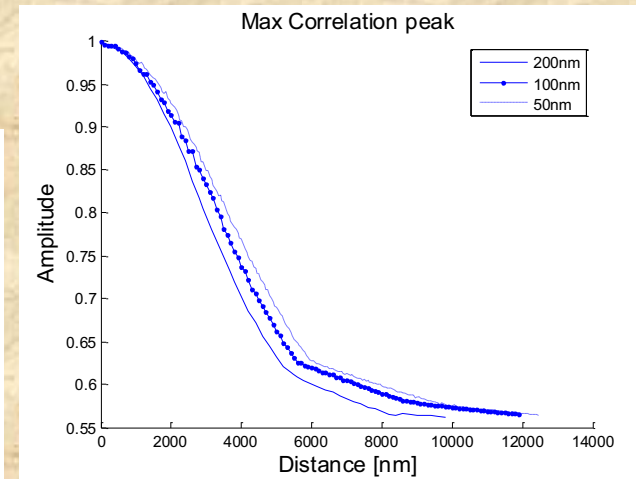


(a) Before contraction. (b) Image of differences (before and during contraction).

Image of the experimental setup.

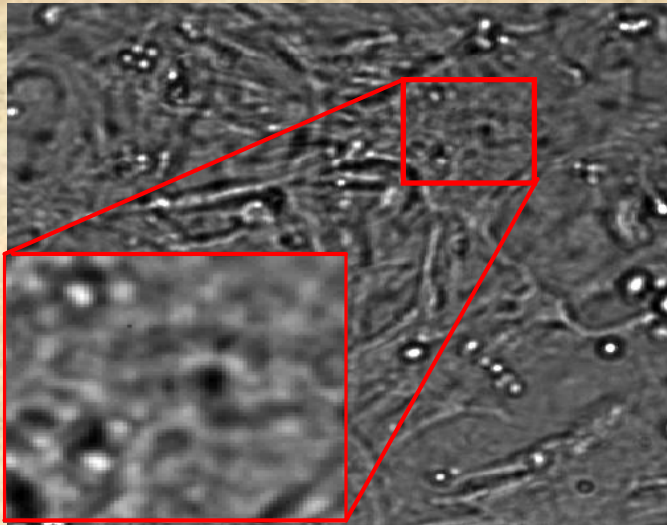


X and Y axis movement in two different video sequences that were obtained using a 10x objective, region of interest of 80x80 pixels and rate of 30 fps. In the lower part of the image one may see the diffused speckle pattern used to perform the movement tracking.

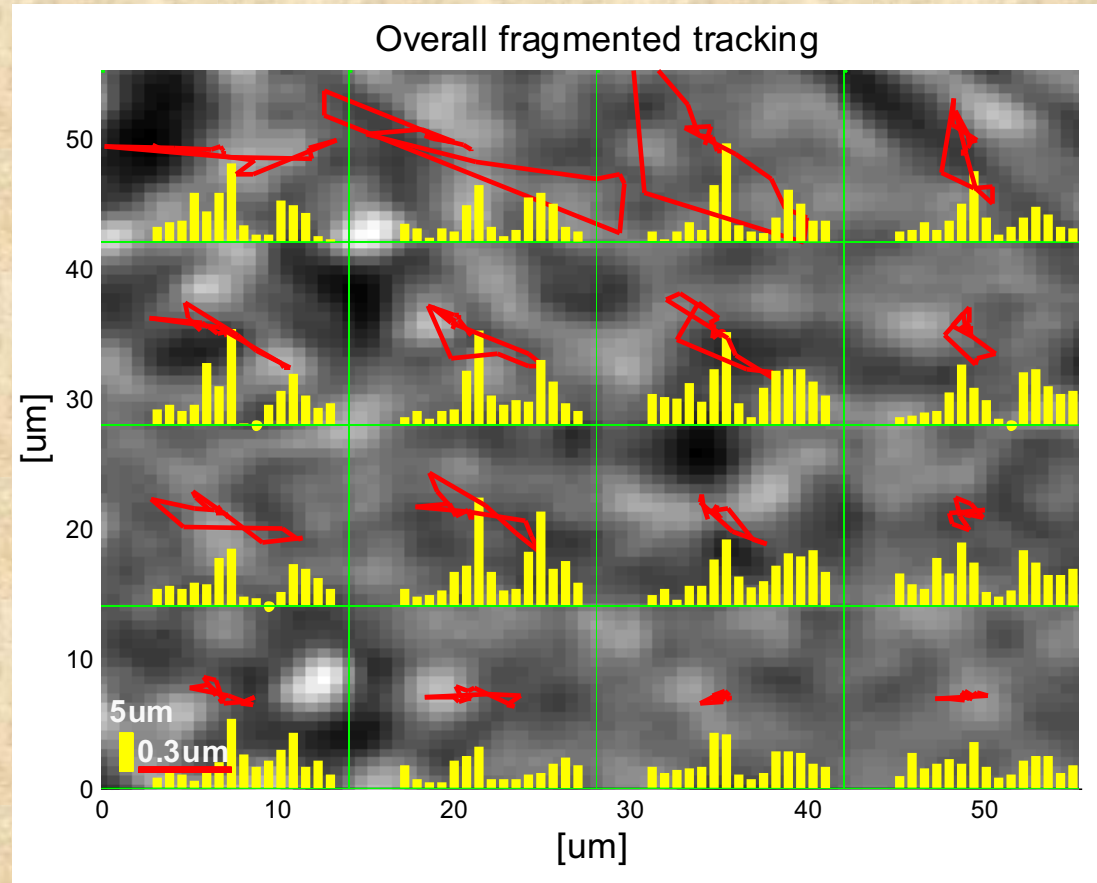


Experimental measurement of the axial movement that is obtained by mapping the amplitude of the correlation peak versus controlled axial shifts.

Opto-Phone: Hearing with Light

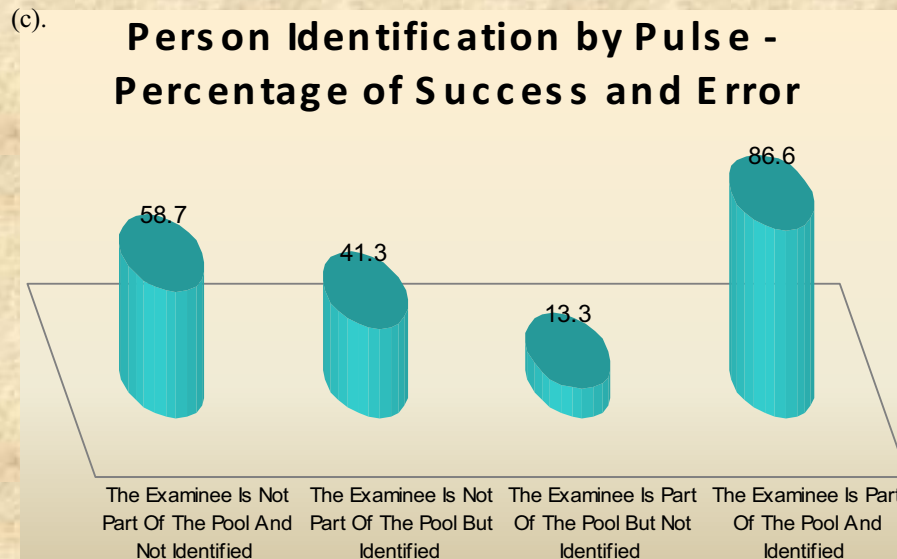
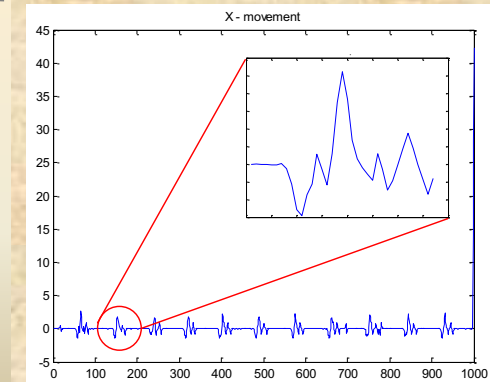
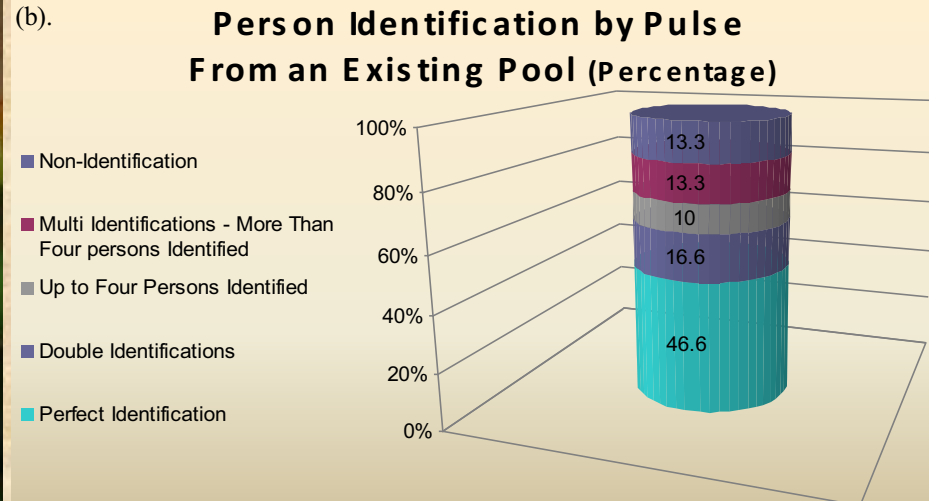
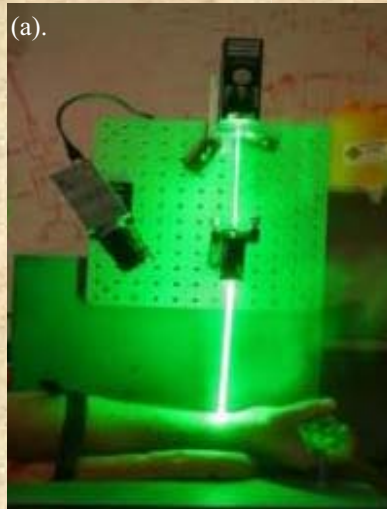


White illumination muscular cell image, with marked area of inside part of the cell that had been chosen for fragmented processing.



Overall time-variant 3-D movement of fragmented cell areas. The red lines represent the X-Y movement, starting from origin (center of each area). The yellow bars represent the axial movement versus time (starting from left to right). In the left bottom corner we marked the scale for the lines and bars as 300nm and 50nm, respectively.

Current on-going project: tracking neuronal synapses movement

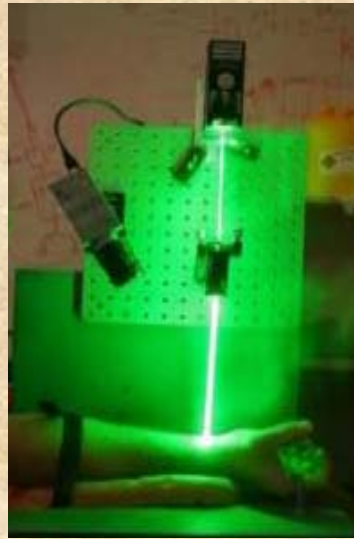
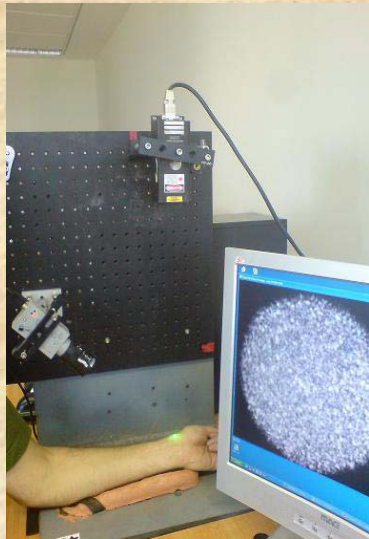
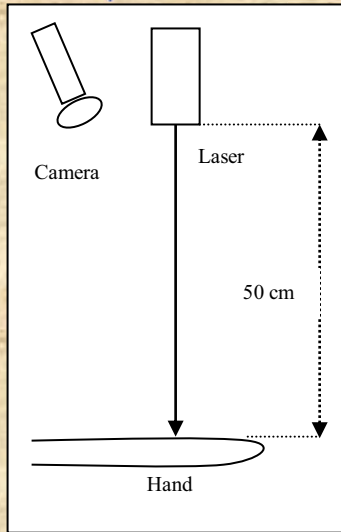


(a). The measurement configuration.

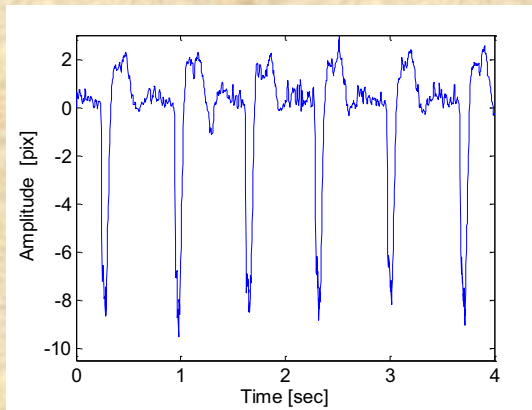
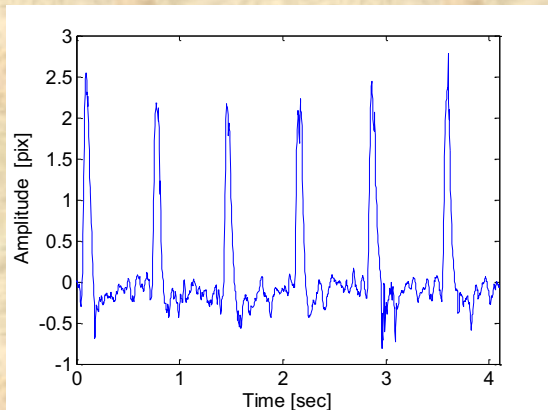
(b). Identification of subjects from an existing pool.

(c). Percentages of success and error.

Remote heart beats monitoring

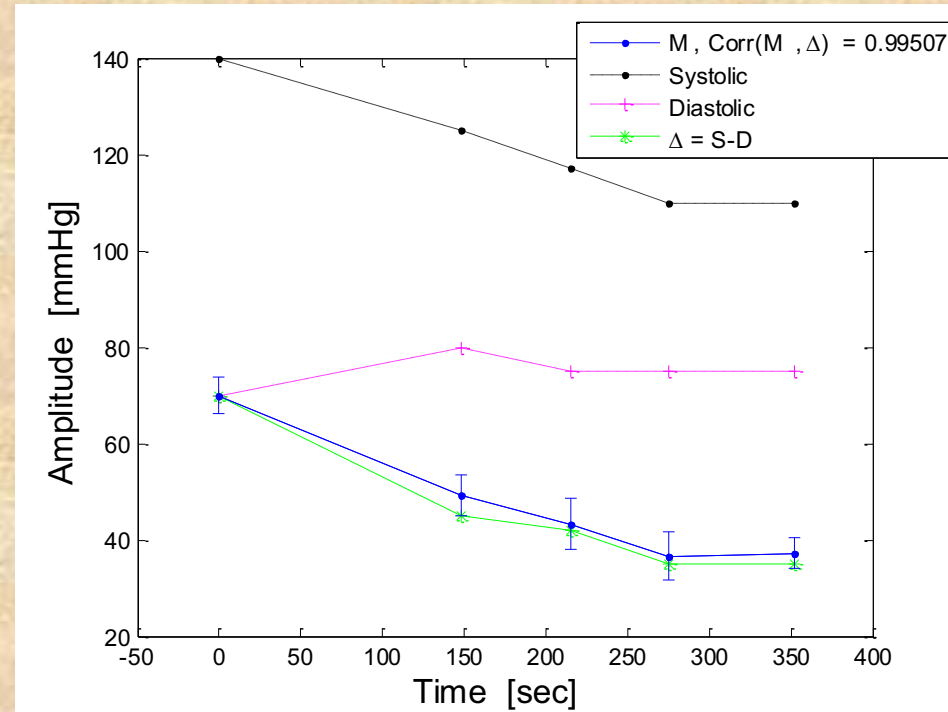
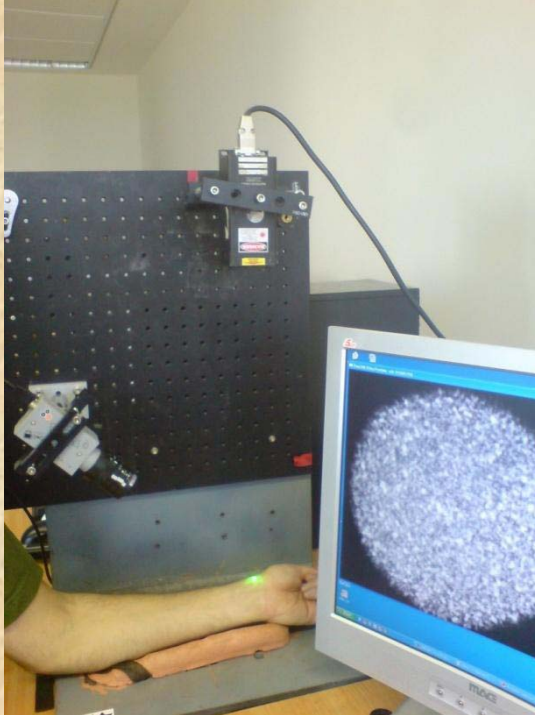


The implemented optical configuration for remote measuring of heart beats and blood pulse pressure from subject's hand

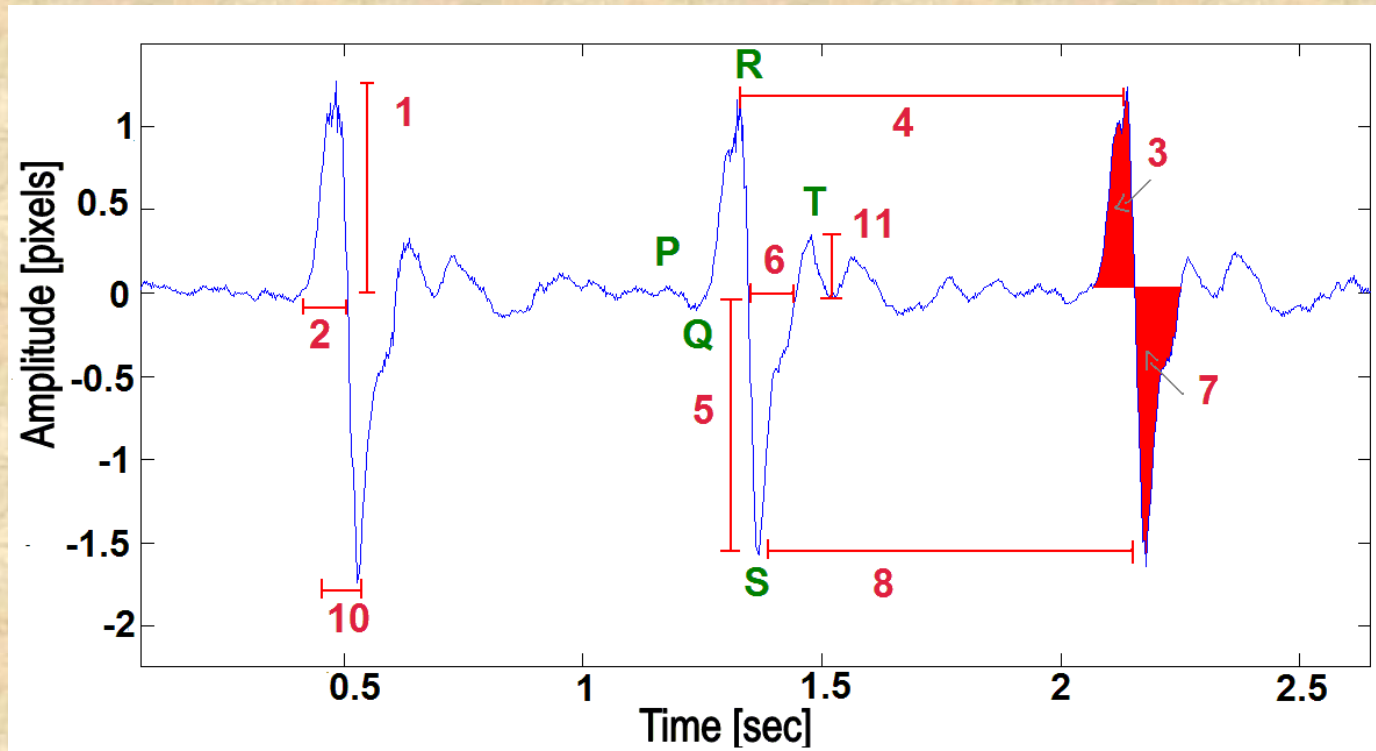


Temporal plot of the outcome from the system used in the clinical trials for two different participants.

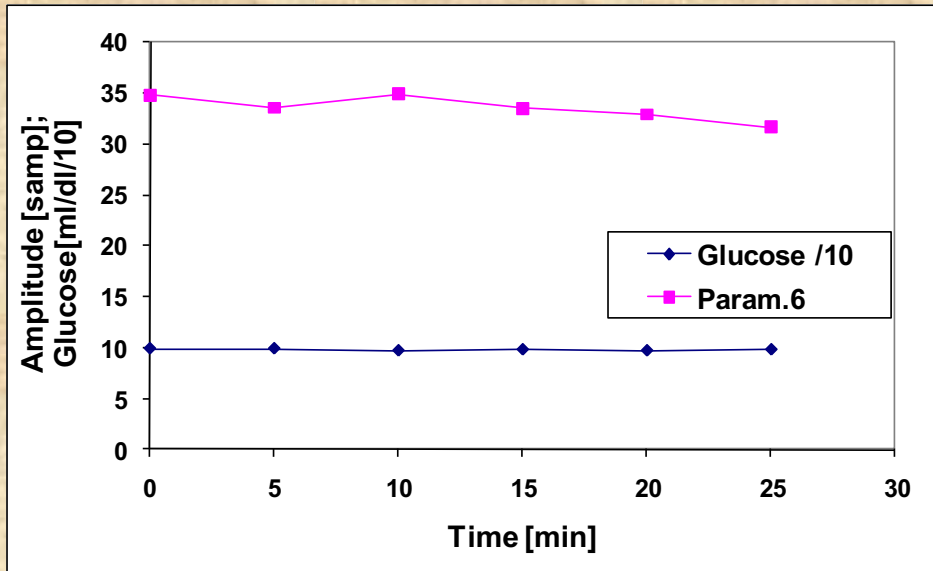
Results: Blood pressure measurement



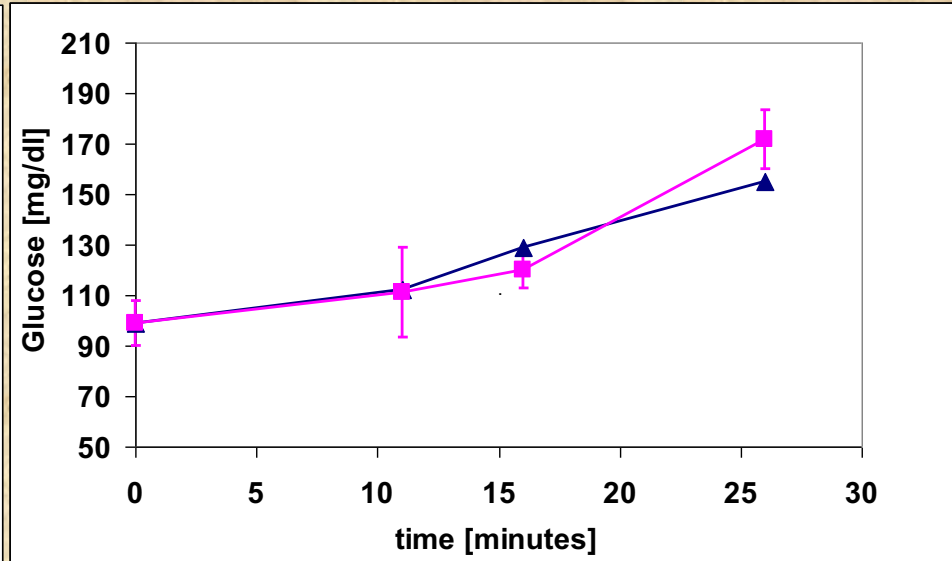
An example of the obtained remote blood pulse pressure measurement using the proposed device for one subject participating in the clinical test group. The reference pulse pressure is shown by the green curve (denoted as Δ) was obtained using manual sleeve based reference measurement device. The blue curve (denoted as M) is the measurement obtained using the proposed optical technique. The time duration of the measurement was 350sec. The sampling of the camera was performed at 300Hz. One may see that strong correlation exists between the green (reference) curve and the blue curve obtained by the developed approach.



Temporal plot of the outcome from the system used in the clinical tests with the graphical description of the observed parameters.

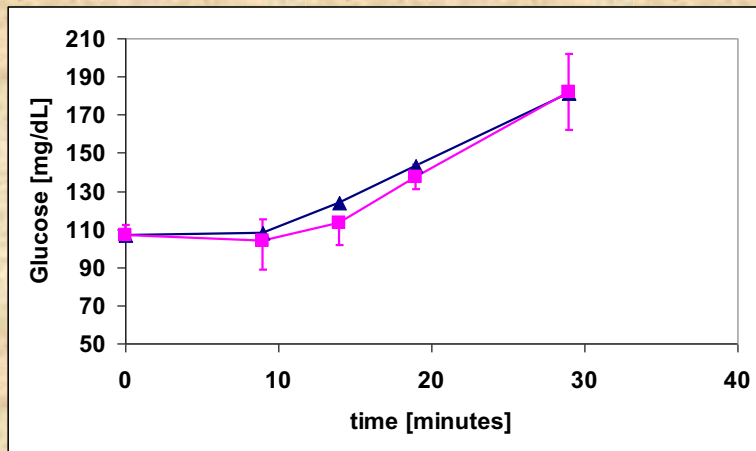


Stability of the system: constant glucose level in blood (denoted by blue line with triangles) and the estimated parameter 6 (denoted by magenta line with rectangles). Glucose level is given in units of 0.1[ml/dl] (representing a constant level of 100 [ml/dl]), while the estimated optical values are given in pixels.

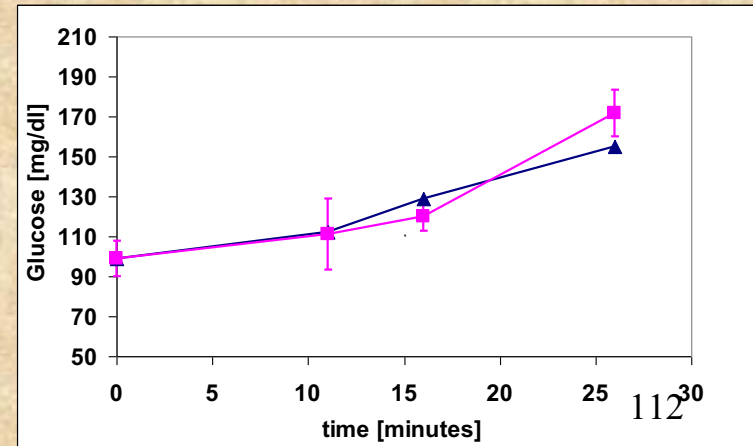


Data of subject #1: Glucose level in blood and amplitude of positive peak (parameter #1). Glucose level is denoted by blue line with triangles and the optically measured parameter is denoted by magenta line with rectangles.

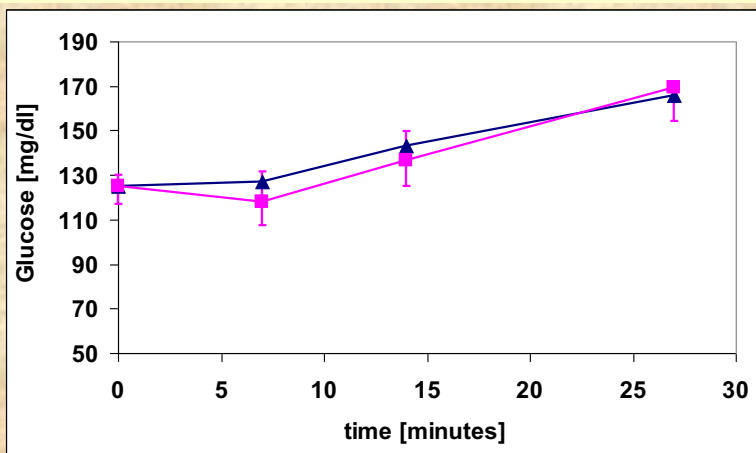
Remote glucose level monitoring



Data of subject #3: Glucose level in blood and amplitude of positive peak (parameter #1). Glucose level is denoted by blue line with triangles and the optically measured parameter is denoted by magenta line with rectangles.

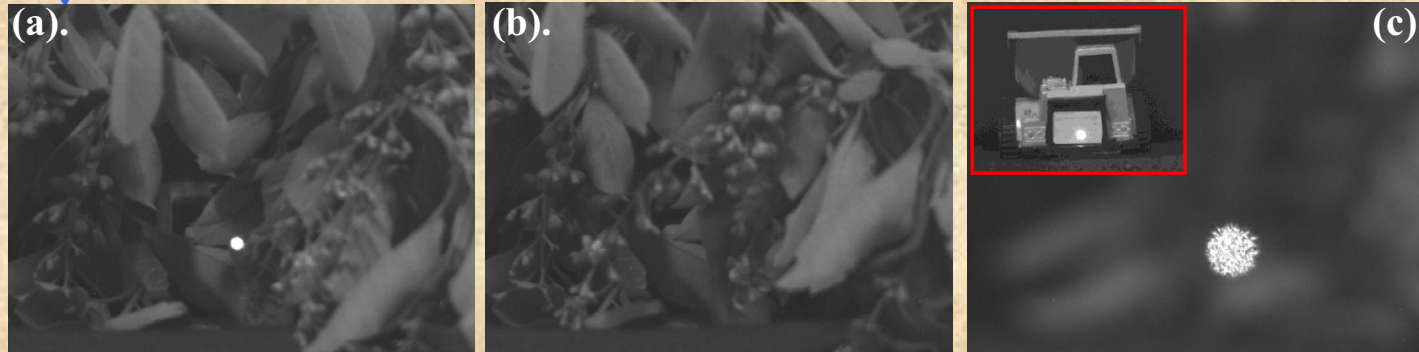


Data of subject #1: Glucose level in blood and amplitude of positive peak (parameter #1). Glucose level is denoted by blue line with triangles and the optically measured parameter is denoted by magenta line with rectangles.

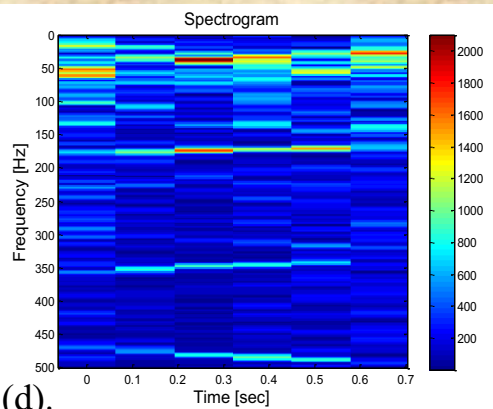


Data of subject #4: Glucose level in blood and amplitude of positive peak (parameter #1). Glucose level is denoted by blue line with triangles and the optically measured parameter is denoted by magenta line with rectangles.

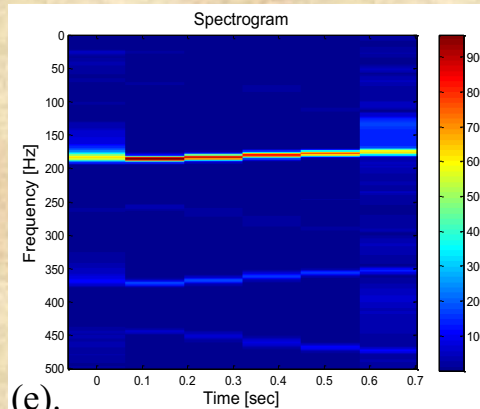
Results: Detection of occluded objects I



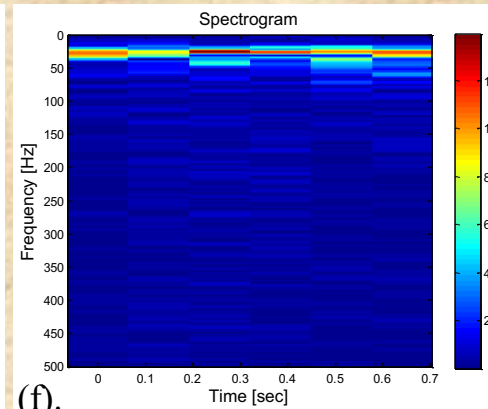
(a). Camouflaged object. (b). Camouflage without the object. (c). The object (upper left part) and the low resolution camouflaged scenery.



(d).



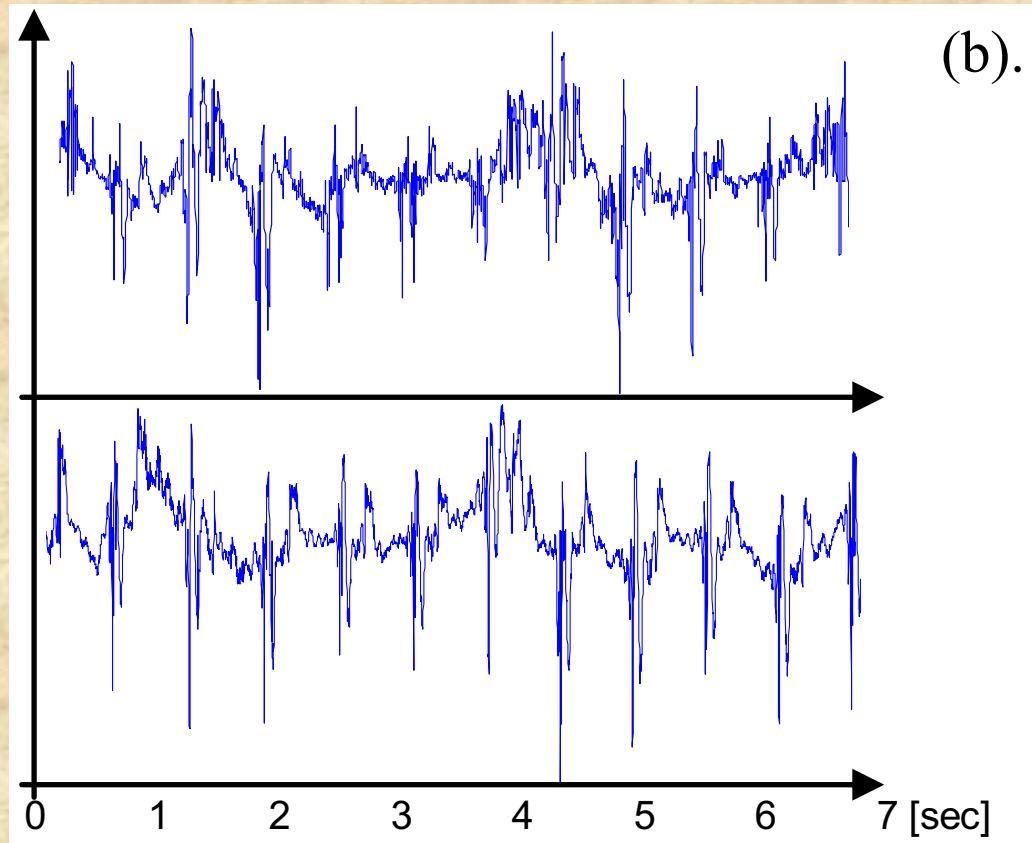
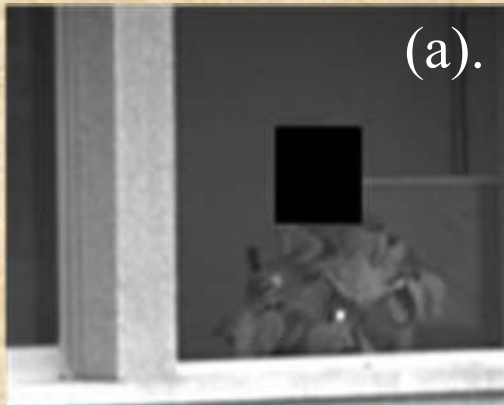
(e).



(f).

(d). The spectrogram of the camouflaged object with its engine turned on. (e). The spectrogram of the object with its engine turned on and without the camouflage. (f). The spectrogram of the camouflaged object without turning on its engine.

***Results: Detection of
occluded objects II***



(a). The scenario of the experiment. (b). Experimental results: upper recording is of the camouflaged subject. Lower recording is the same subject without the camouflage.



Outline

- **Introduction**
- **The “SW Adaptation” Process**
- **Diffraction type Super Resolution**
- **Geometrical type Super Resolution**
- **Hearing with light**
- **Conclusions**



Conclusions:

- **Resolution of optical system is restricted by various terms.**
- **SW Adaptation process is a useful tool for designing super-resolution systems.**
- **A generalization for handling more types of resolution restrictions was introduced for large variety of applications.**
- **Examples of achieving super resolution effects were viewed.**
- **New approach for “hearing” with light was demonstrated.**